Chapter 5

Spin Transfer Torque

韩伟

量子材料科学中心

2018年11月23日

Outline

1. Spin transfer torque

2. Spin orbit torque and spin Hall effect

3. Spin orbit torque and Rashba-Edestein effect

Review of last class

1. Theory and observation of spin transfer torque

2. Spin transfer torque and spin pumping

3. Spin transfer torque in MTJ and Domain wall motion

4. Spin transfer torque in domain wall motion

5. Thermal spin transfer torque

6. Pure Spin current transfer torque

Review of last class

John Slonczewski



Luc Berger



This class

1. Spin orbit torque

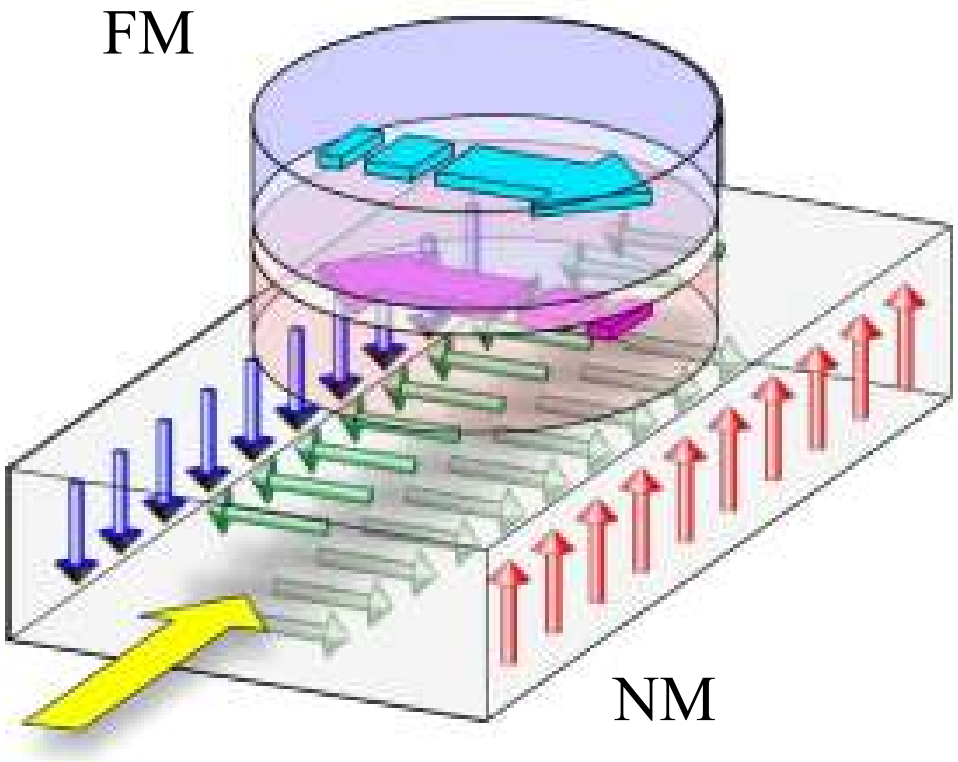
2. Spin Hall effect

3. Rashba-Edelstein effect

Outline

1. Spin orbit torque

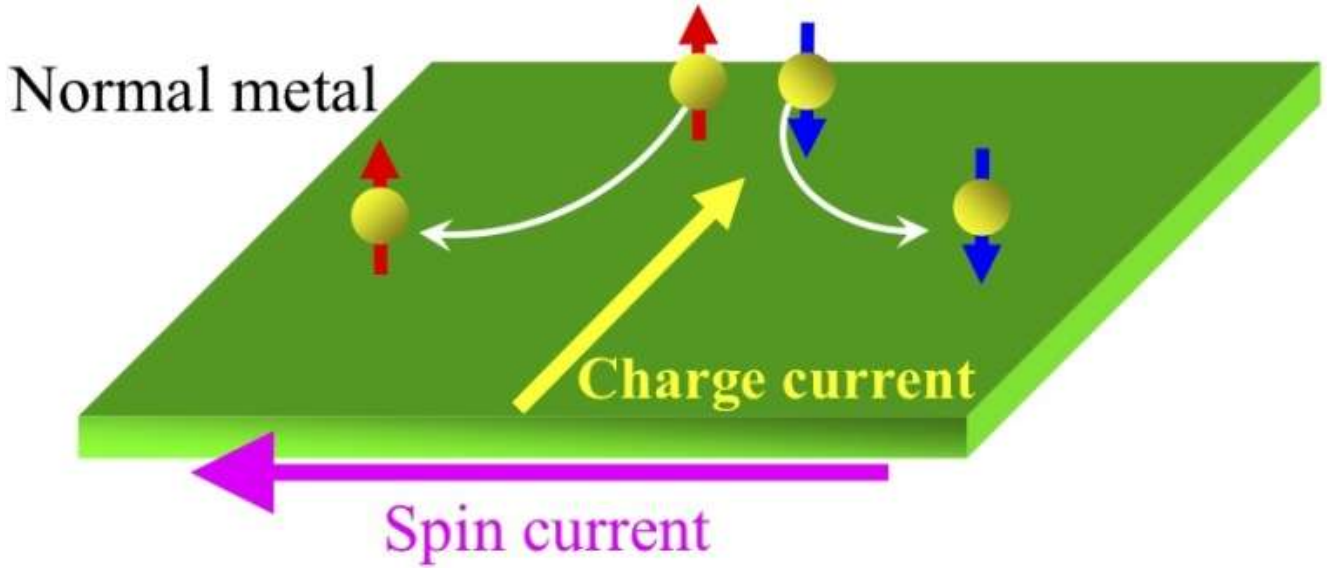
Spin orbit torque



$$\tau_{ST} = \frac{\hbar}{2}\hat{m} \times (\hat{\sigma} \times \hat{m})$$

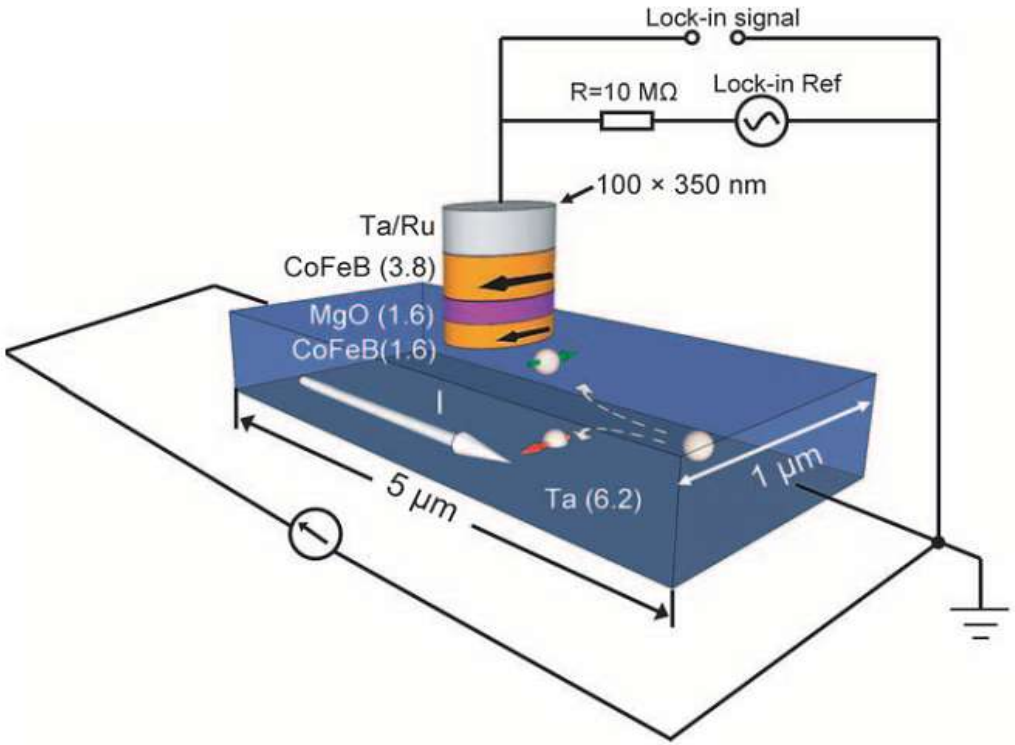
Spin orbit torque

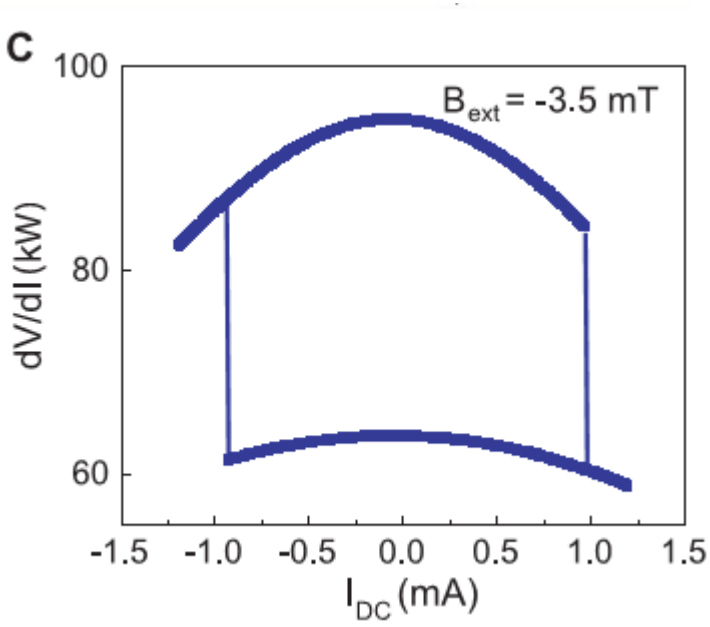
Spin Hall effect



D'yakonov, M. I. & Perel', J. Exp. Theor. Phys. Lett. 13, 467-469, (1971).
Hirsch, J. E. Phys. Rev. Lett. 83, 1834-1837, (1999).
Zhang, S. Phys. Rev. Lett. 85, 393-396, (2000).

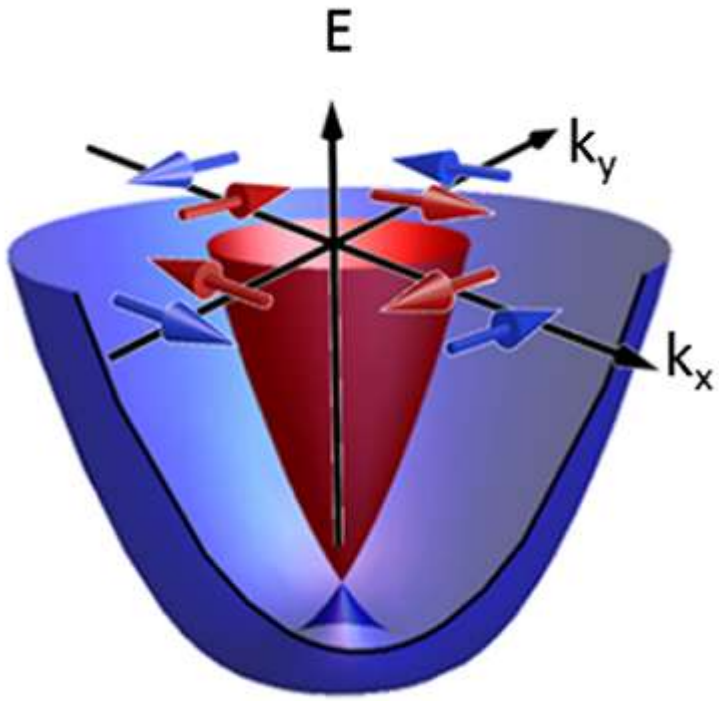
Spin orbit torque

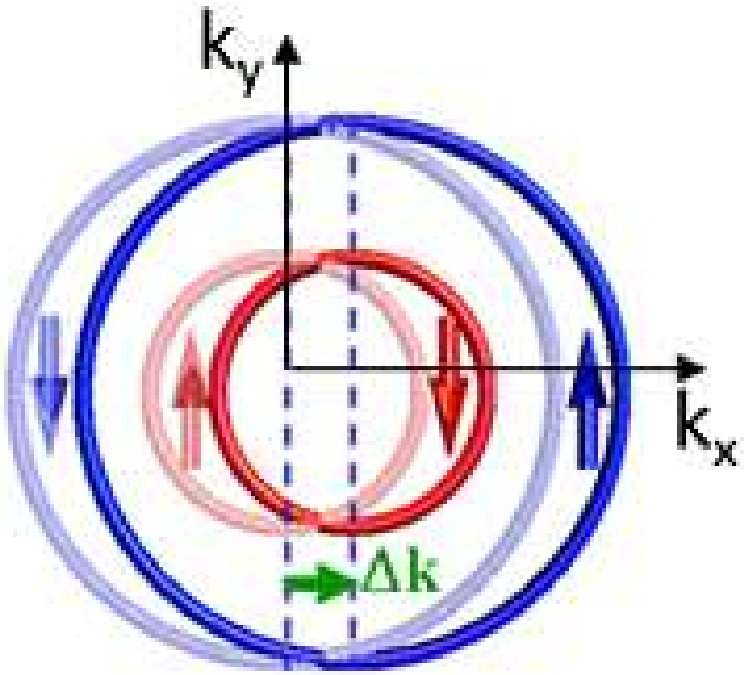




Liu, et al, Science (2012)

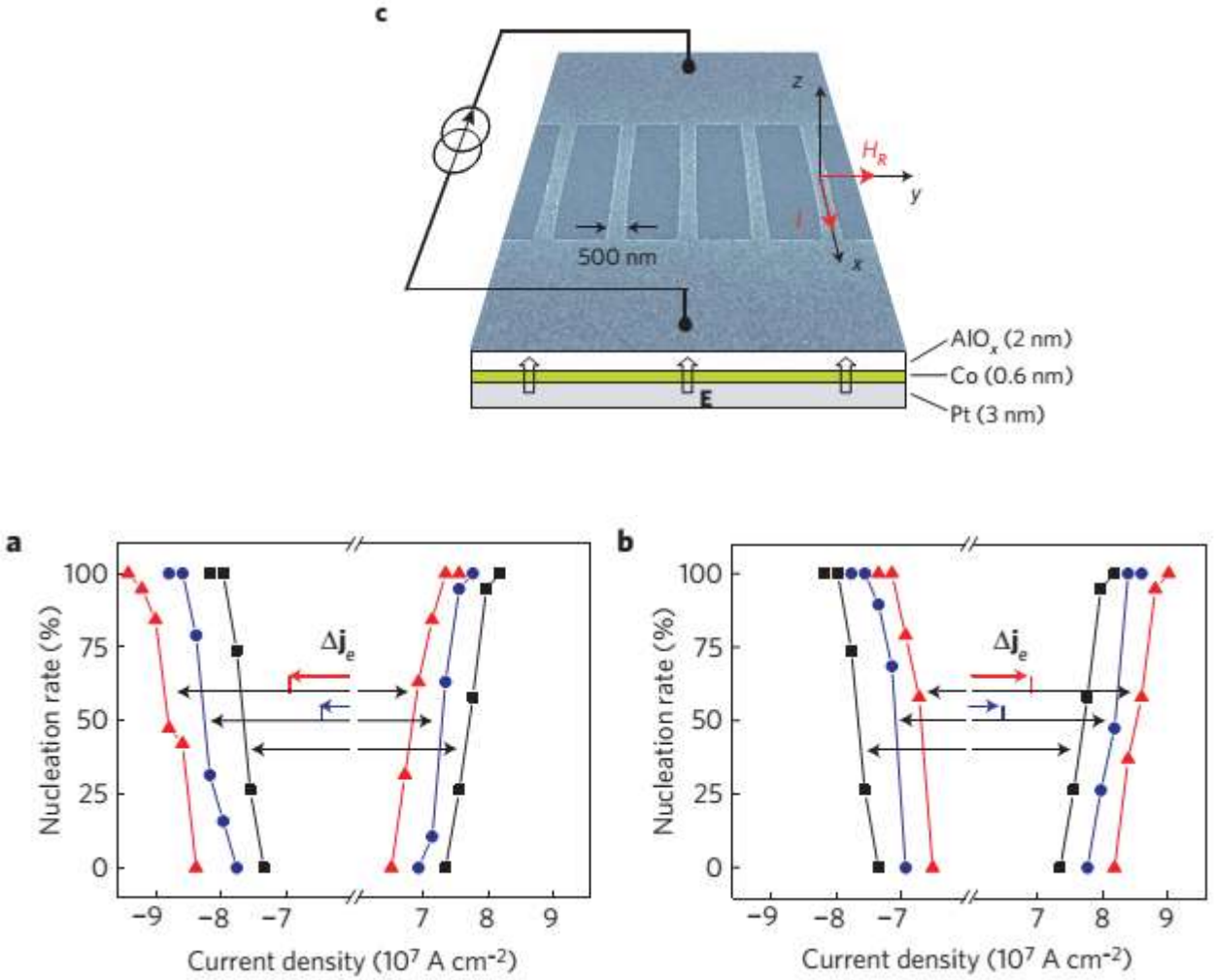
Spin orbit torque





V. M. Edelstein, Solid State Commun. 73, 233 (1990)
A. Manchon, et al, Nat. Mater. 14, 871 (2015)
J. C. R. Sánchez, et al, Phys. Rev. Lett. 116, 096602 (2016)

Spin orbit torque

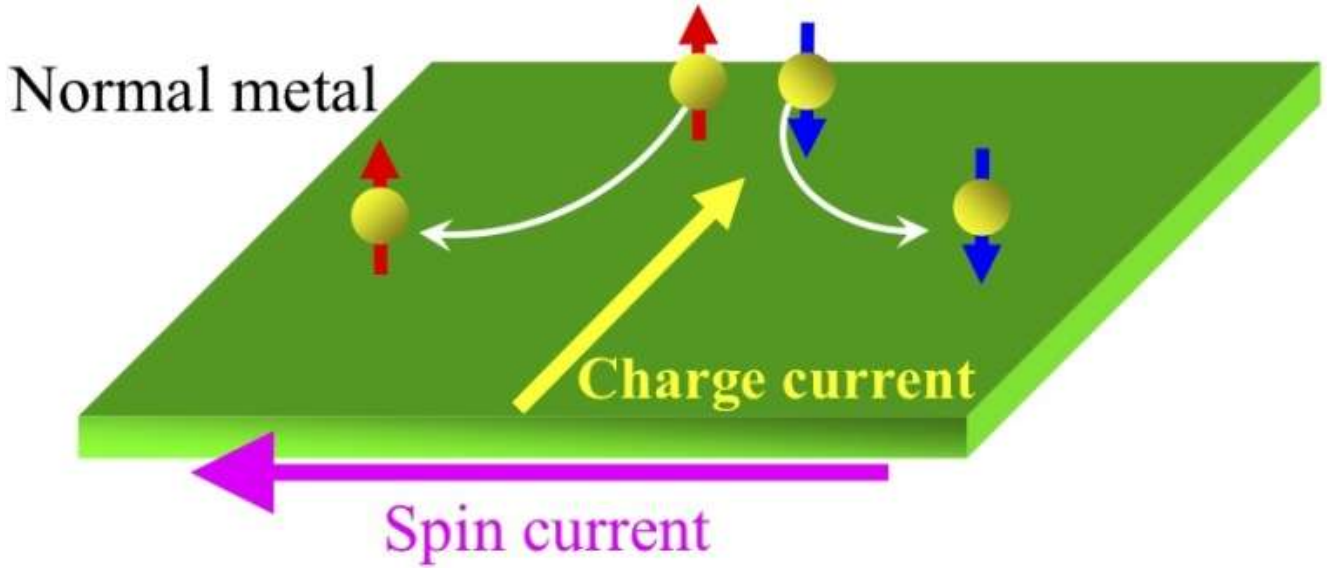


Miron, et al, Nature Materials (2011)

Outline

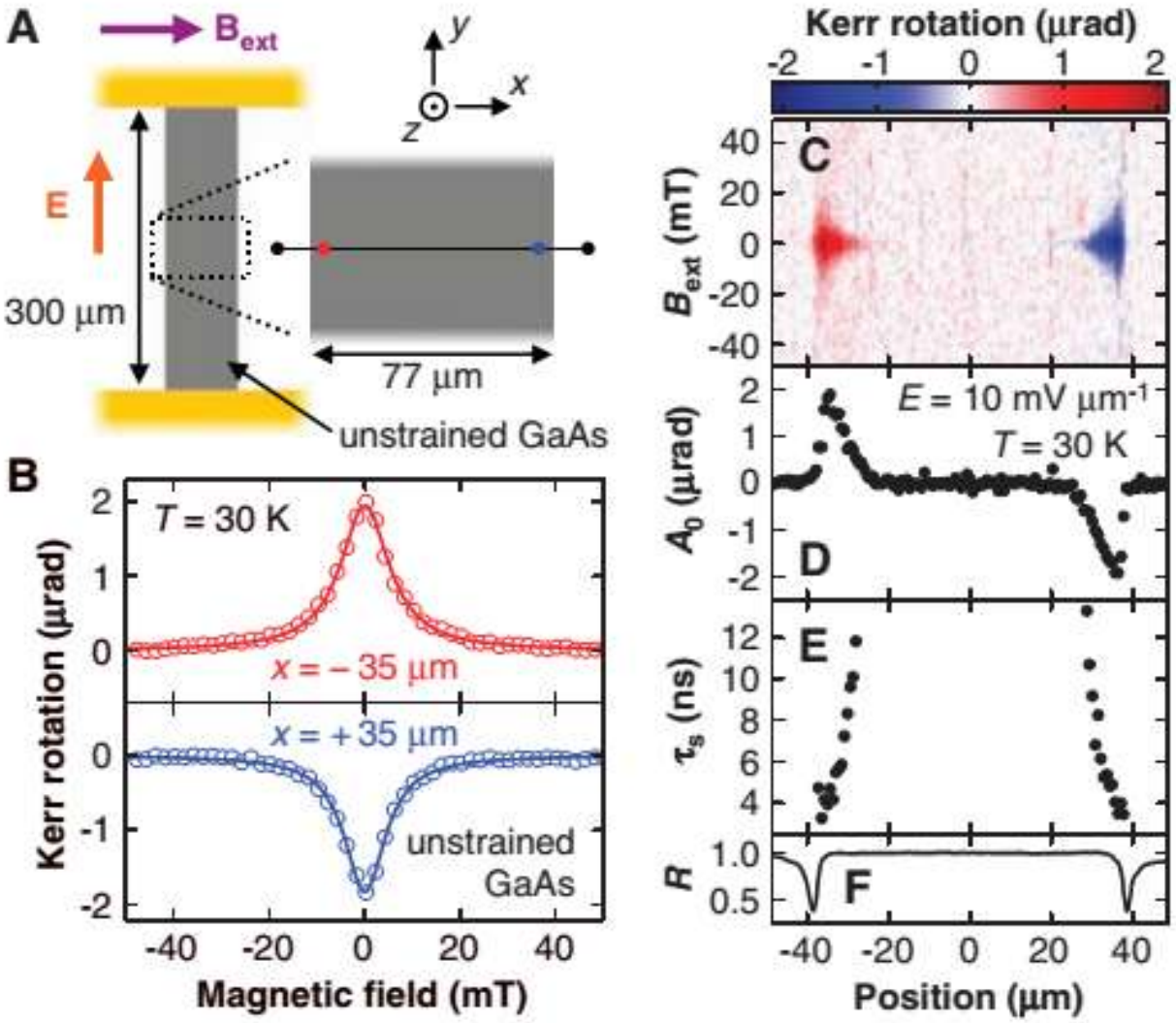
2. Spin Hall effect

Spin Hall effect



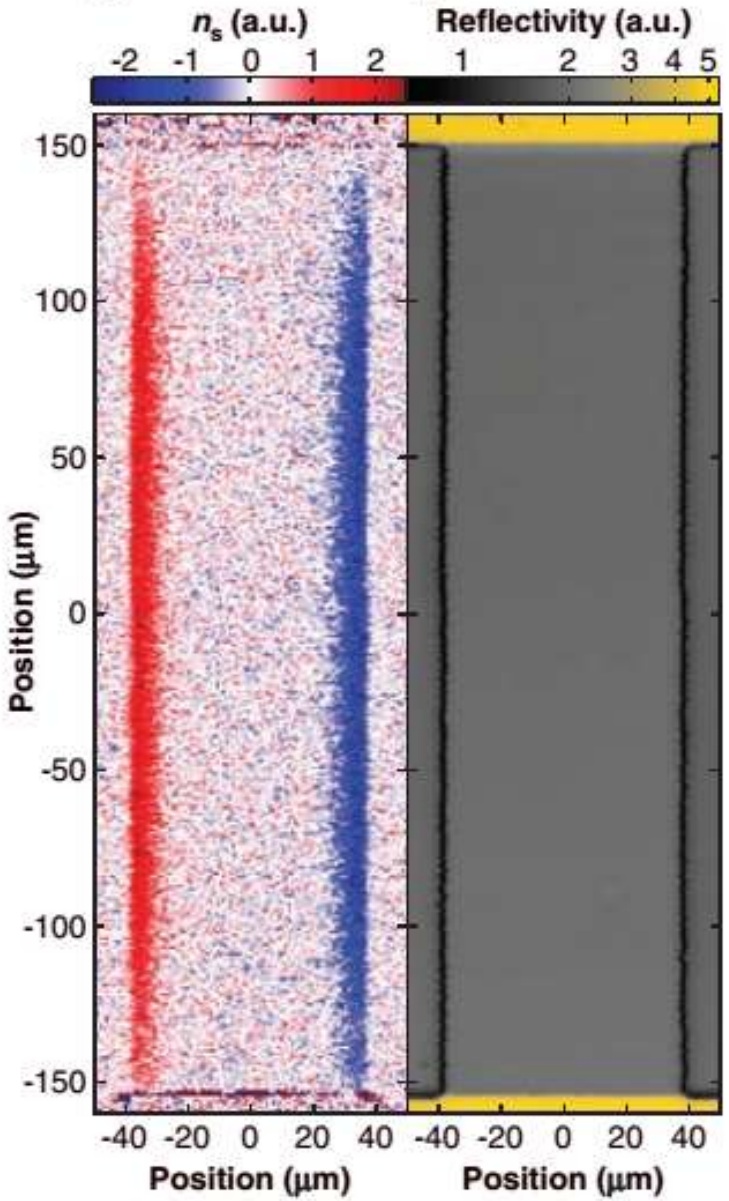
D'yakonov, M. I. & Perel', J. Exp. Theor. Phys. Lett. 13, 467-469, (1971).
Hirsch, J. E. Phys. Rev. Lett. 83, 1834-1837, (1999).
Zhang, S. Phys. Rev. Lett. 85, 393-396, (2000).

First observation of SHE

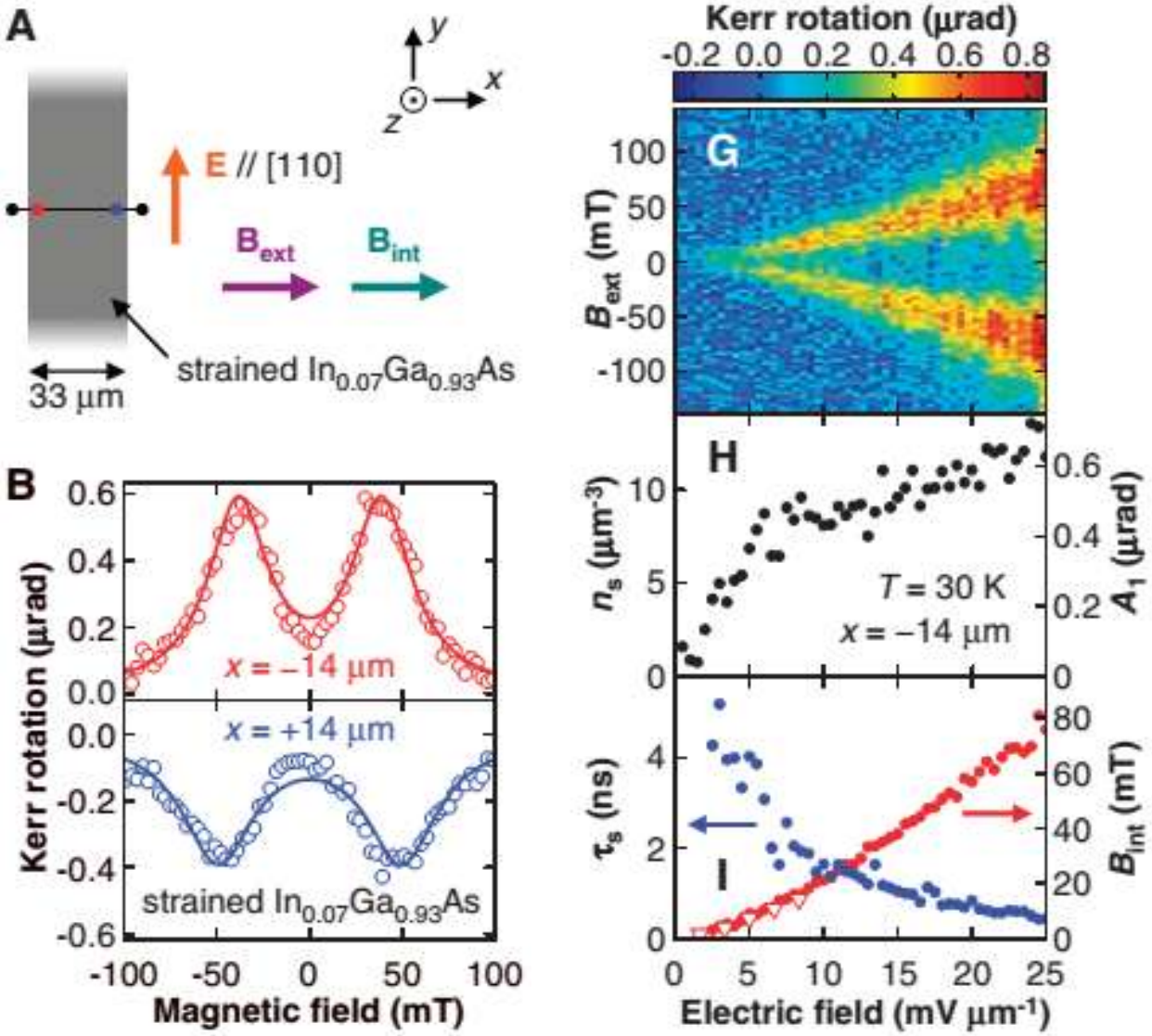


Kato, et al, Science (2004)

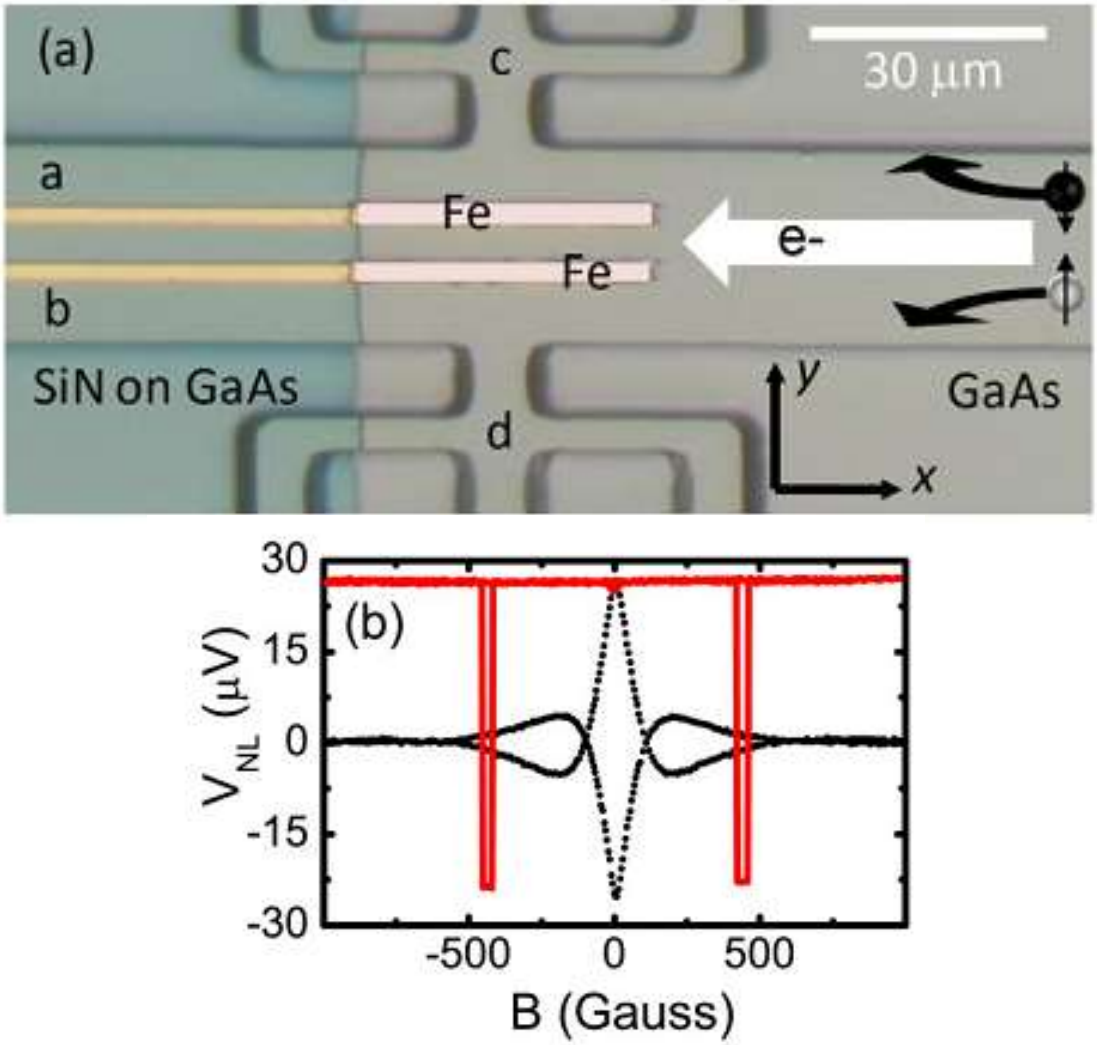
First observation of SHE



First observation of SHE

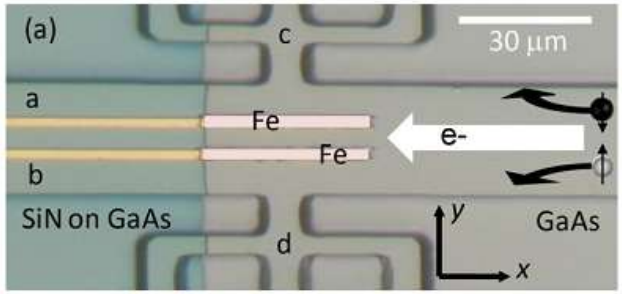


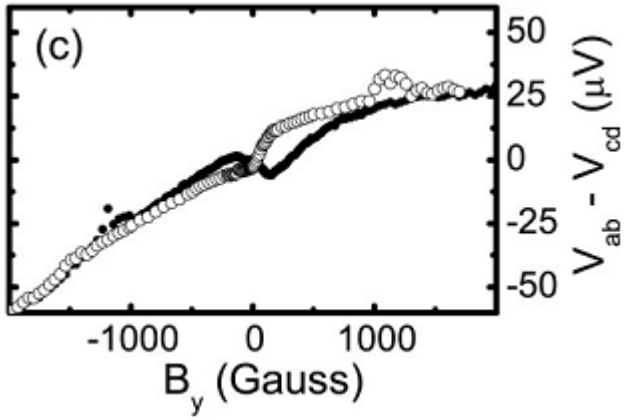
Electrical measurement

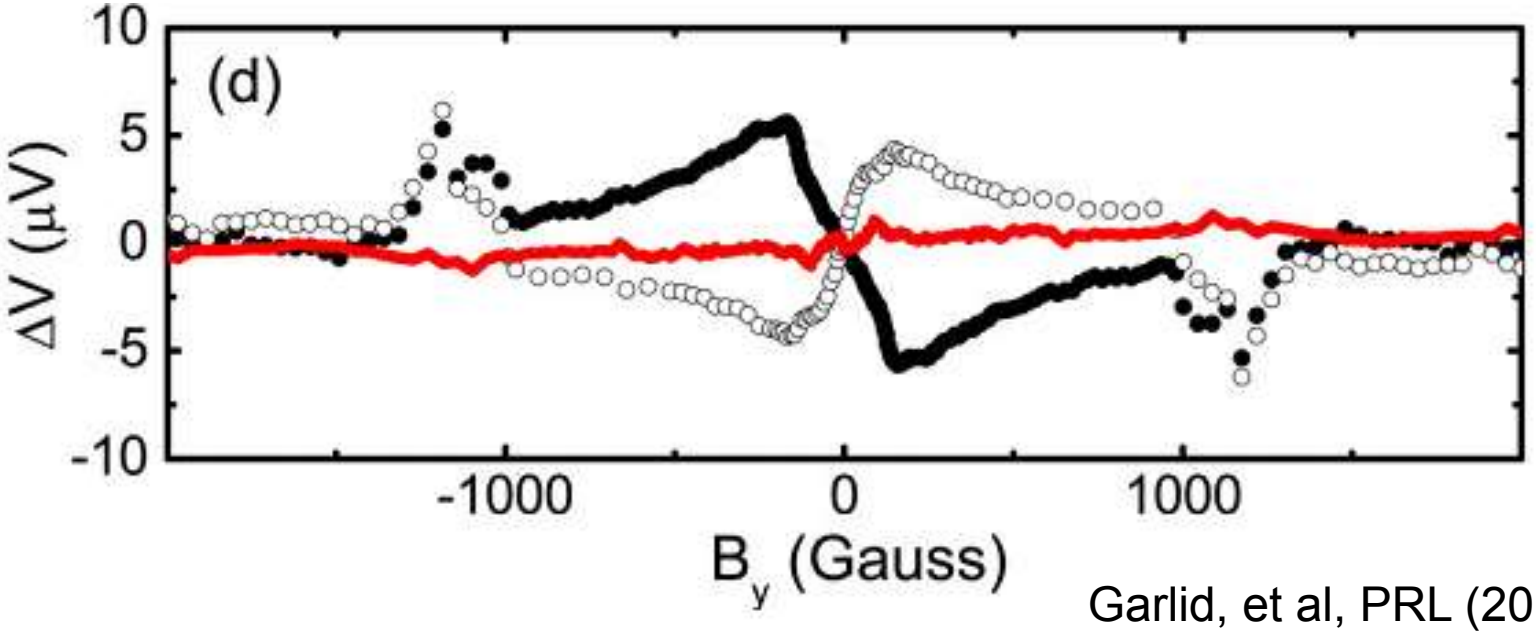


Garlid, et al, PRL (2010)

Electrical measurement

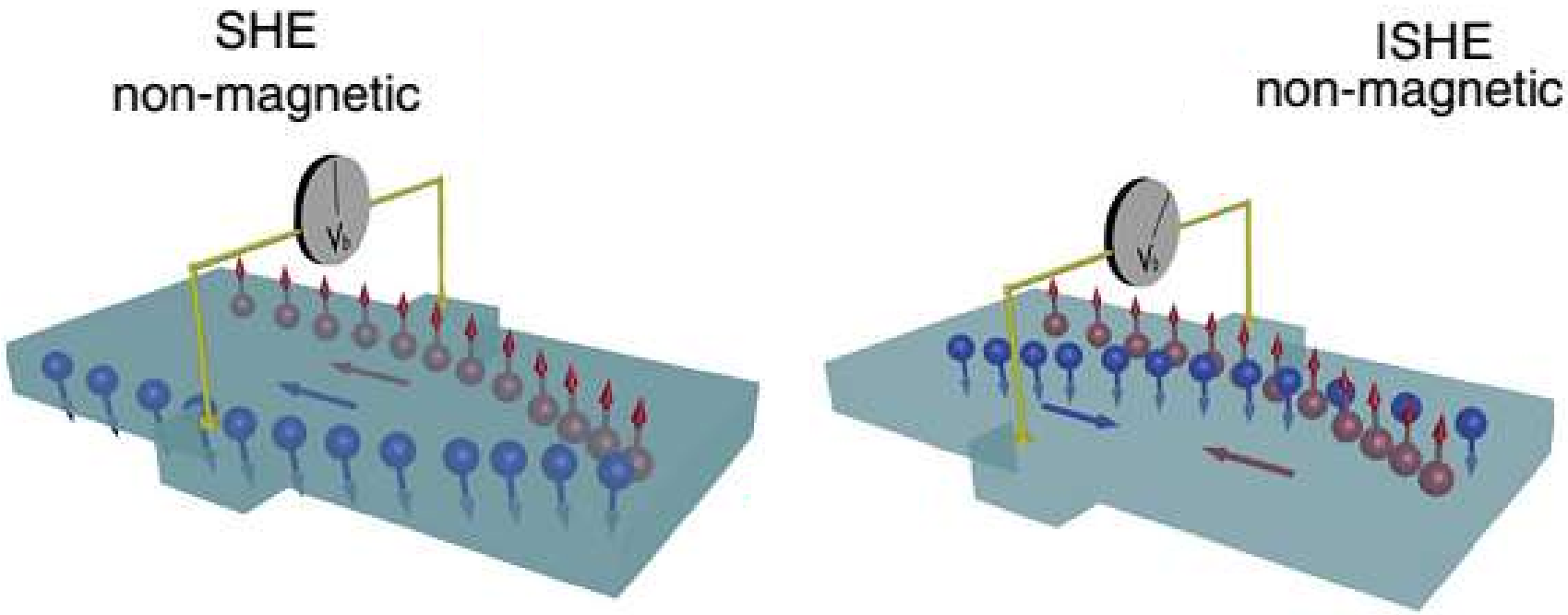




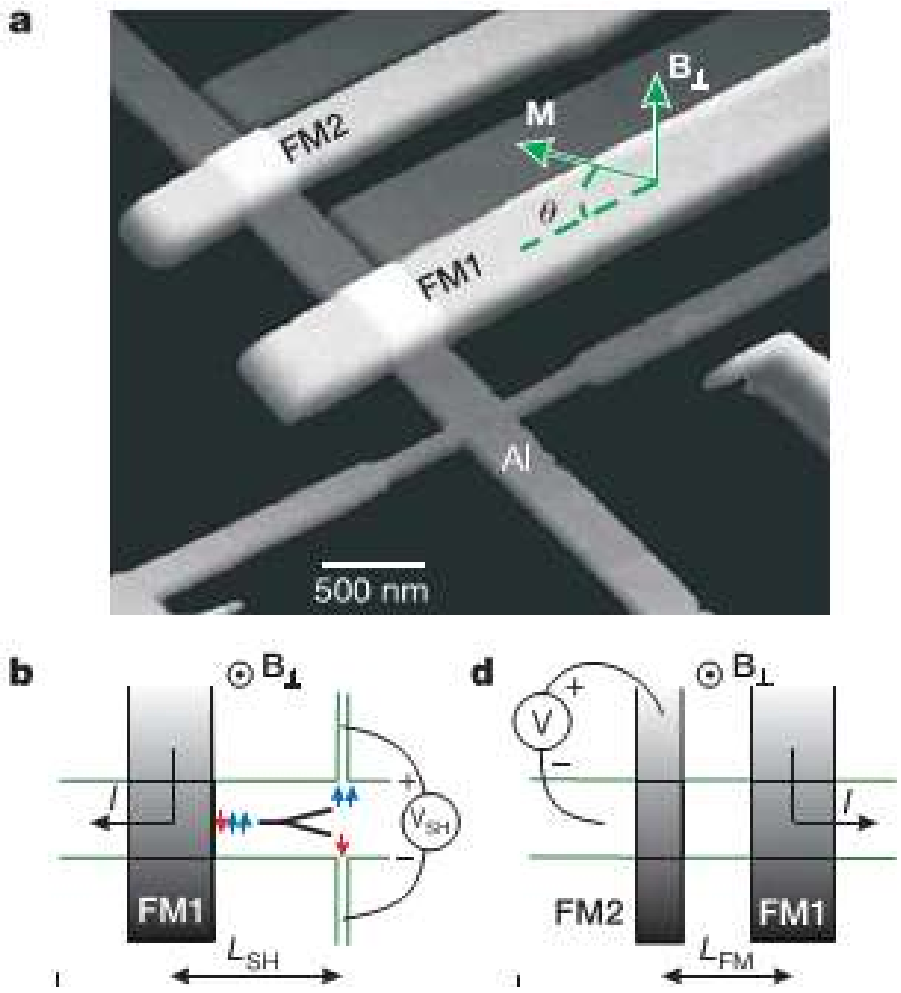


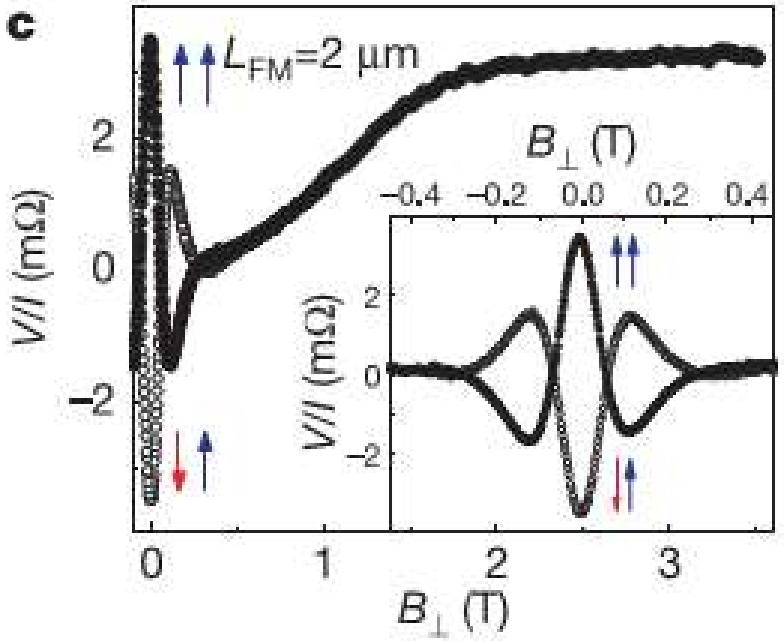
Garlid, et al, PRL (2010)

SHE vs ISHE



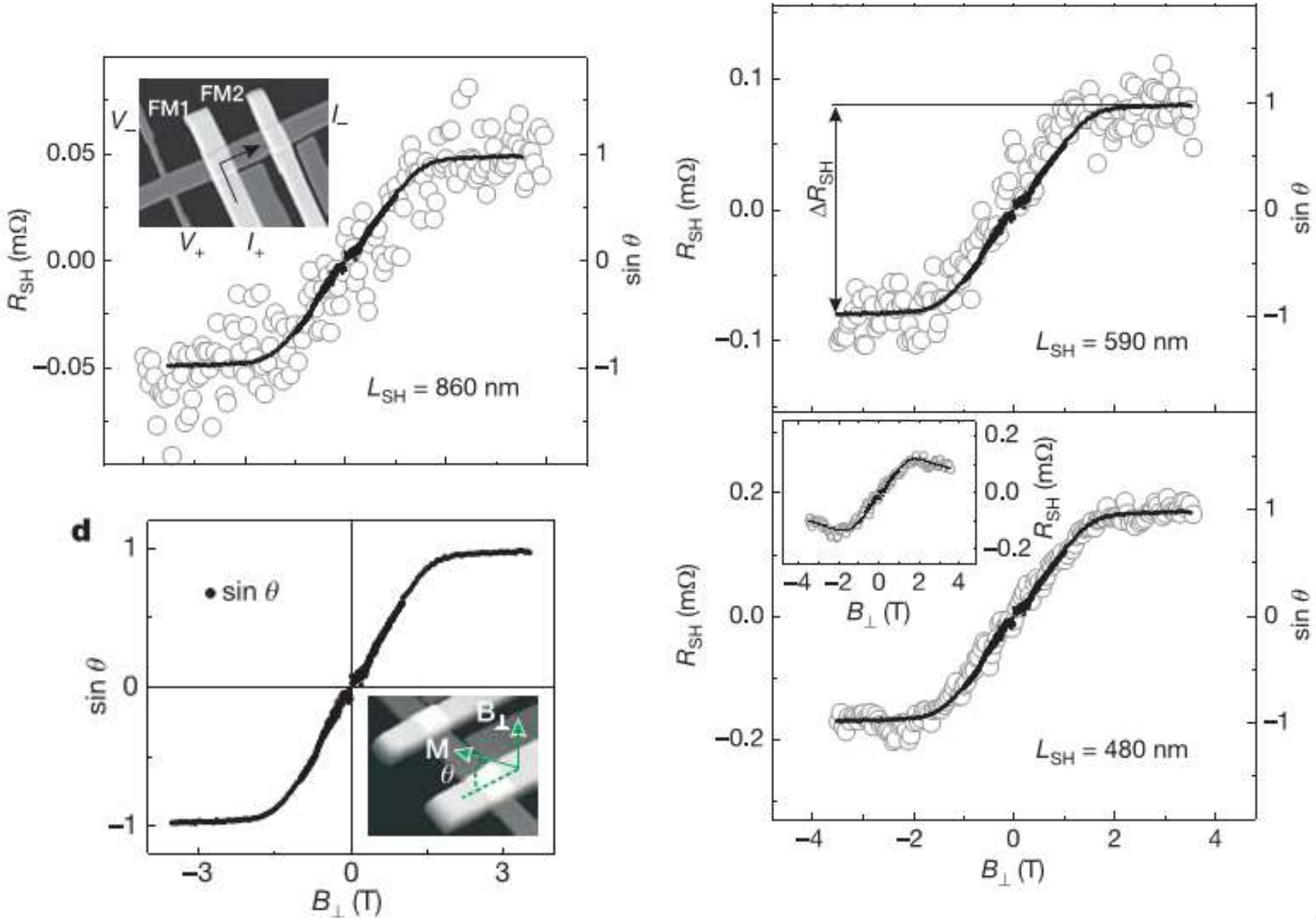
Spin injection and spin Hall



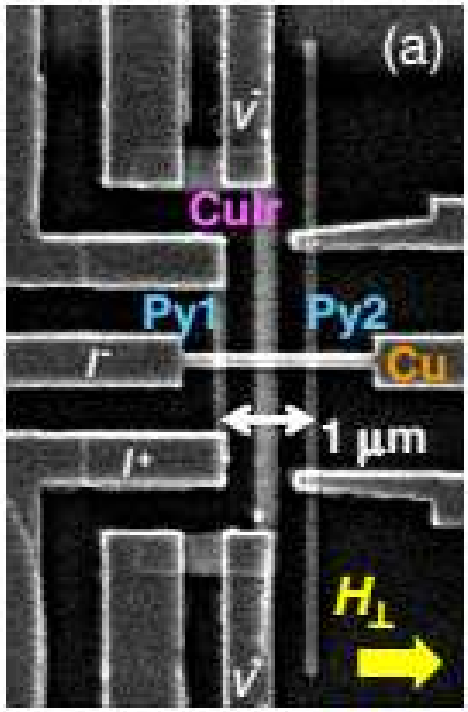


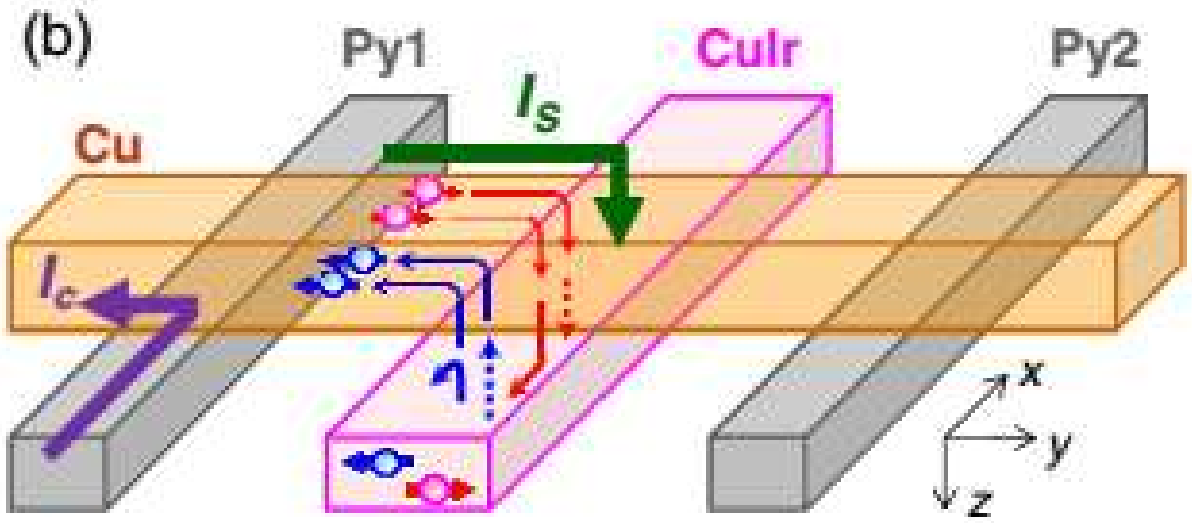
Valenzuela, et al, Nature (2006)

Spin injection and spin Hall



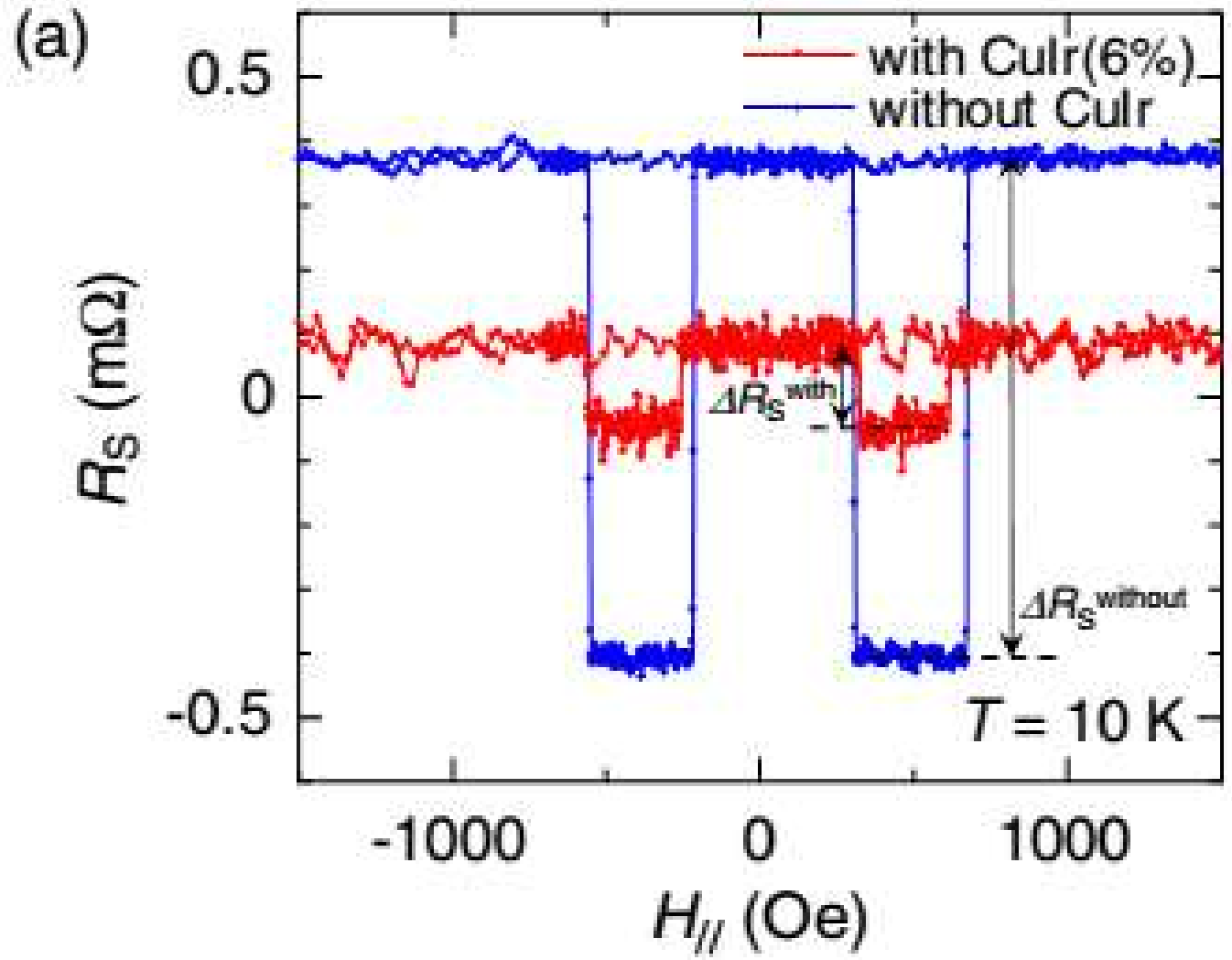
Spin diffusion and absorption



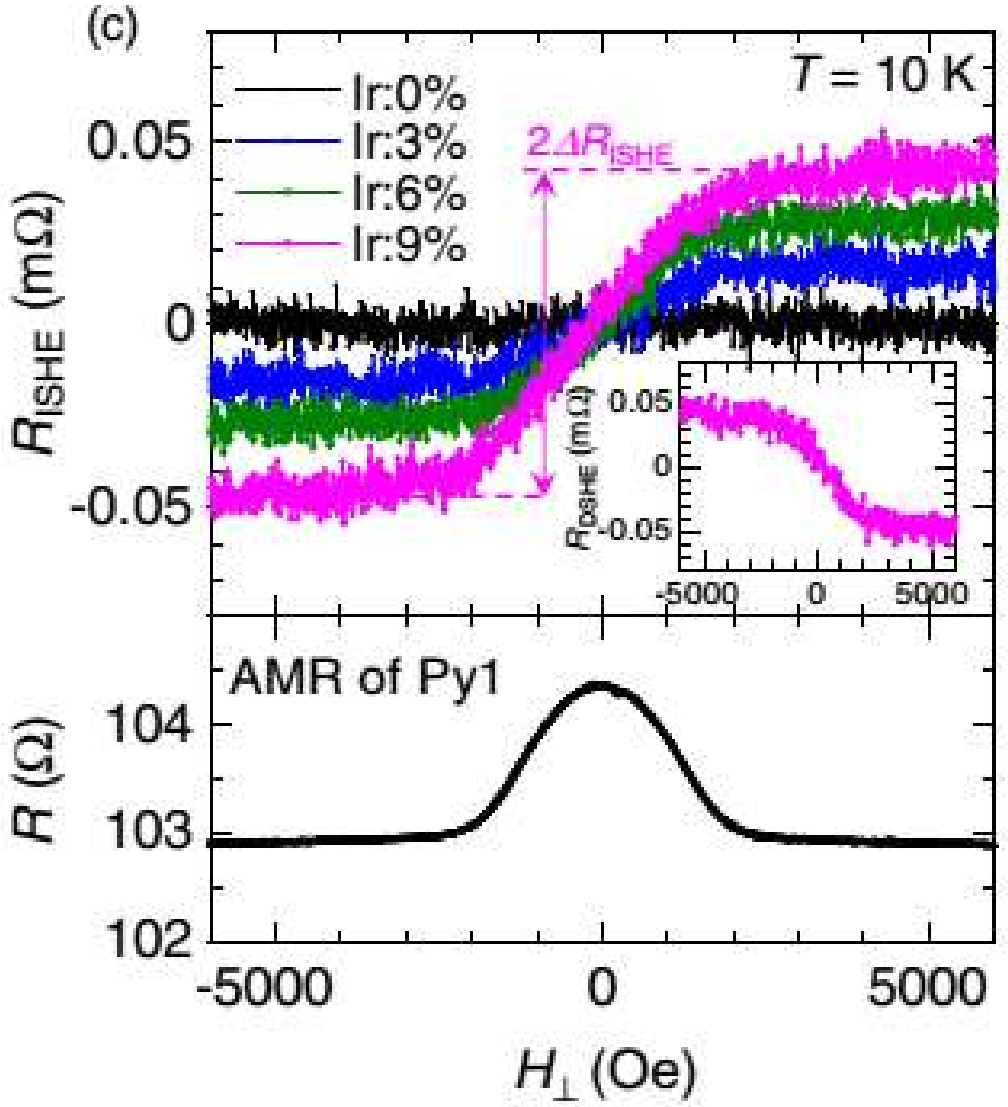


Olejnik, et al, PRL (2012)

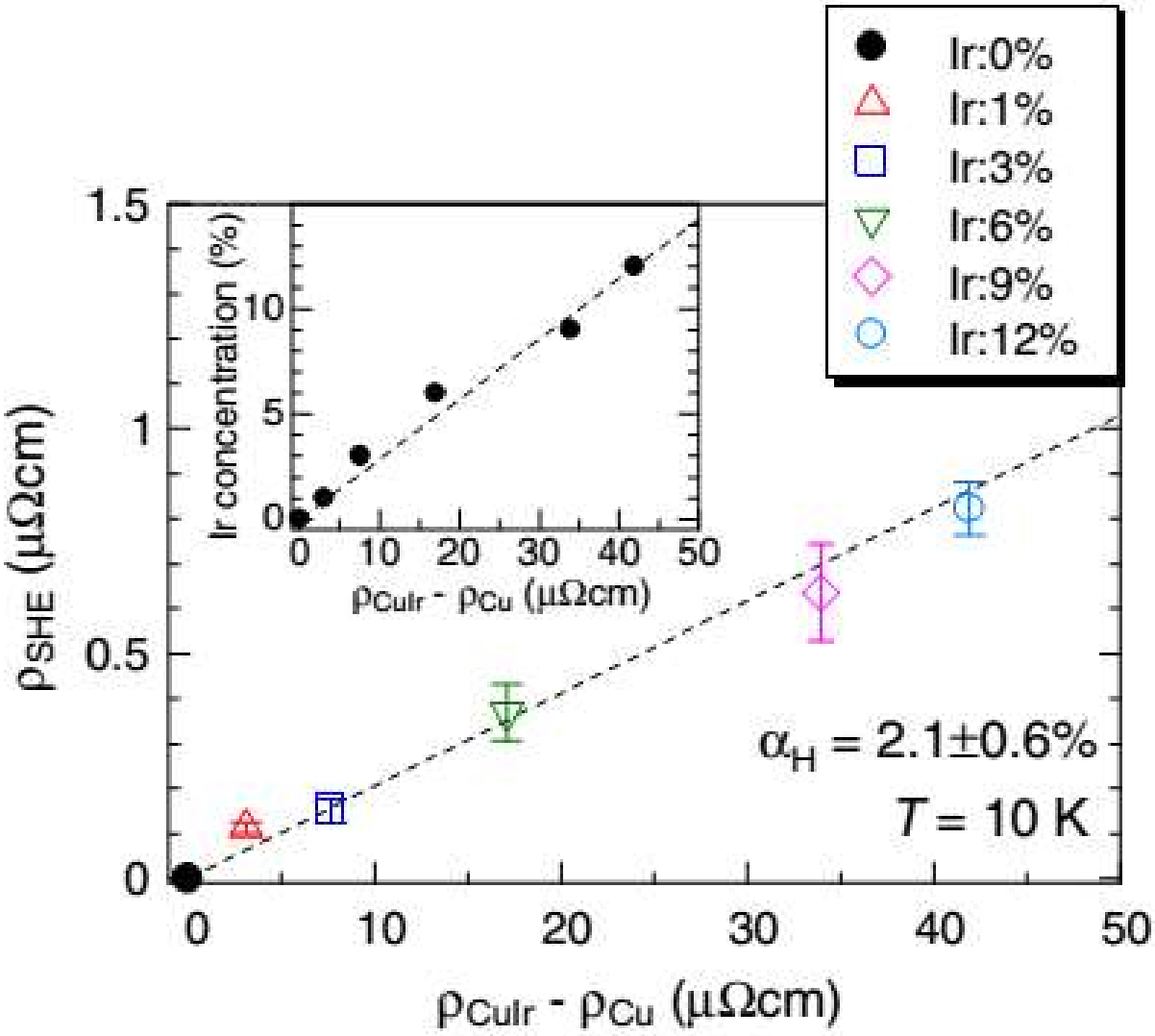
Spin diffusion and absorption



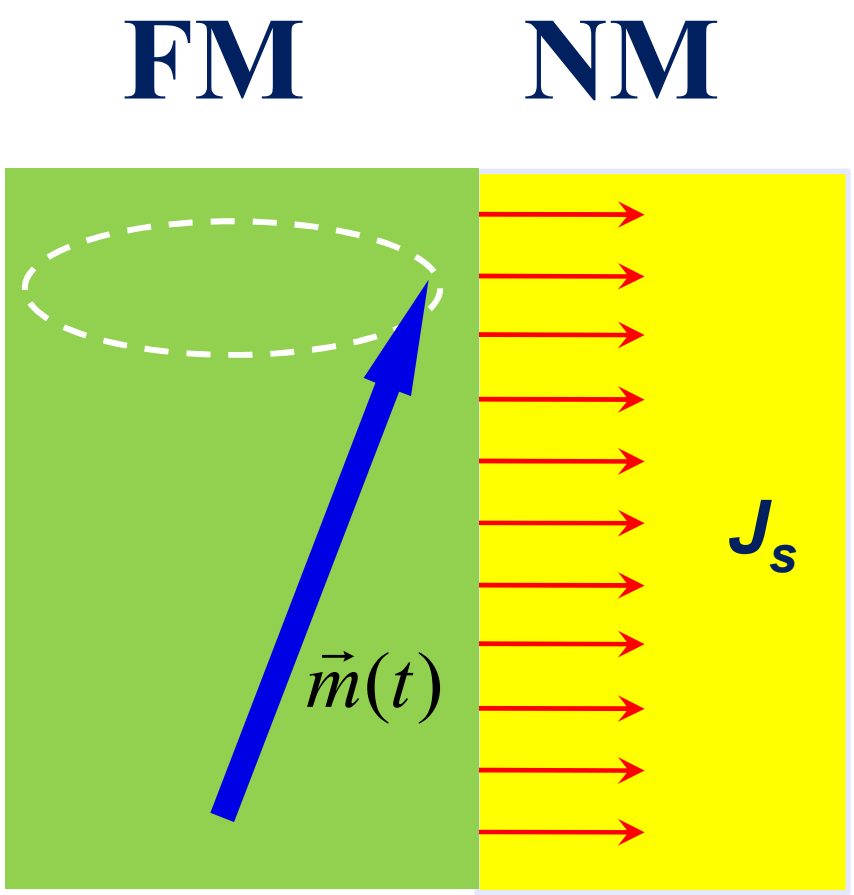
Spin diffusion and absorption



Spin diffusion and absorption



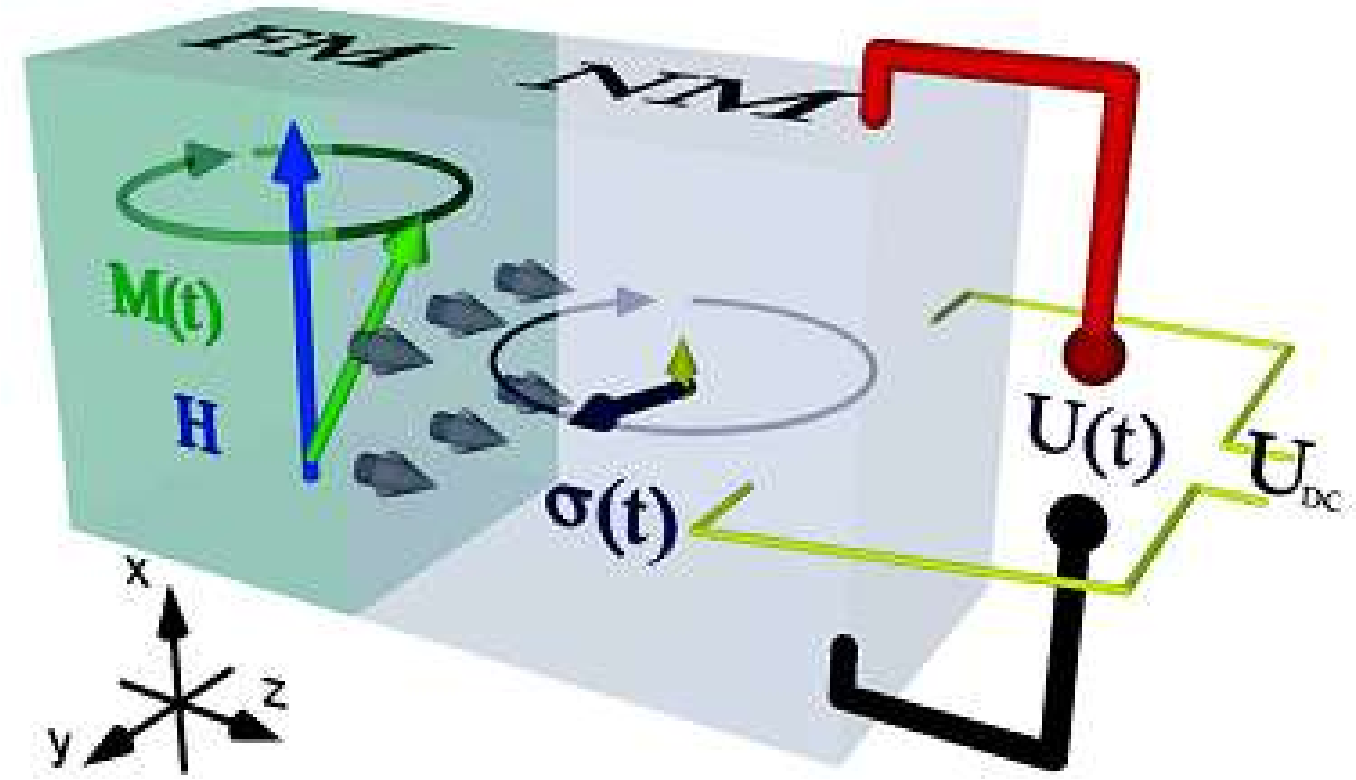
Spin angular momentum



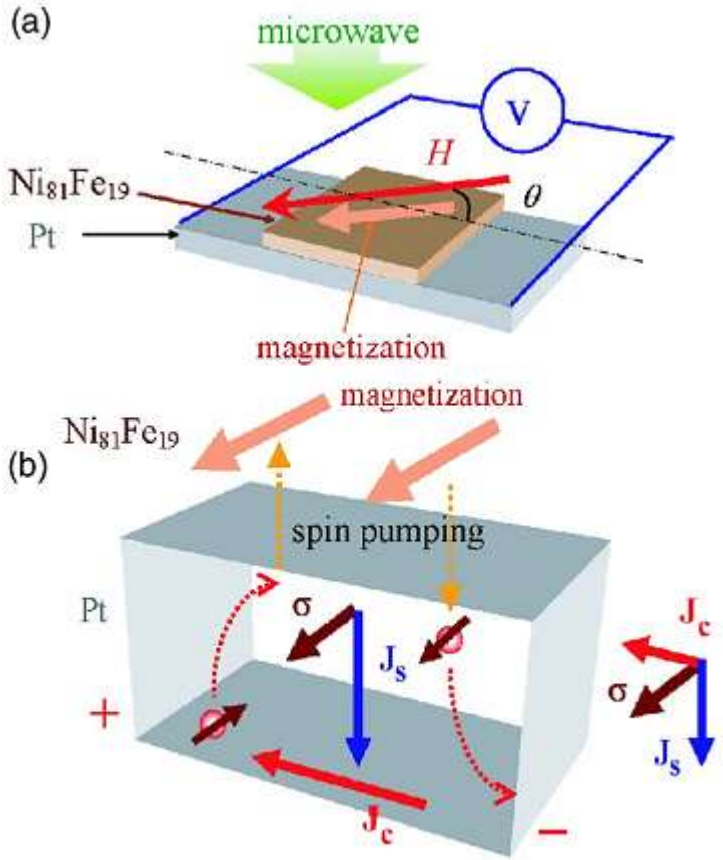
$$\vec{J}_S = \frac{\hbar g_r^{\uparrow\downarrow}}{4\pi M^2}\left(\vec{M} \times \frac{\partial \vec{M}}{\partial t}\right)$$

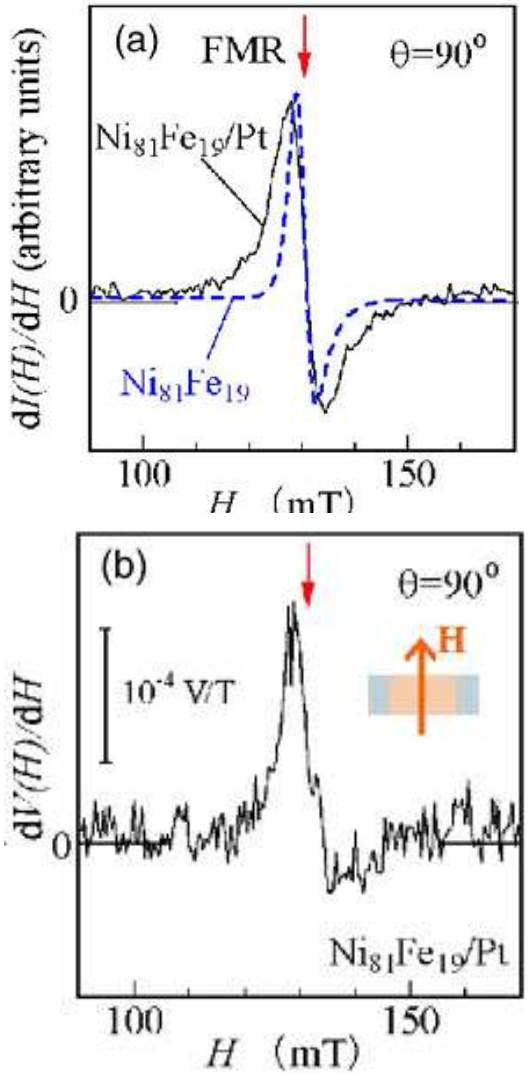
Precessing magnetization in FM layer pump spin current into NM layer (Angular momentum conservatoin)

Spin pumping and ISHE



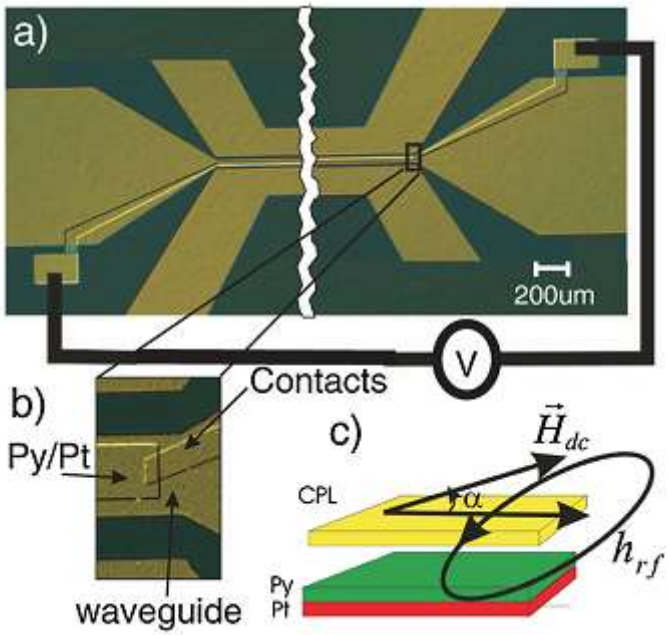
Spin pumping

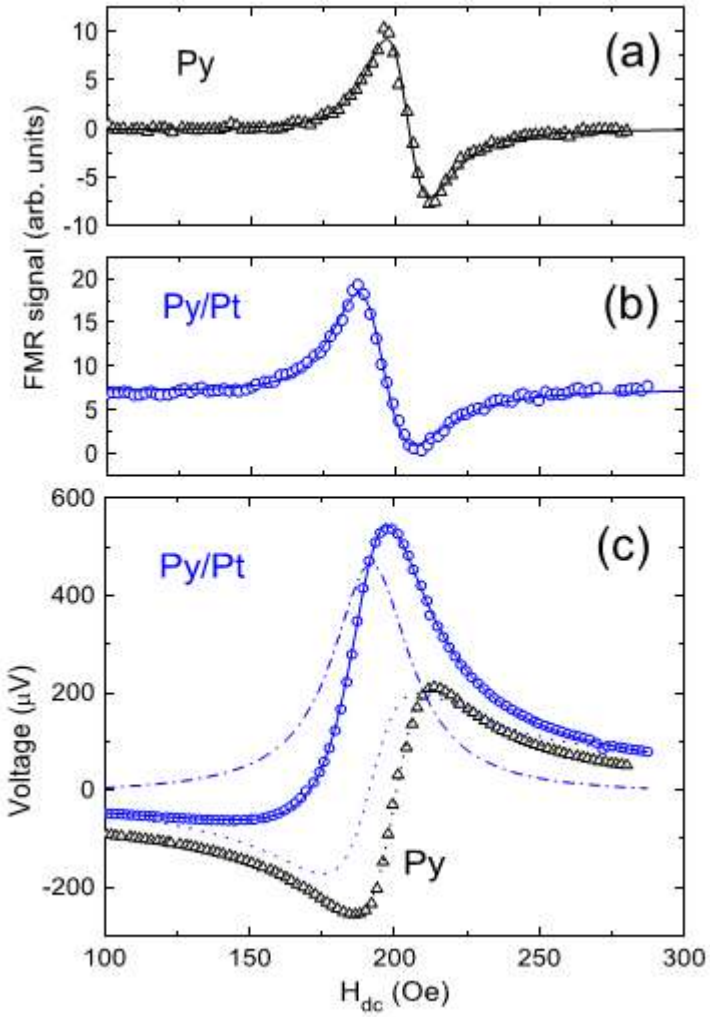




Saitoh, et al, ARL (2006)

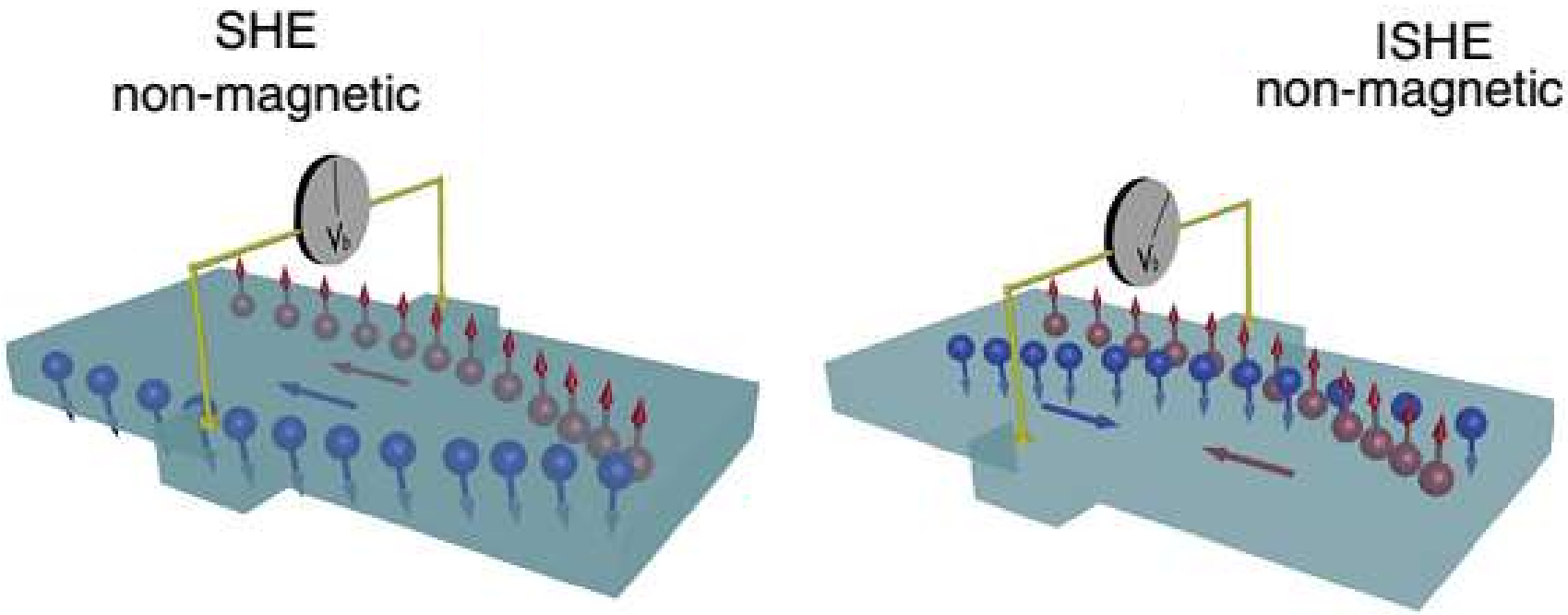
Spin pumping and ISHE



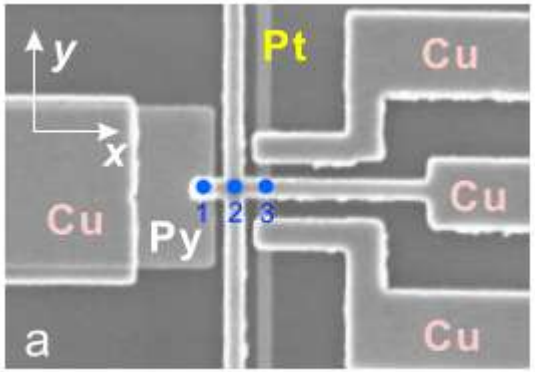


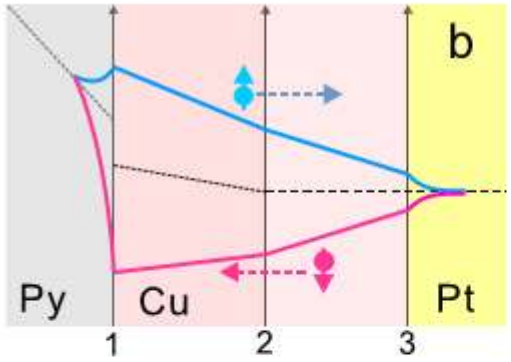
Mosendz, et al, PRL (2010)

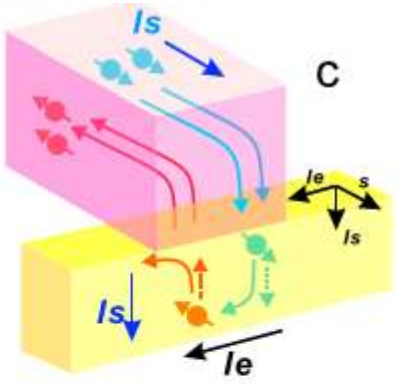
SHE vs ISHE

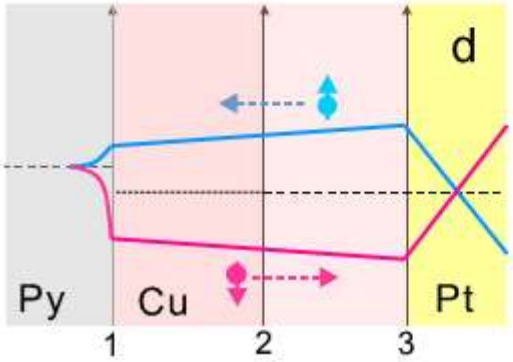


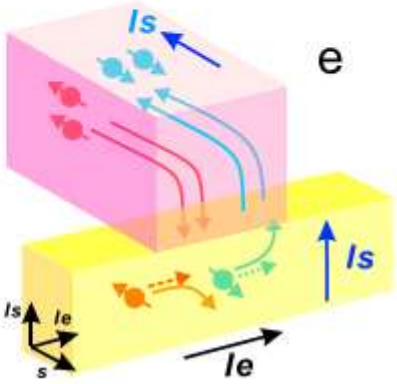
SHE vs. ISHE


y
x
Pt
Cu
Cu
Py
Cu
1 2 3
Cu
a


b
Py
Cu
Pt
1
2
3

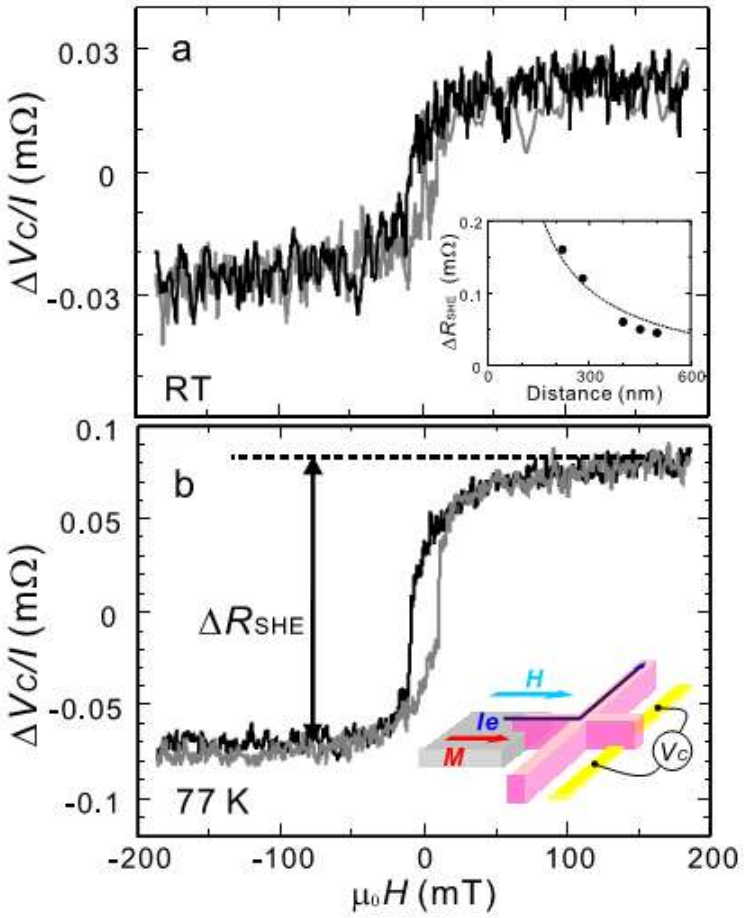

Is
c
Ie
s
Is
Is
Ie


d
Py
Cu
Pt
1
2
3

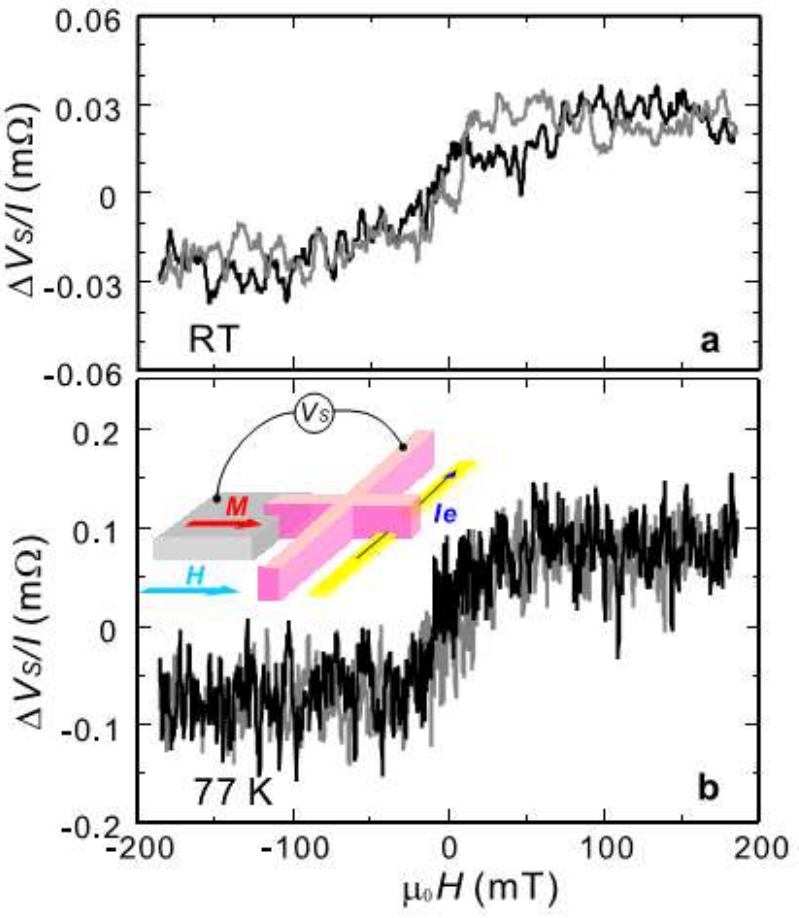

Is
e
Is
Is
Ie
s
Ie

SHE vs. ISHE

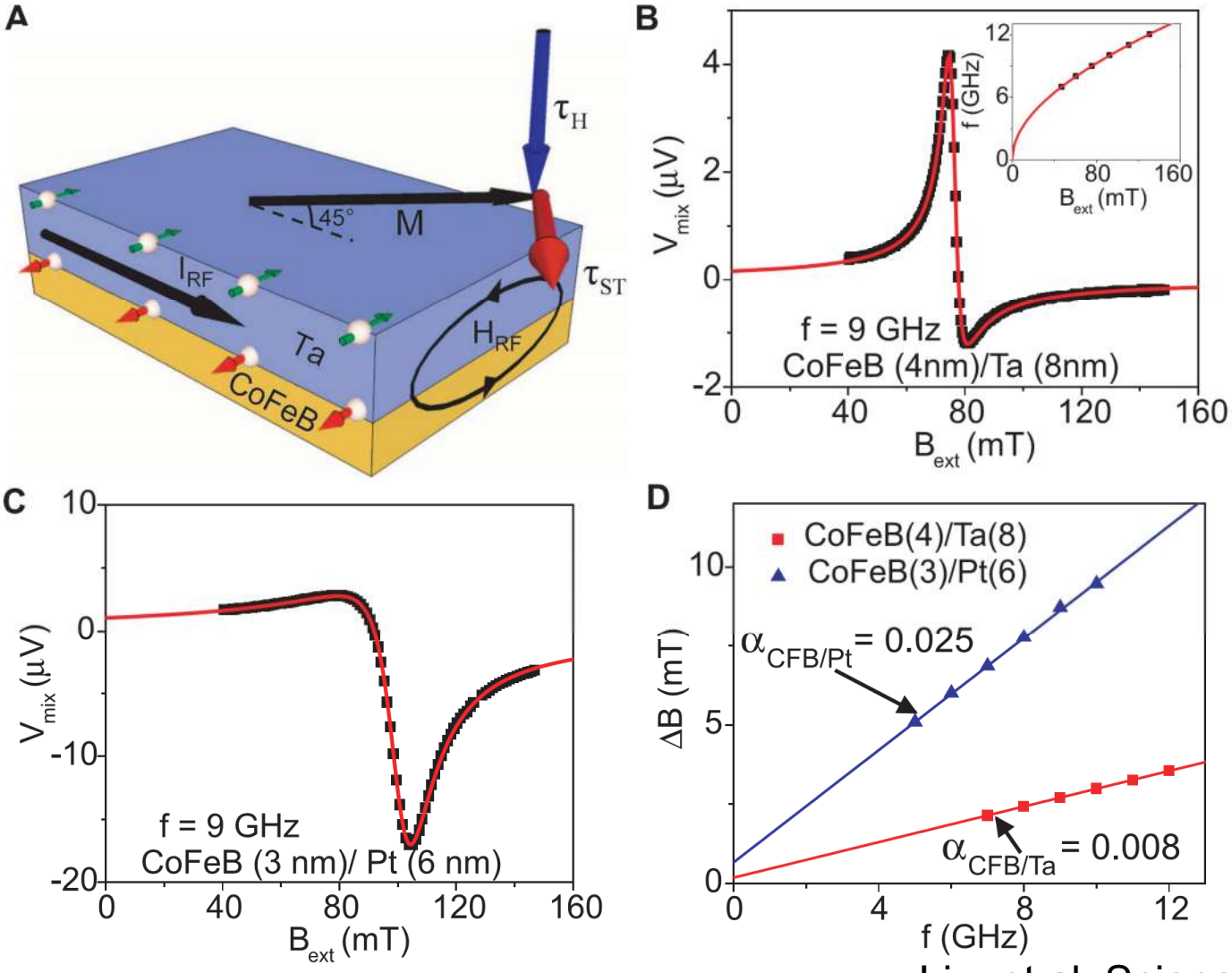
ISHE



SHE

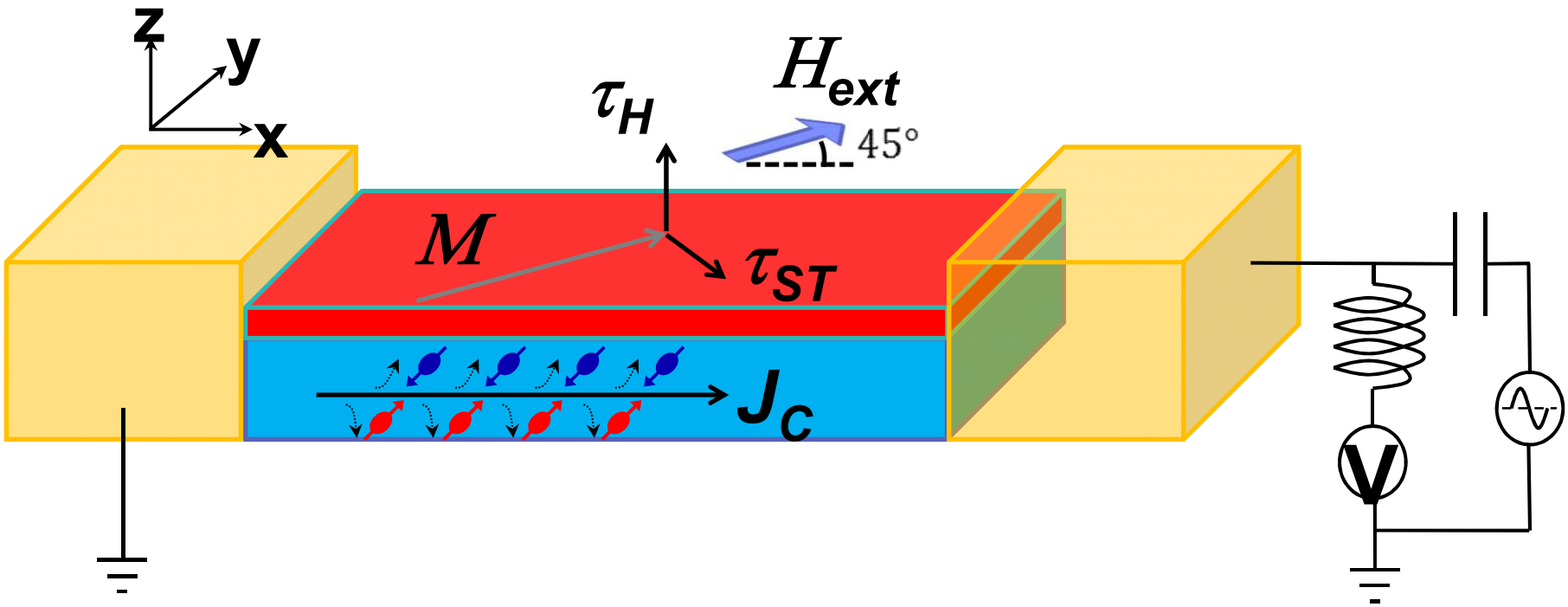


Spin Hall torque



Liu, et al, Science (2012)

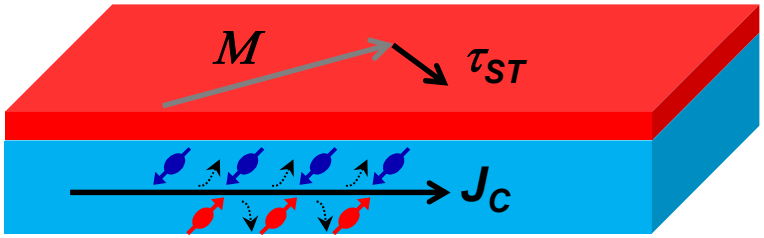
Spin Hall torque



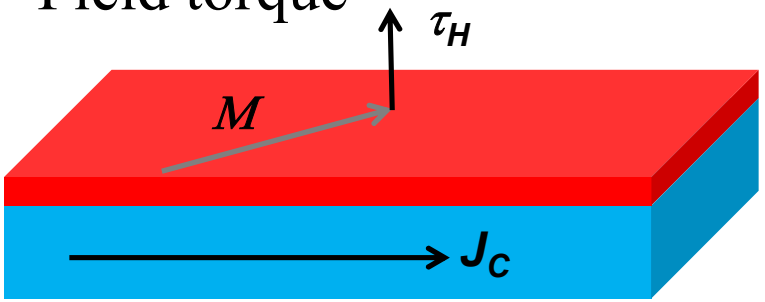
Liu, et al, PRL (2011)

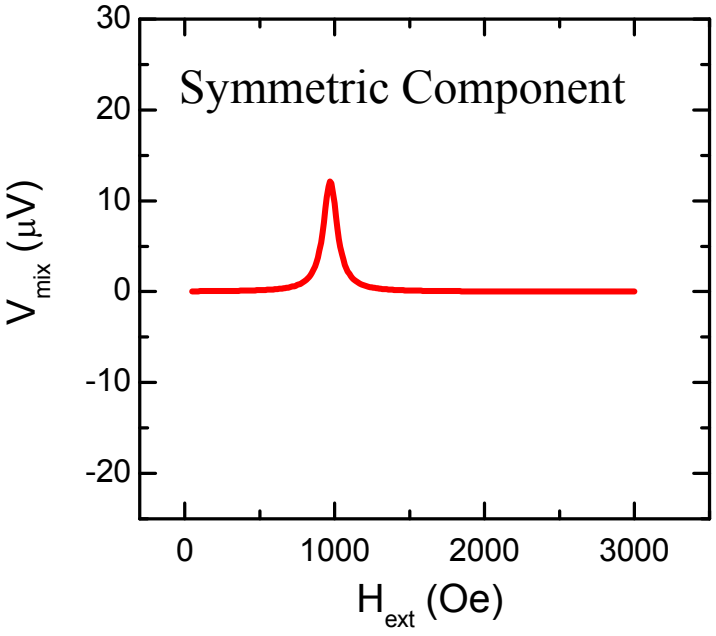
Spin Hall torque

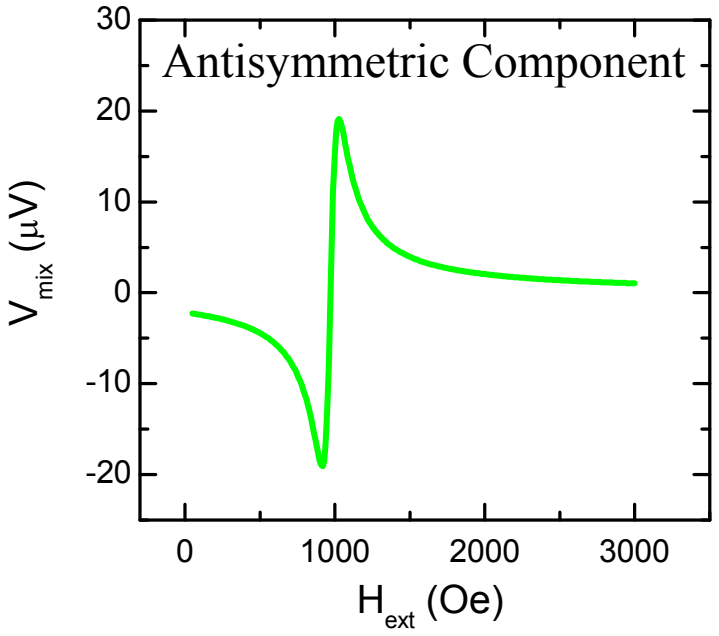
Spin Hall torque



Field torque

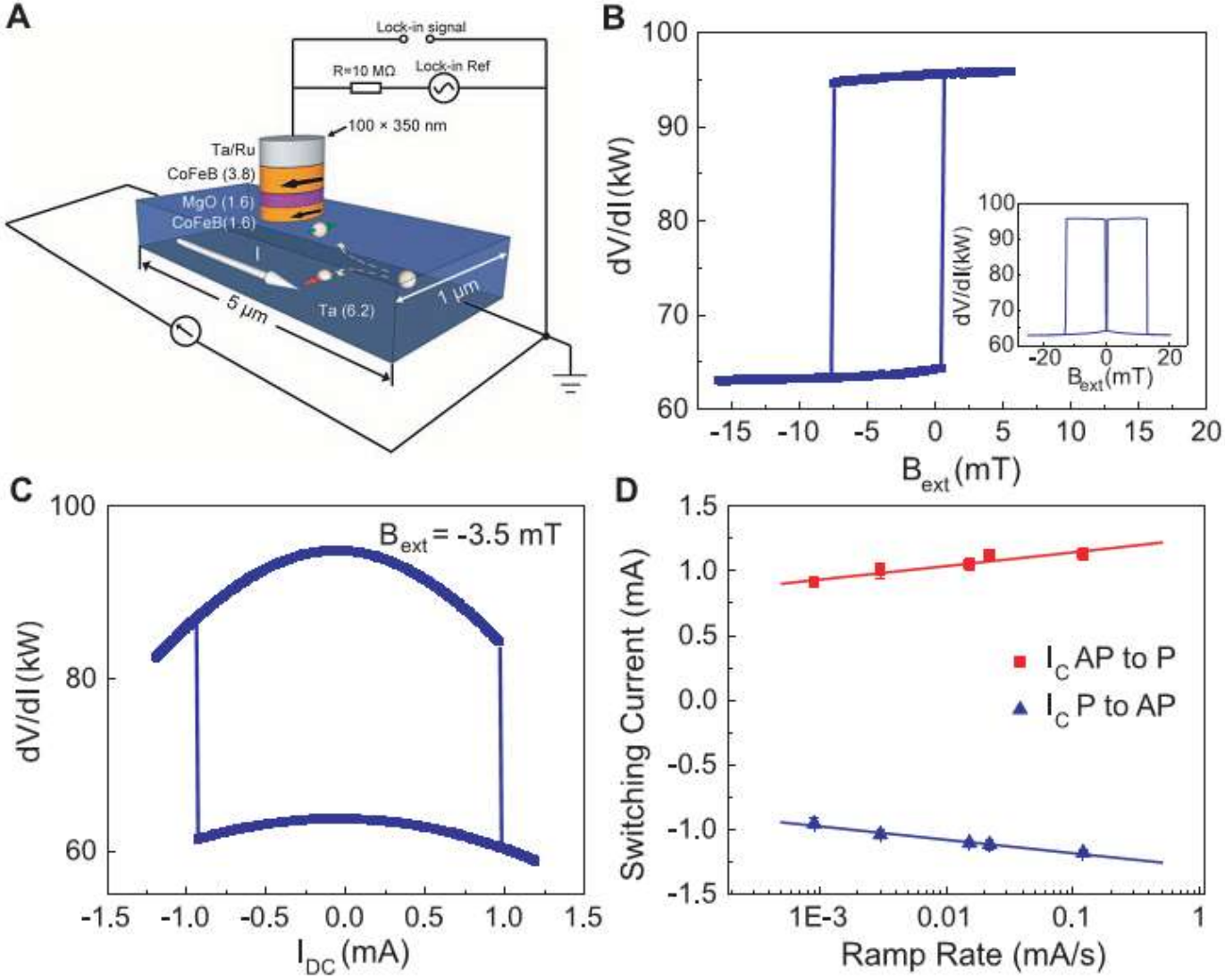




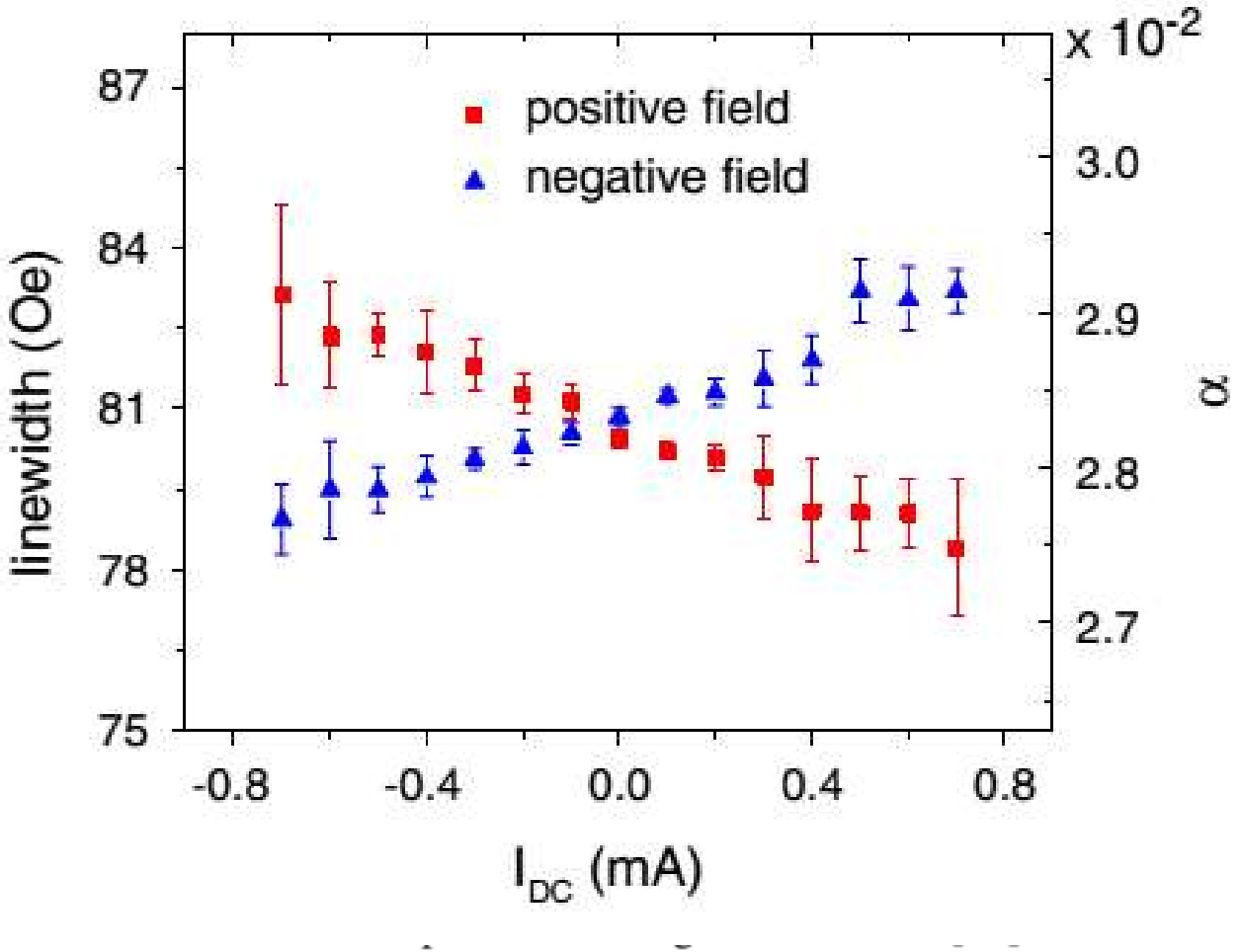


$$SHA = \frac{S}{A}\frac{e\mu_0 M_s t d}{\hbar}[1 + (4\pi M_{eff}/H_{ext})]^{1/2}$$

Spin Hall torque



Spin Hall torque



$$\Delta = \frac{2\pi f}{\gamma}\left(\alpha + \frac{\sin\theta}{(H_{\text{ext}} + 2\pi M_{\text{eff}})\mu_0 M_S t}\frac{\hbar J_S}{2e}\right).$$

1) Large spin Hall in AFM

PRL 112, 017205 (2014) PHYSICAL REVIEW LETTERS week ending 10 JANUARY 2014

Anomalous Hall Effect Arising from Noncollinear Antiferromagnetism

Hua Chen, Qian Niu, and A. H. MacDonald
Department of Physics, University of Texas at Austin, Austin, Texas 78712, USA
(Received 3 October 2013; published 10 January 2014)

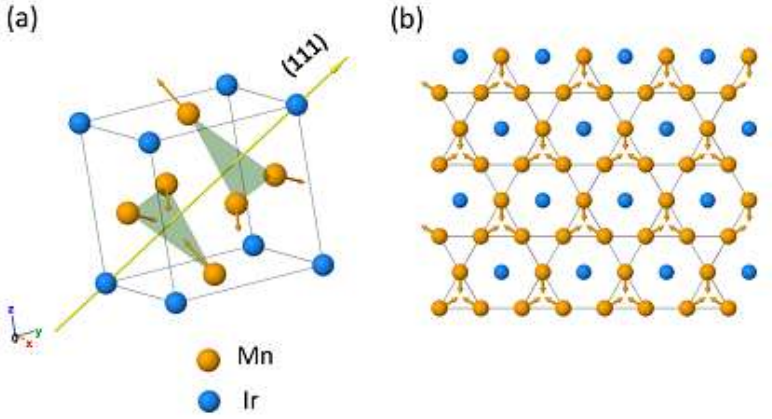


FIG. 1 (color online). Structure of Mn_3Ir. (a) Unit cell of Mn_3Ir with triangular antiferromagnetic order. (b) An individual (111) plane of Mn_3Ir. The Mn atoms form a kagome lattice.

- **Large spin orbit coupling of Ir transfer to Mn.**
- **Non-collinear antiferromagnetism**

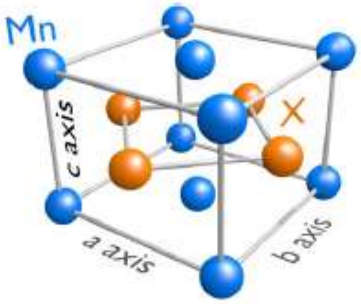
1) Large spin Hall in AFM

PRL 113, 196602 (2014) PHYSICAL REVIEW LETTERS week ending 7 NOVEMBER 2014

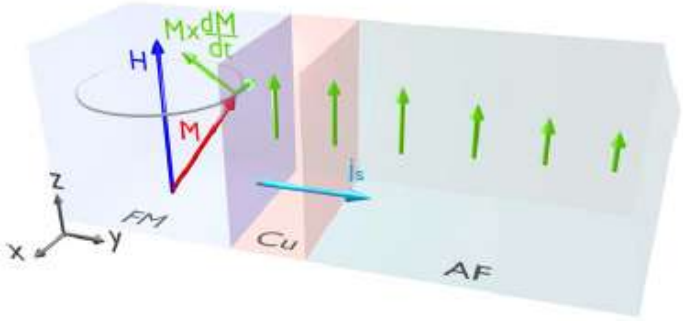
Spin Hall Effects in Metallic Antiferromagnets

Wei Zhang, Matthias B. Jungfleisch, Wanjun Jiang, John E. Pearson, and Axel Hoffmann
Materials Science Division, Argonne National Laboratory, Argonne, Illinois 60439, USA

Frank Freimuth and Yuriy Mokrousov
Peter Grünberg Institut and Institute for Advanced Simulation, Forschungszentrum Jülich and JARA, D-52425 Jülich, Germany
(Received 12 August 2014; published 4 November 2014)



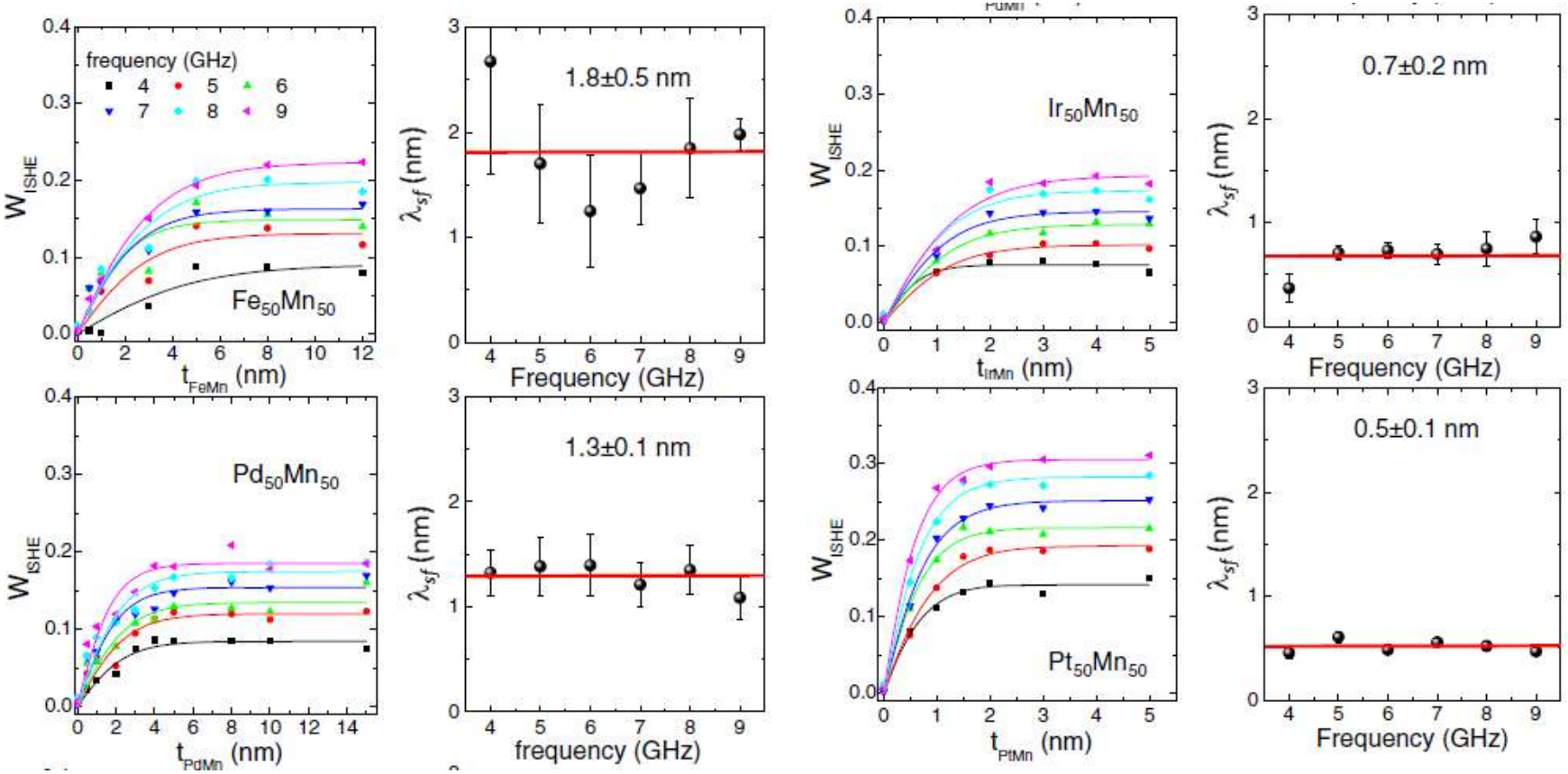
Crystal structure of CuAu- Ⅰ -type Afs



Schematic of spin pumping and spin Hall effect

Zhang, et al, PRL (2014)

1) Large spin Hall in AFM



Thickness dependence shows spin diffusion length to be short ~1nm

$Fe_{50}Mn_{50}$
$Pd_{50}Mn_{50}$

$Ir_{50}Mn_{50}$
$Pt_{50}Mn_{50}$

1) Large spin Hall in AFM

Spin Hall angle

0.008 ± 0.002 for FeMn

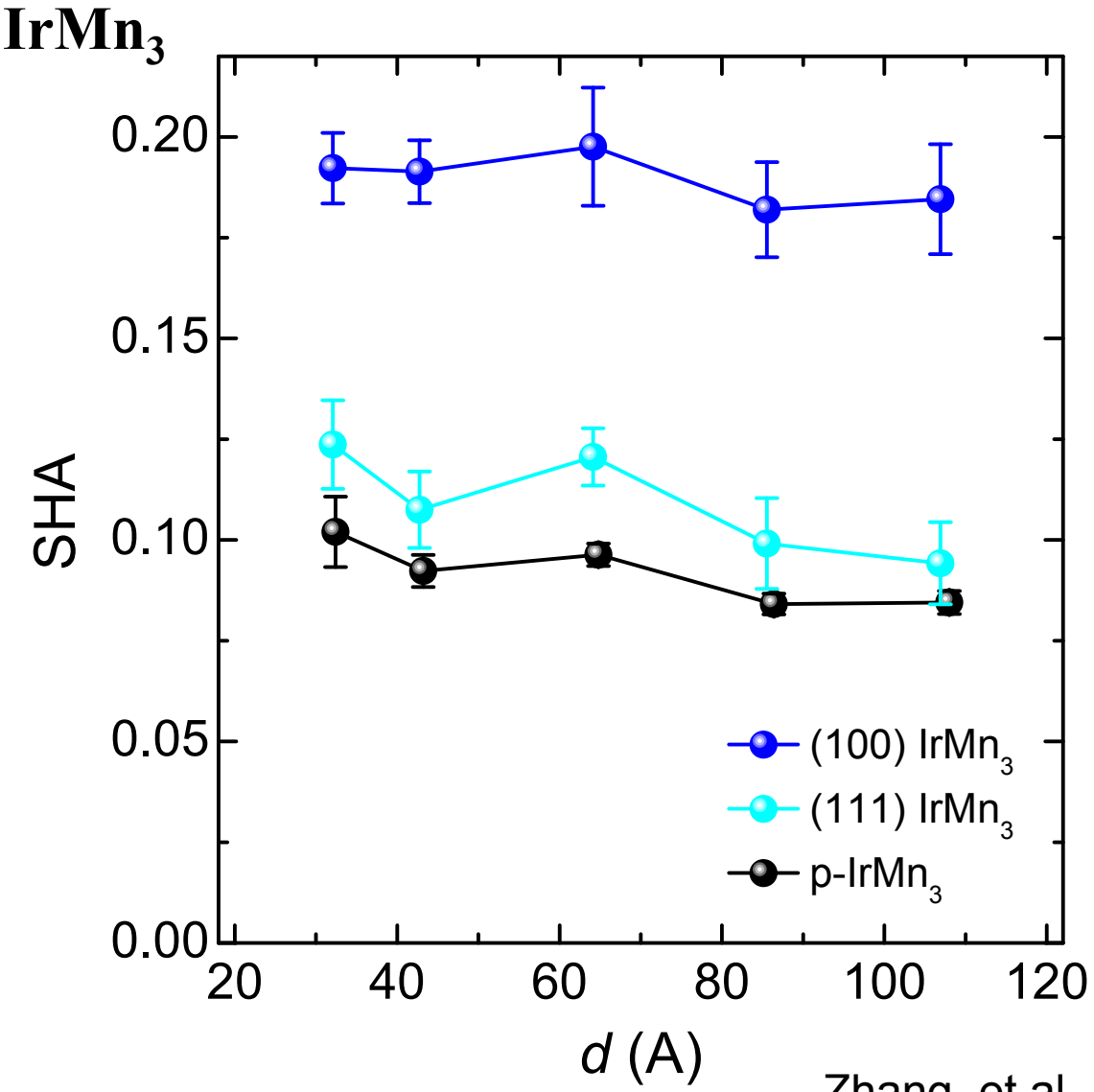
0.015 ± 0.005 for PdMn

0.022 ± 0.005 for IrMn

0.060 ± 0.010 for PtMn Large value, comparable to Pt

		σ^x_{yz}	σ^x_{zy}	σ^y_{zx}	σ^y_{xz}	σ^z_{xy}	σ^z_{yx}	$\bar{\sigma}$	σ_{av}	σ_{exp}
PtMn	*c* axis	303.9	–219.9	219.9	–303.9	60.3	–60.3	194.7	125.2	182.9
	a axis	30.4	–10.5	52.3	–260.9	92.5	–96.5	90.5		
IrMn	*c* axis	372.8	–59.7	59.7	–372.8	40.9	–40.9	157.8	41.6	40.8
	a axis	–21.3	–94.6	126.3	–351.6	–325.1	325.1	–16.5		
PdMn	*c* axis	69.5	–17.0	17.0	–69.5	17.8	–17.8	34.8	3.9	33.6
	a axis	0.0	3.5	7.4	–66.8	–70.8	69.8	–11.6		
FeMn	*c* axis	51.9	48.4	–47.6	50.9	–100.3	96.5	–48.6	–59.0	23.9
	a axis	–82.6	85.9	–47.8	47.5	–121.6	0.0	–64.2		

1) Large spin Hall in AFM

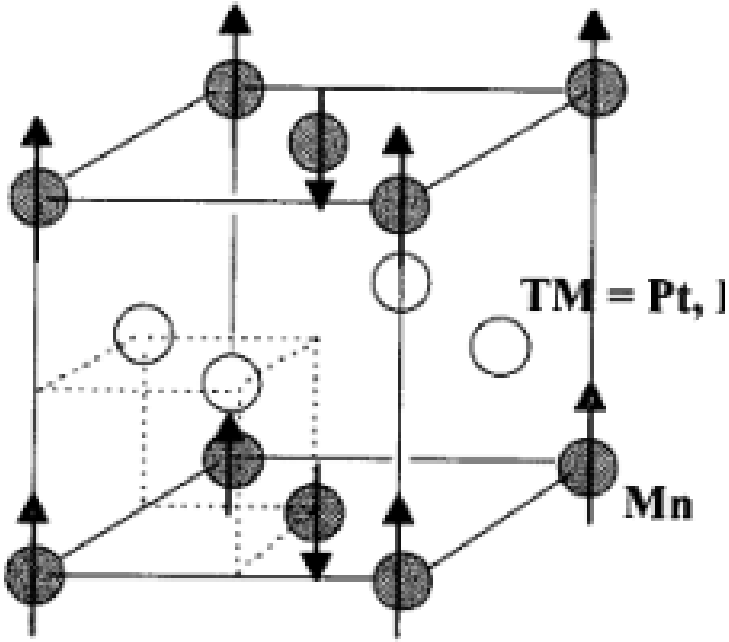


- **The effective SHA is the largest for (100) $IrMn_3$**
- **(111) and polycrystalline IrMn3 show similar SHA.**

Zhang, et al, Science Advances (2012)

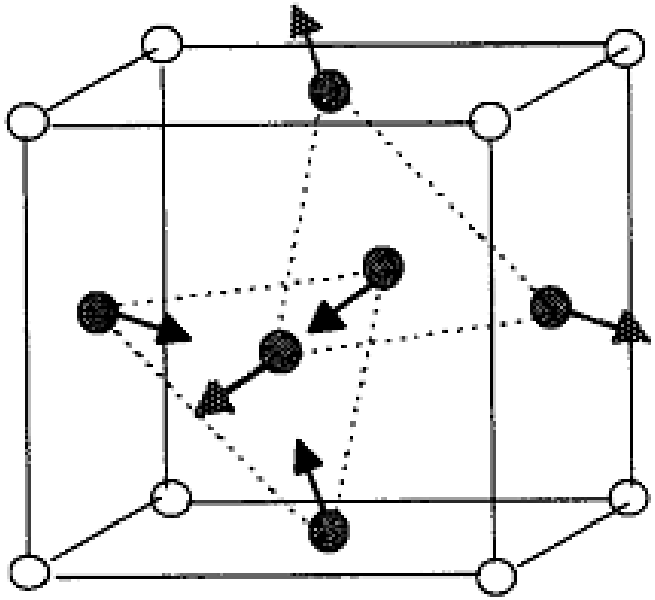
1) Large spin Hall in AFM

IrMn



- **Collinear AFM**

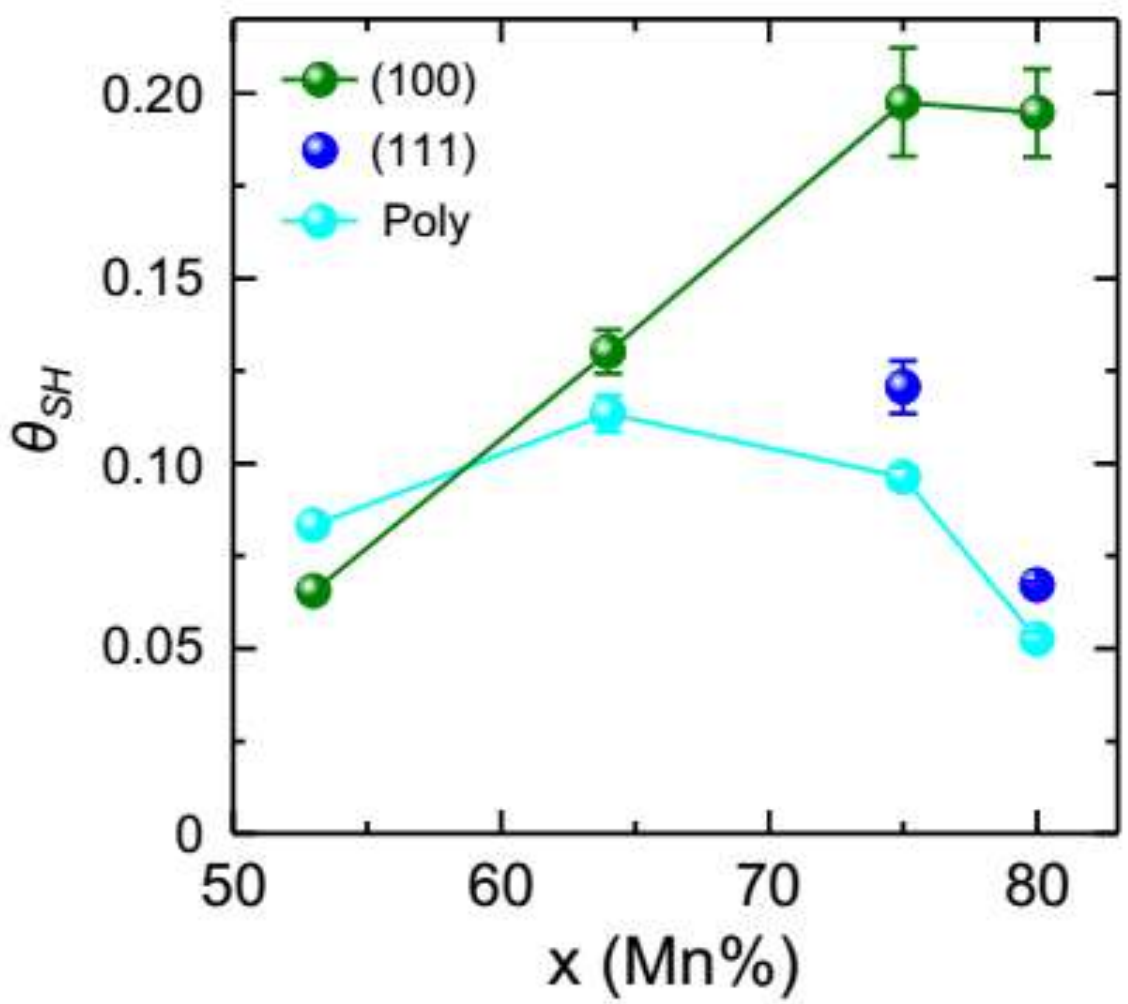
$IrMn_3$



- **Non-Collinear AFM**

Non-collinear AFM spin structure

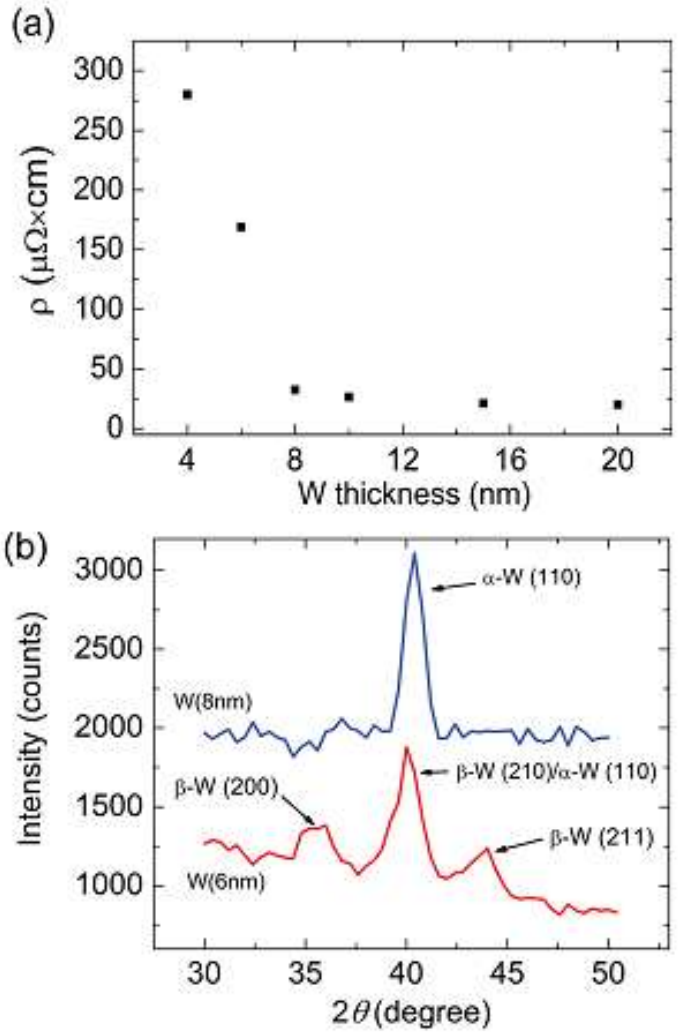
1) Large spin Hall in AFM

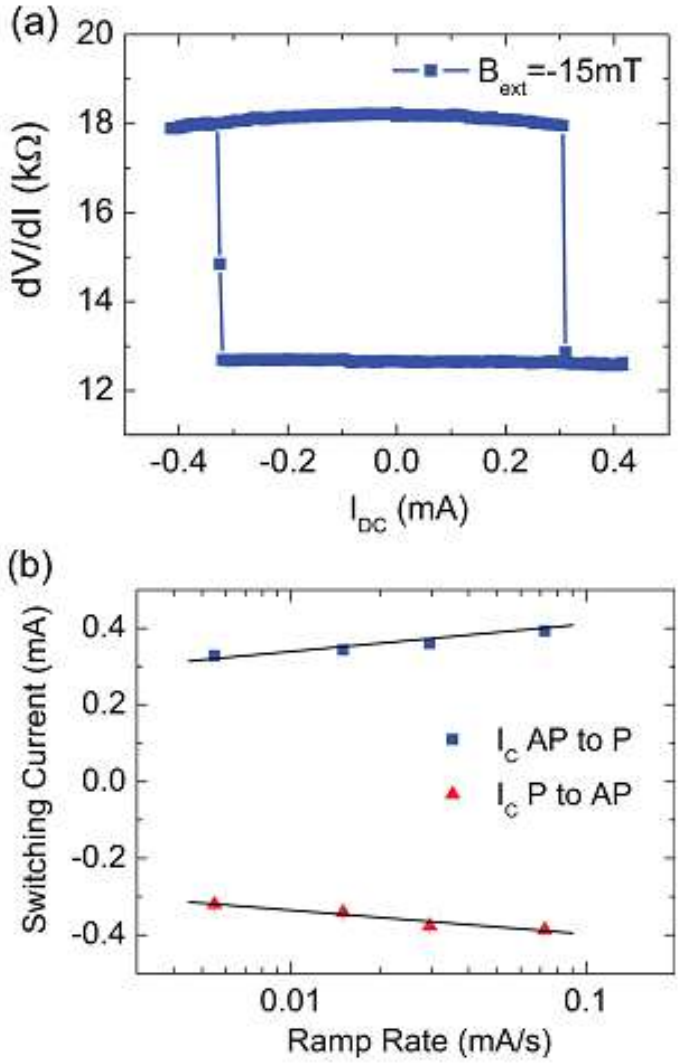


- **Little facet dependence in collinear AFM**

- **Strong Facet dependence in non-collinear AFM**

2) Large spin Hall in Beta-W, Ta



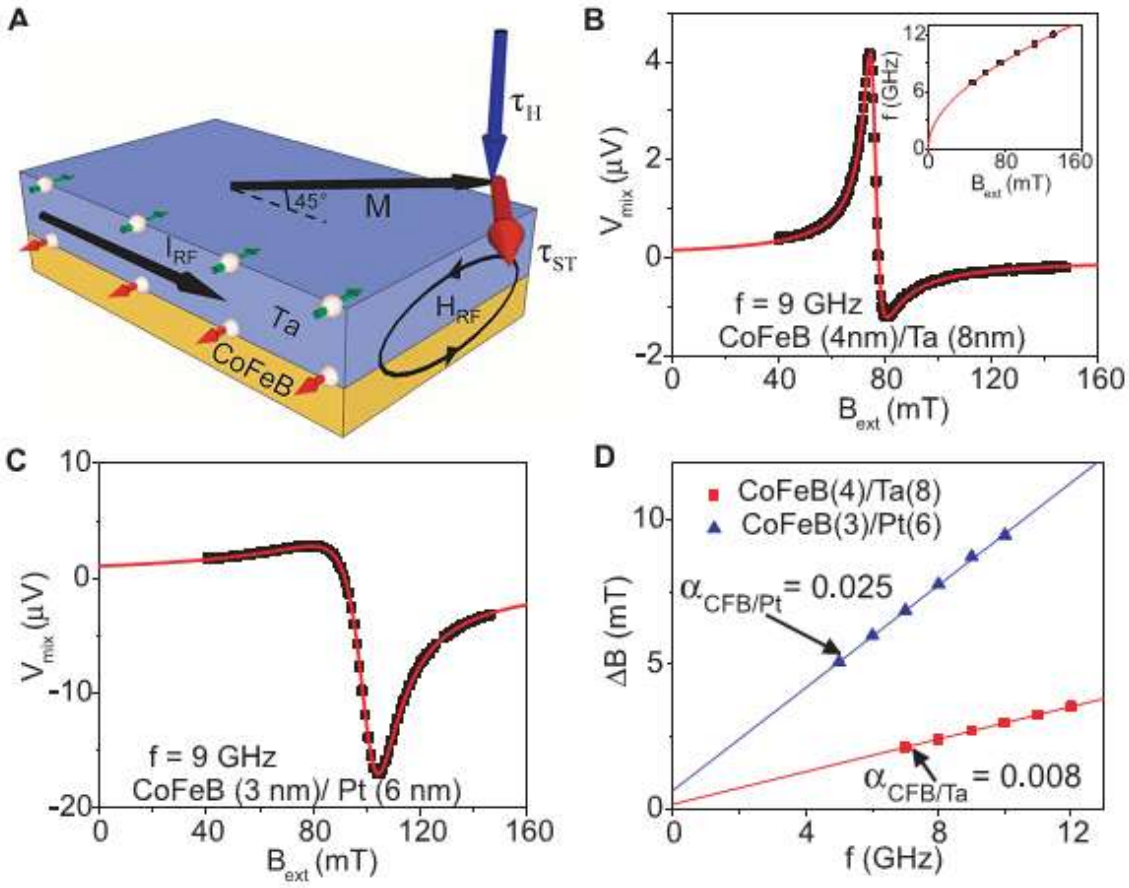


Spin Hall angle: 0.38 +- 0.06

Pai, et al, ARL (2012)

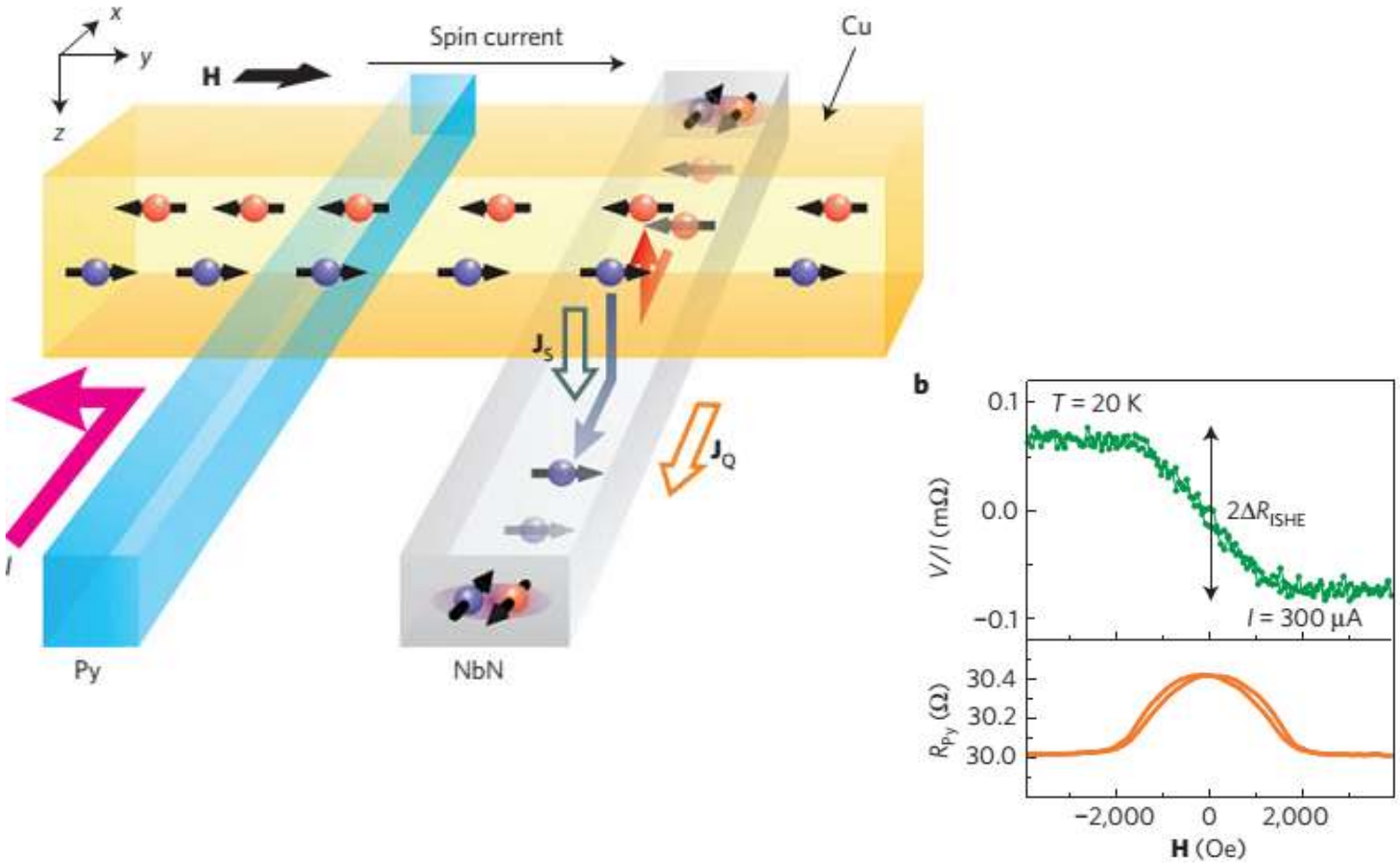
2) Large spin Hall in Beta-W, Ta

Beta-Ta



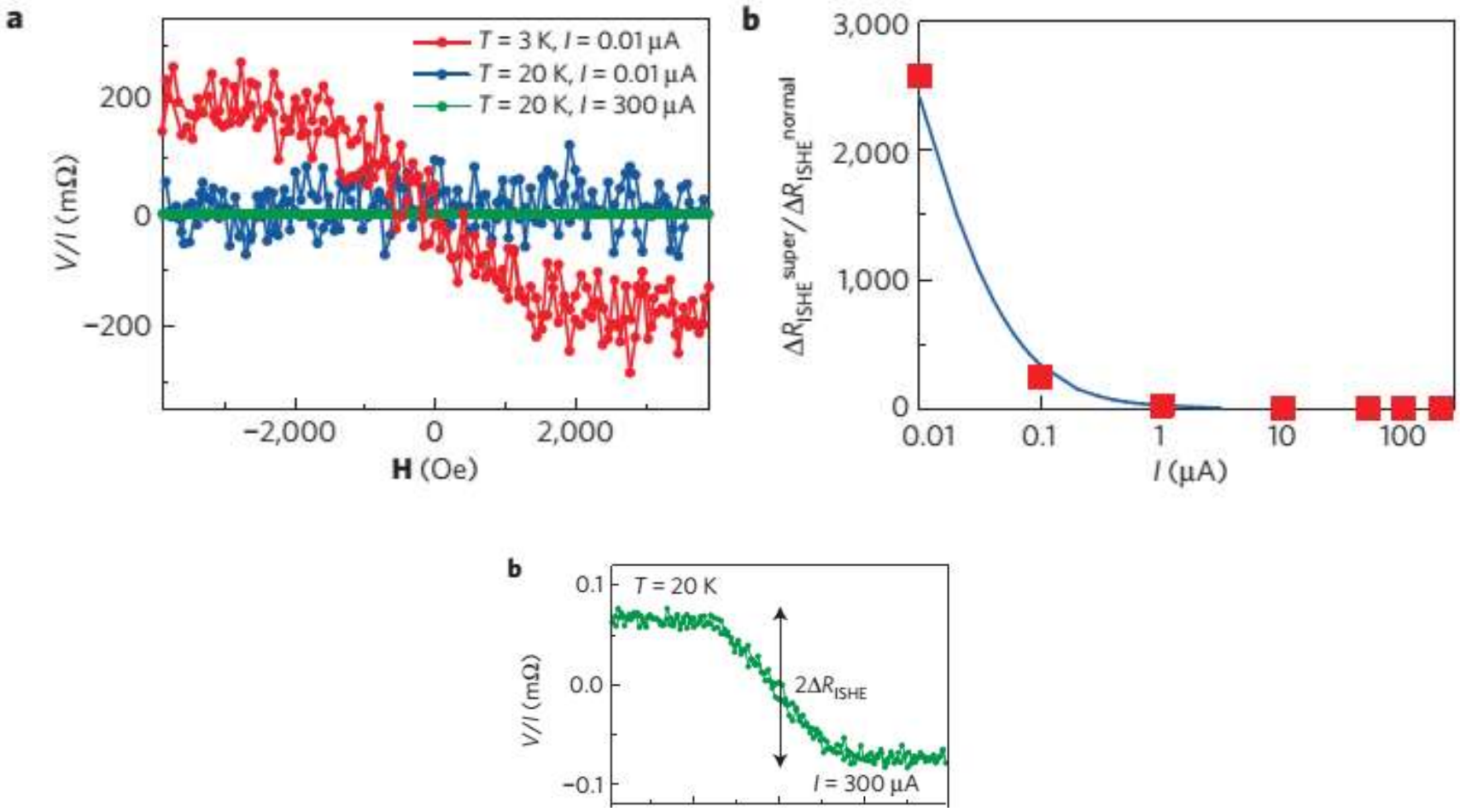
Liu, et al, Science (2012)

3) Large spin Hall in S.C.

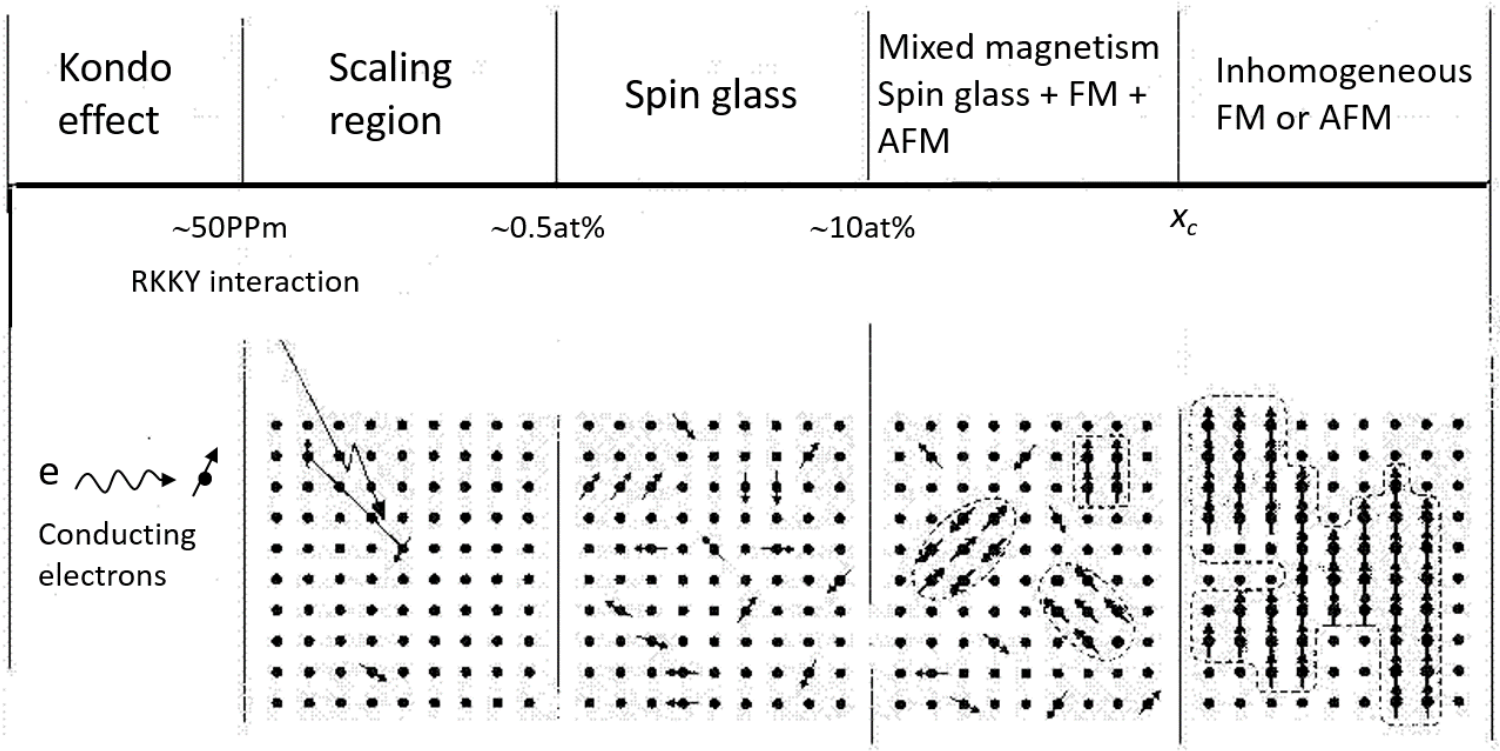


Wakamura, et al, Nature Materials (2015)

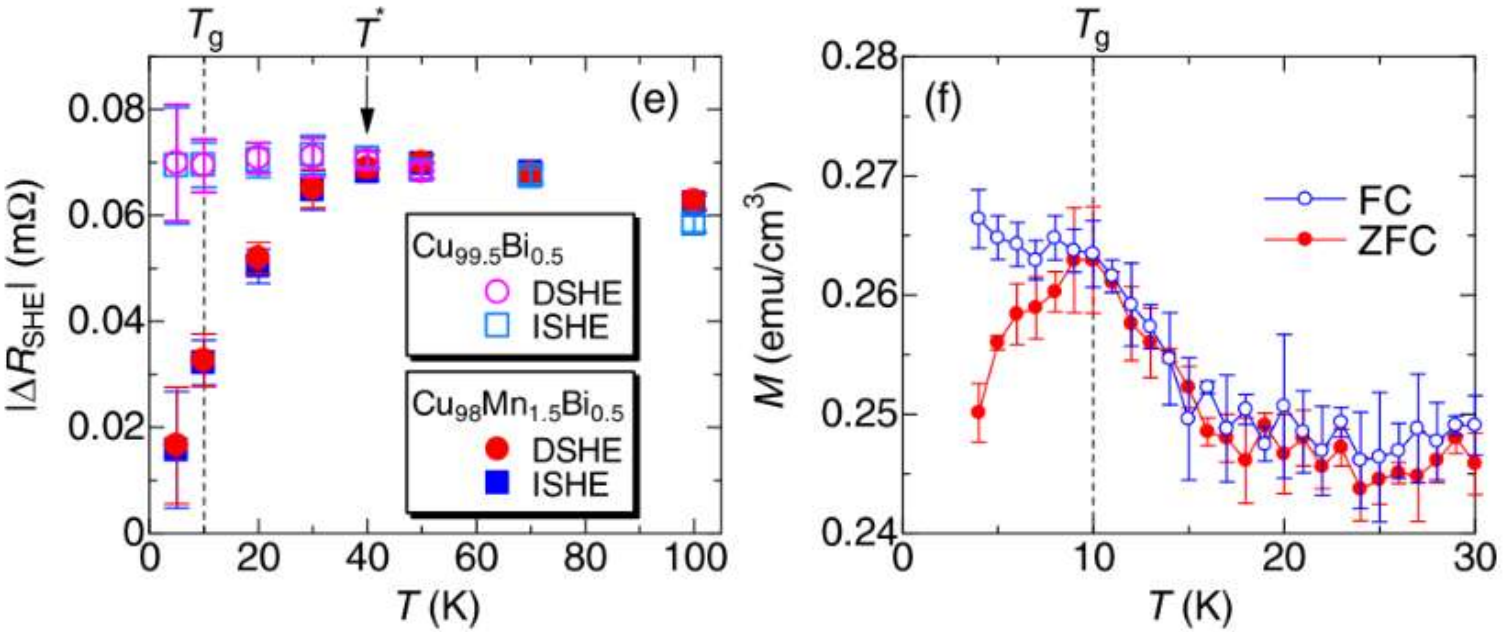
3) Large spin Hall in S.C.



4) Suppression of SHE in spin Glass



4) Suppression of SHE in spin Glass



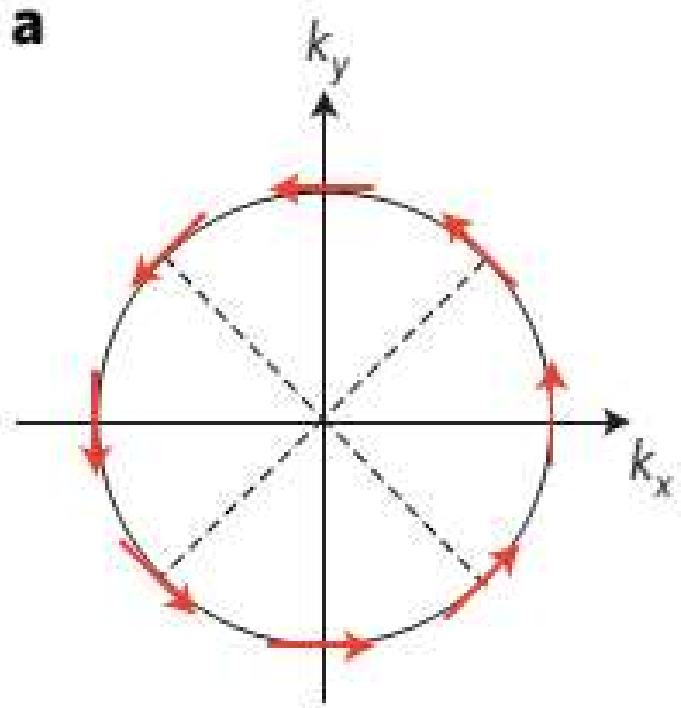
Niimi, et al, PRL (2015)

休息10分钟

Outline

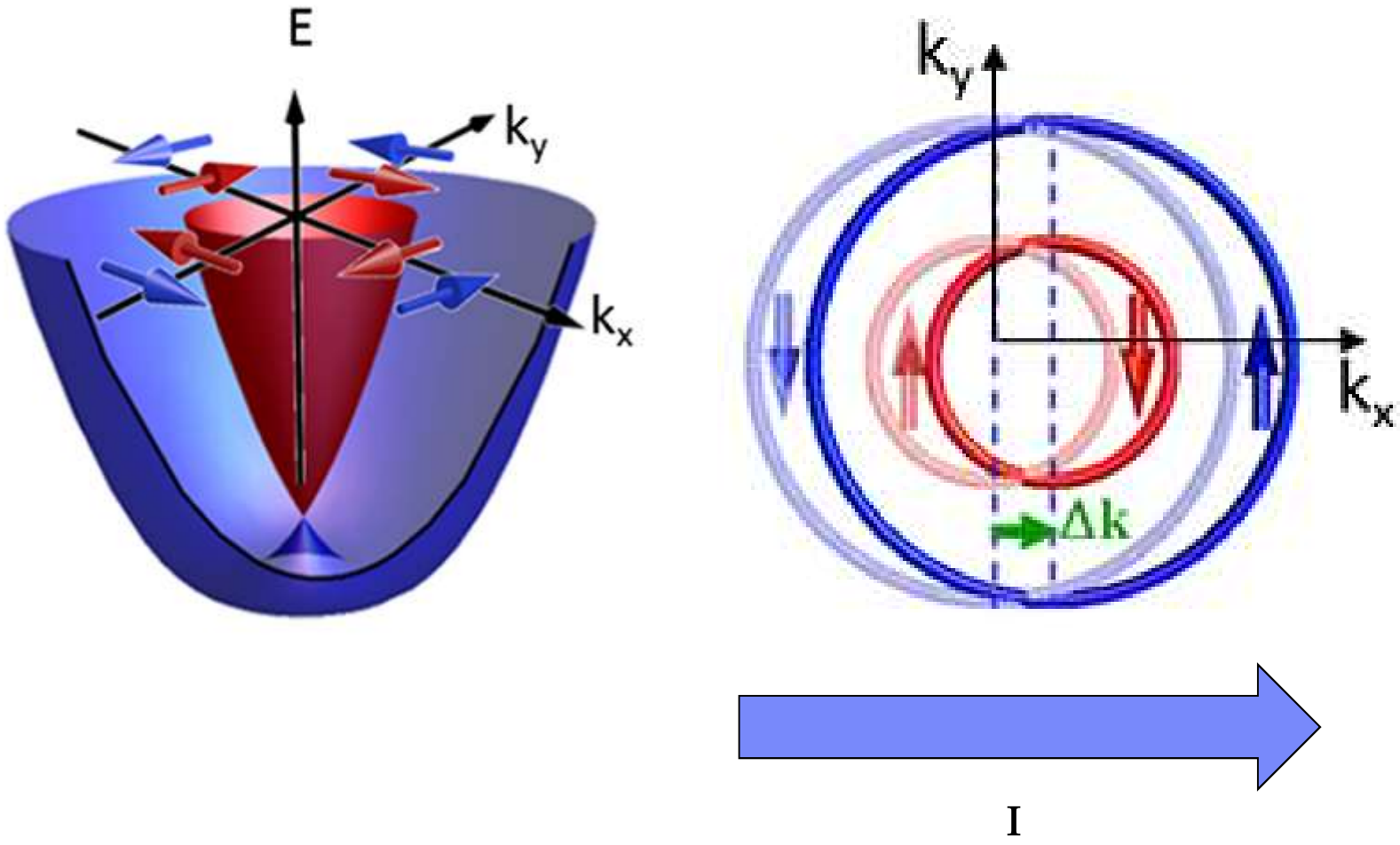
3. Rashba-Edelstein effect

Rashba effect



$$\hat{H}_R = (\alpha_R/\hbar)\,(\mathbf{z} \times \mathbf{p}) \cdot \boldsymbol{\sigma}$$

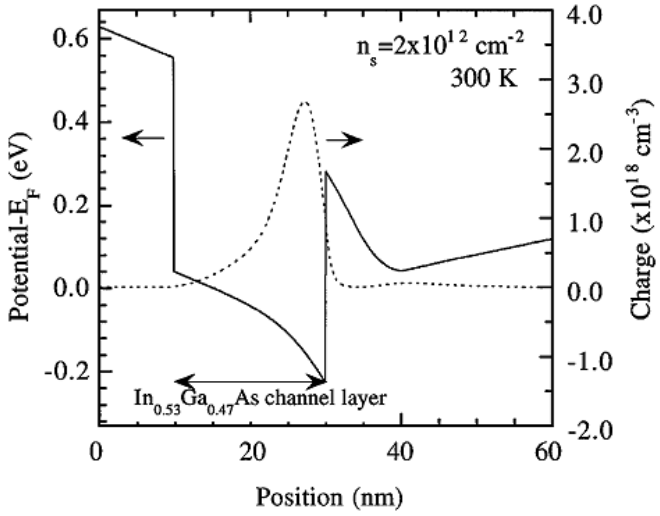
Edelstein effect

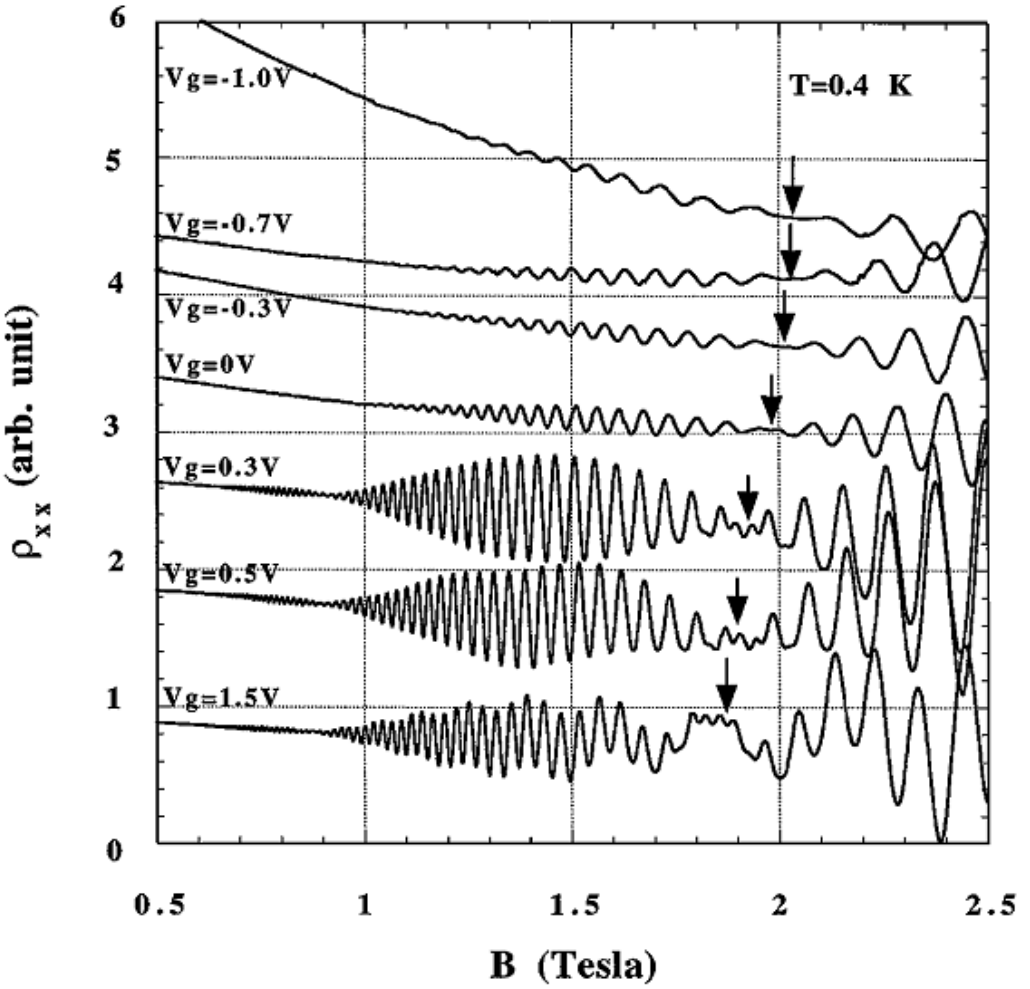


V. M. Edelstein, Solid State Commun. 73, 233 (1990)

Experimental of Rashba effect

InGaAs

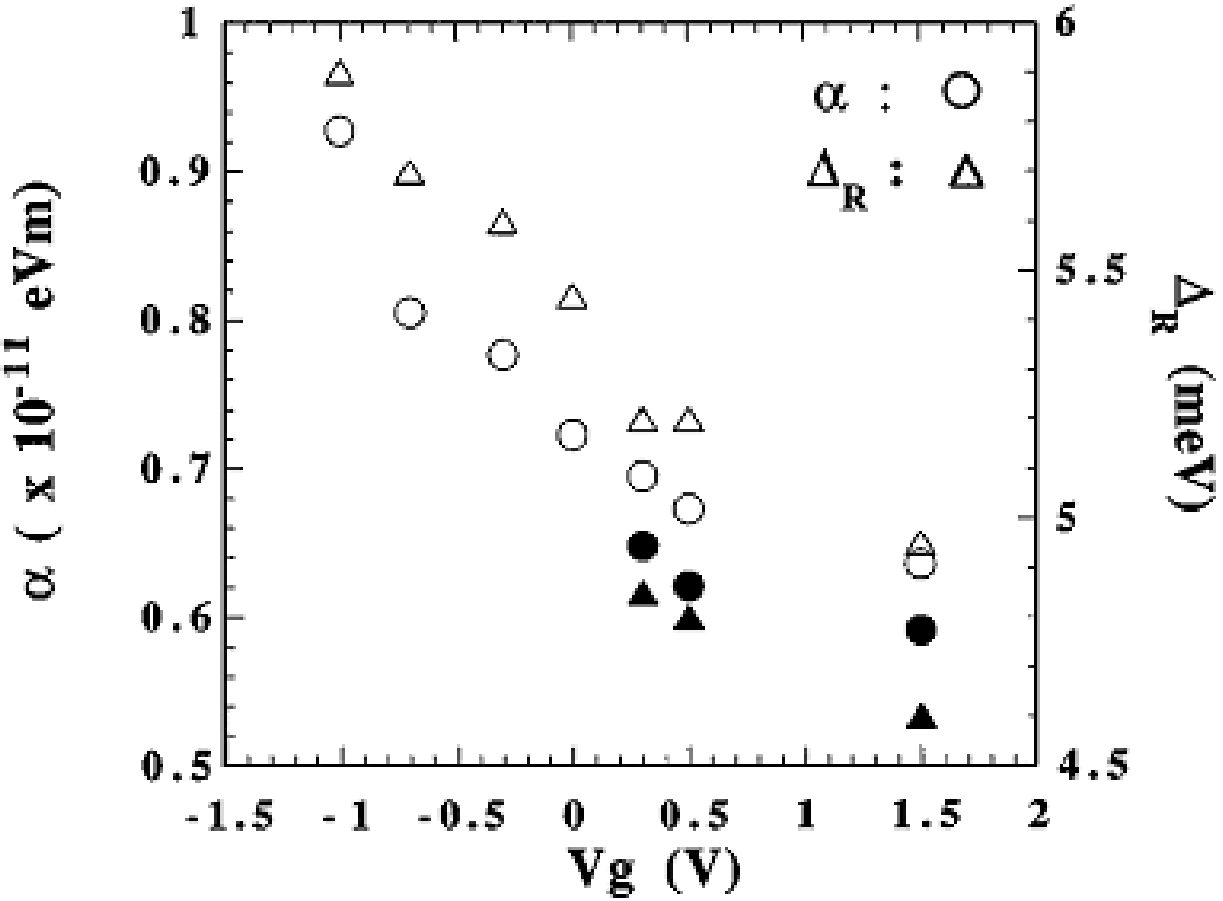




Nitta, et al, PRL (1997)

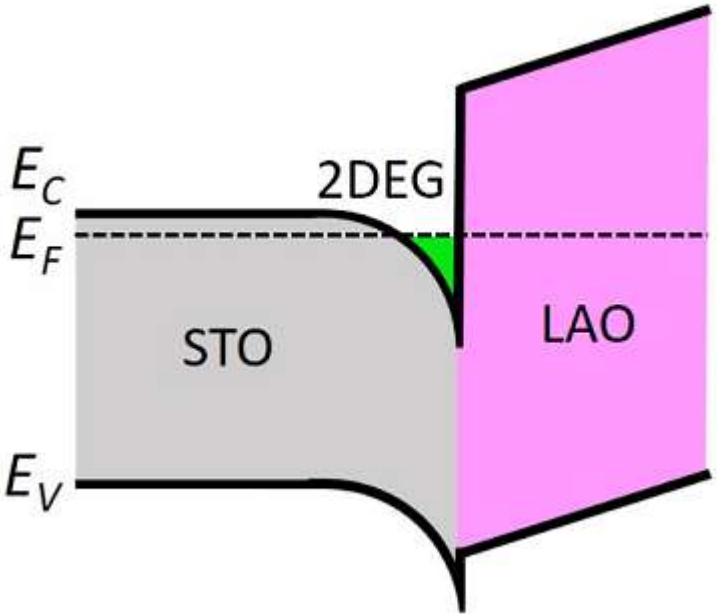
Experimental of Rashba effect

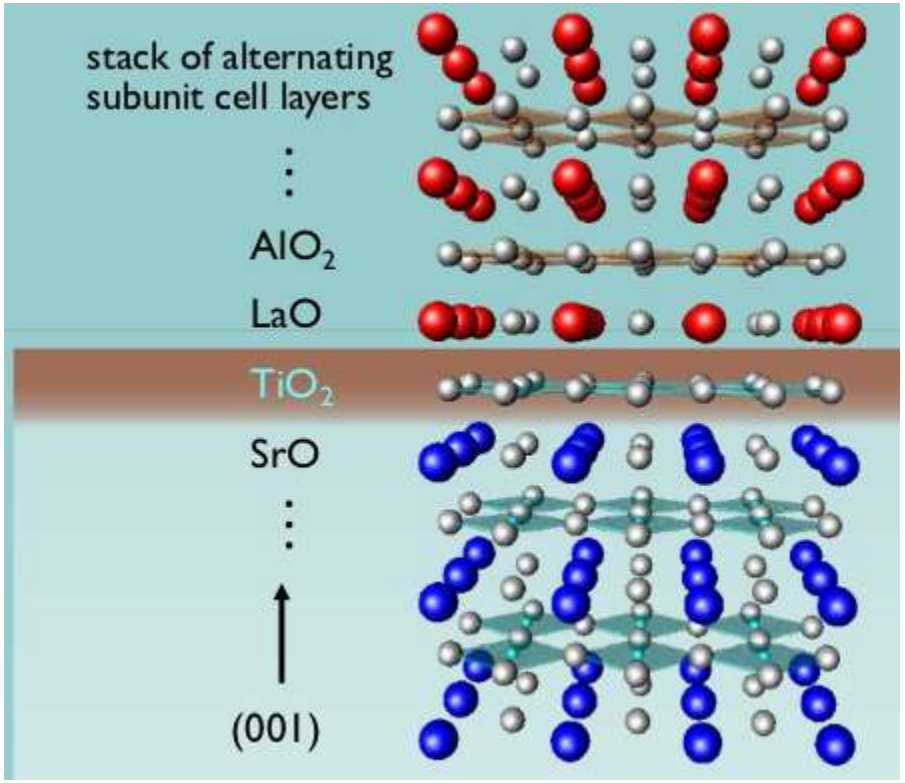
$$E_n^{\pm} = \hbar\omega_c \left[n \pm \frac{1}{2}\sqrt{(1 - gm^*/2)^2 + n\frac{\Delta_R^2}{E_F \hbar\omega_c}} \right]$$



Experimental of Rashba effect

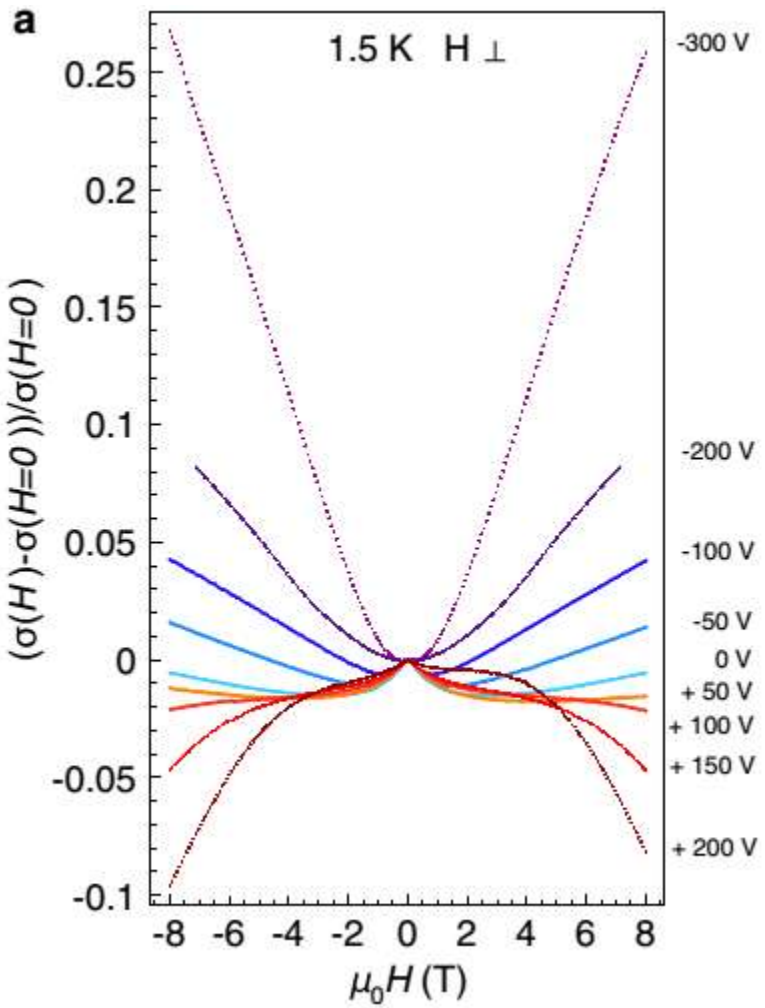
STO-LAO

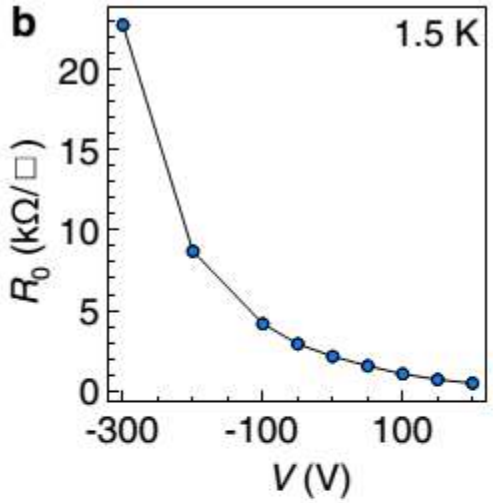


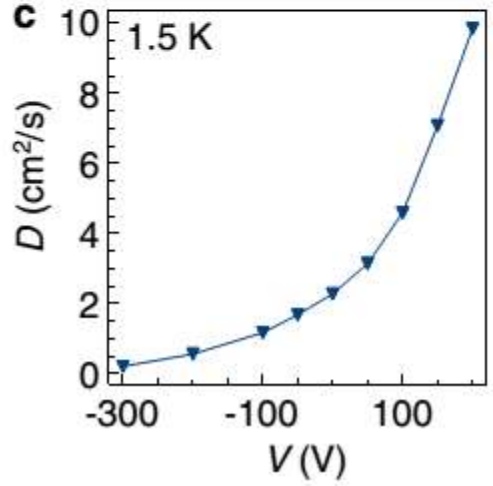


Hwang, et al. Nat. Mater. (2012)

Experimental of Rashba effect

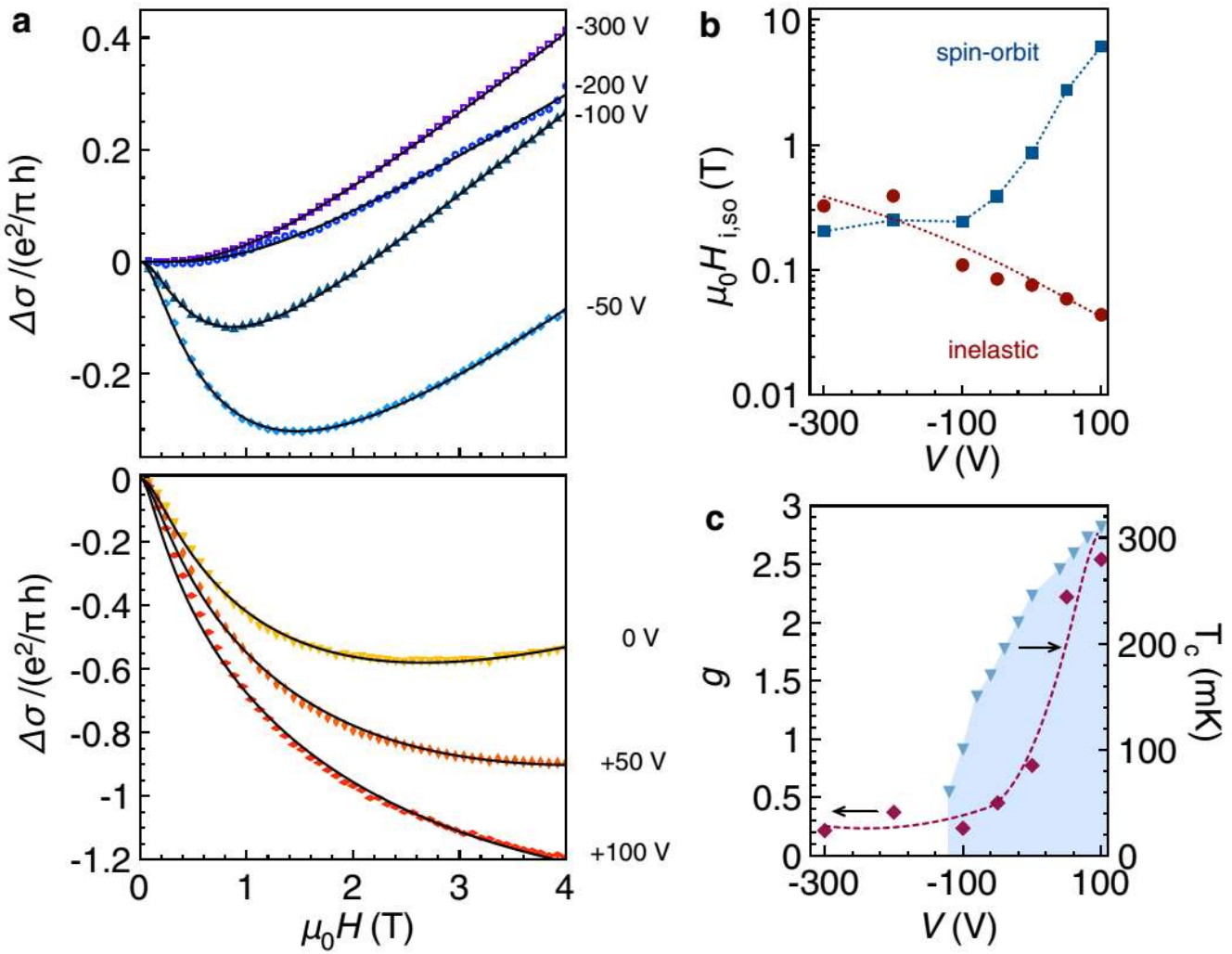




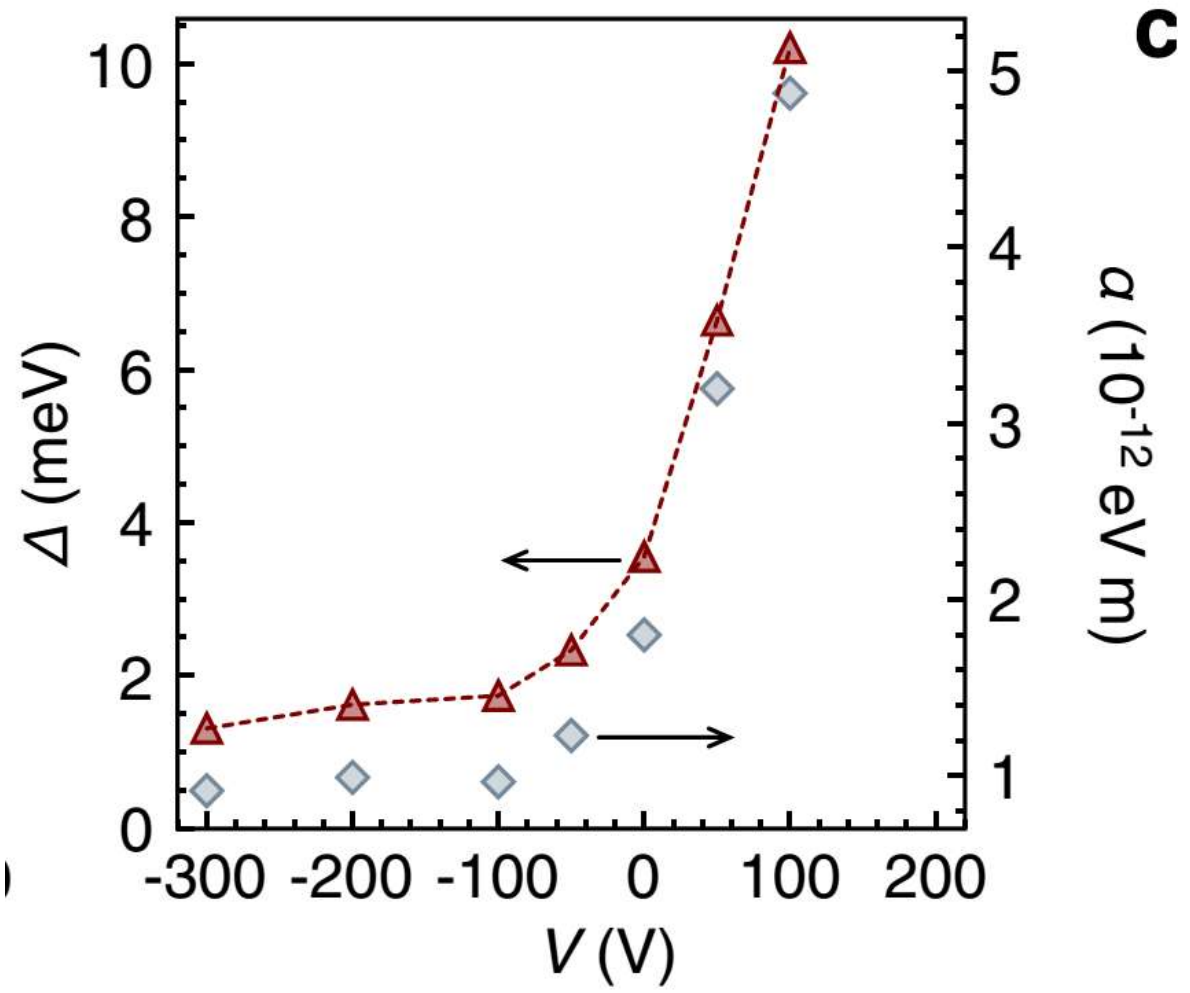


Caviglia, et al. PRL (2010)

Experimental of Rashba effect



Experimental of Rashba effect



Rashba effect

Spin-ARPES of Bi/Ag

$$\hat{H}_{\mathrm{SO}} = \alpha_R \boldsymbol{\sigma} \cdot (\boldsymbol{k}_{\parallel} \times \mathbf{e}_z),$$

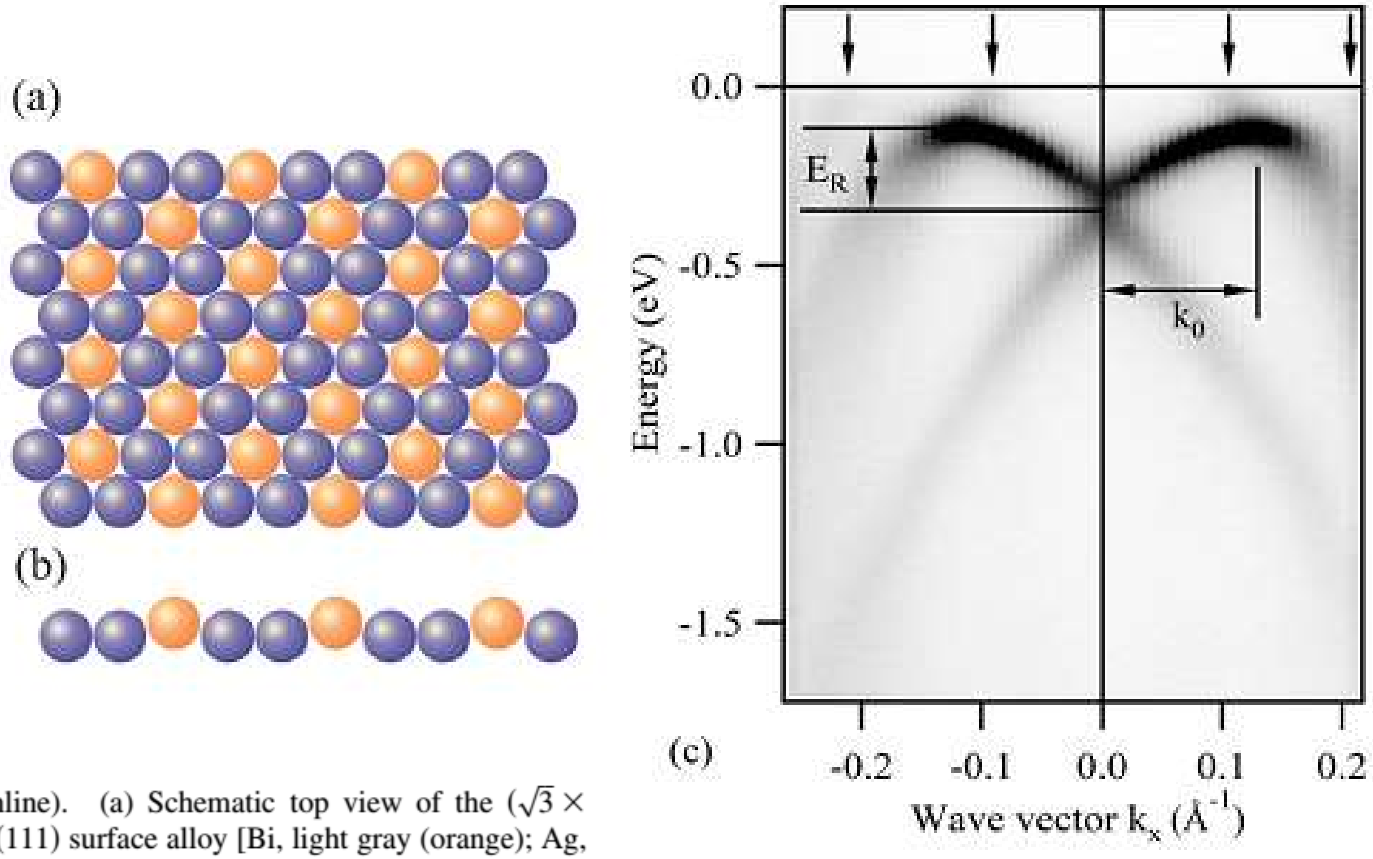
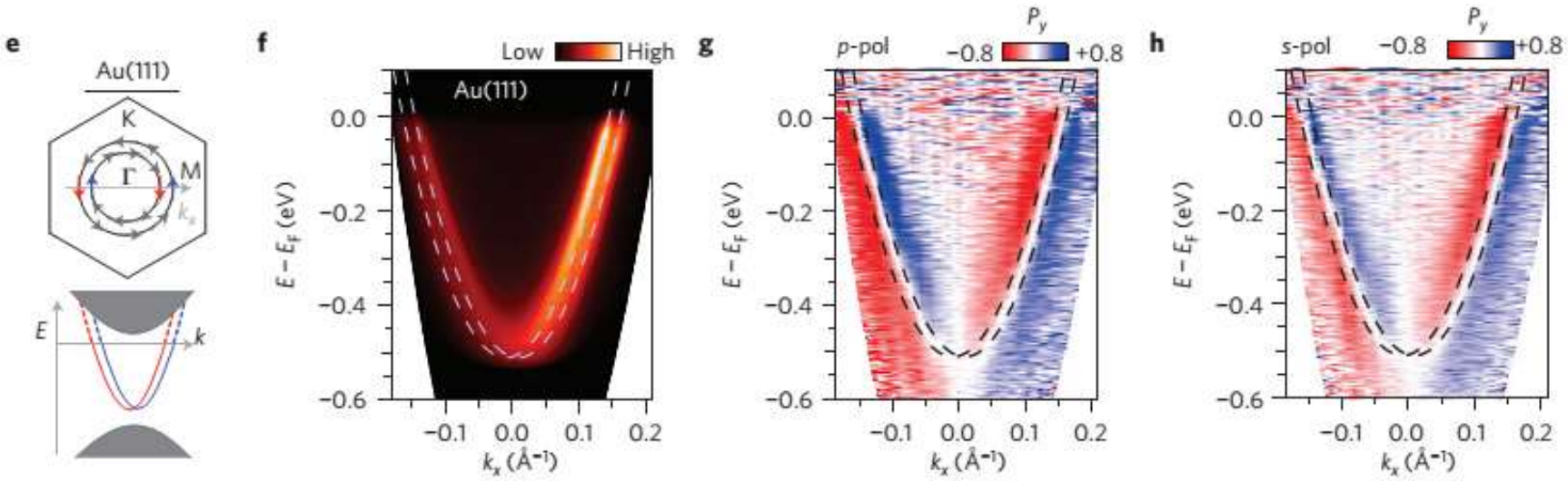


FIG. 1 (color online). (a) Schematic top view of the $(\sqrt{3} \times \sqrt{3})R30°$ Bi/Ag(111) surface alloy [Bi, light gray (orange); Ag, dark gray (blue)]. (b) Side view of the schematic, illustrating the

Ast, et al. PRL (2007)

Rashba effect

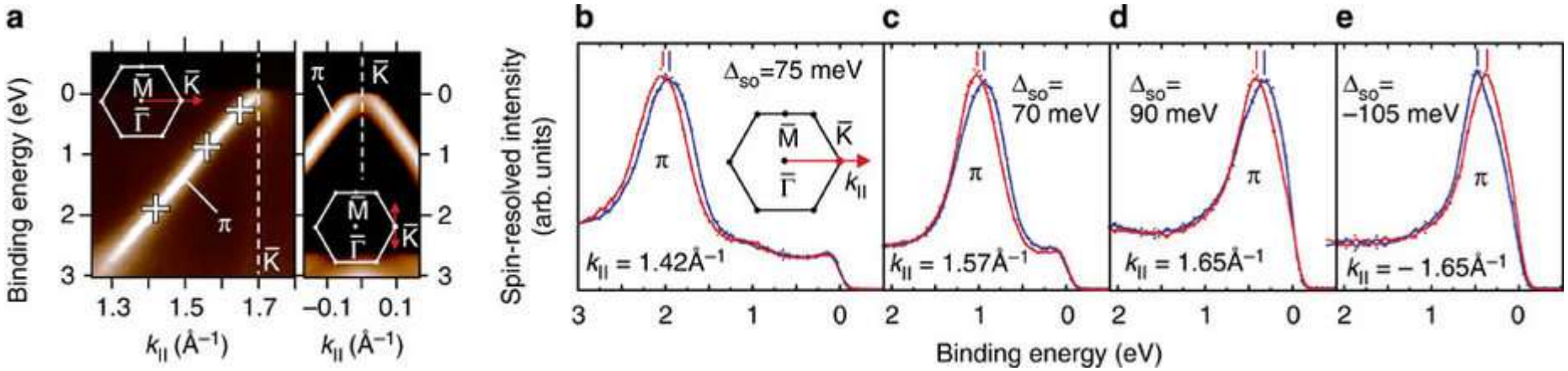
Spin-ARPES of Au (111)



Jozwiak, et al. Nature Physics (2013)

Rashba effect

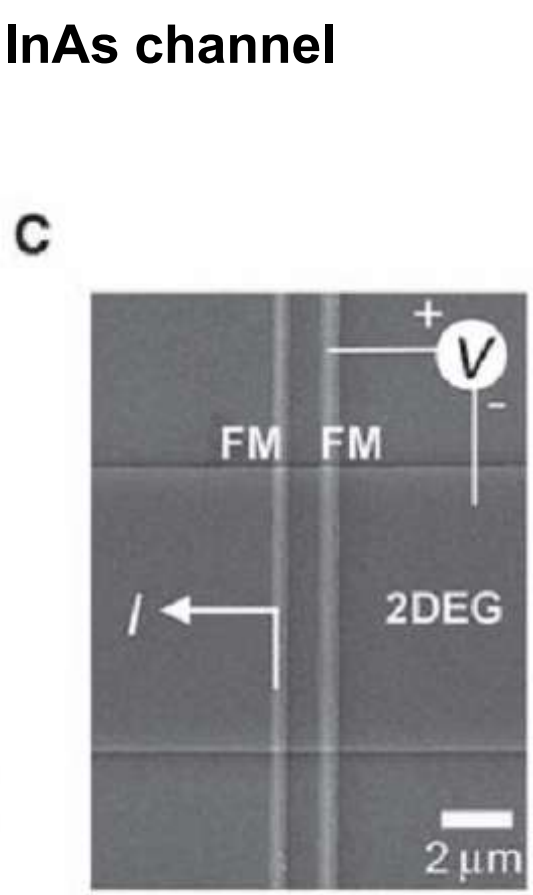
Spin-ARPES of Graphene/Au (111)

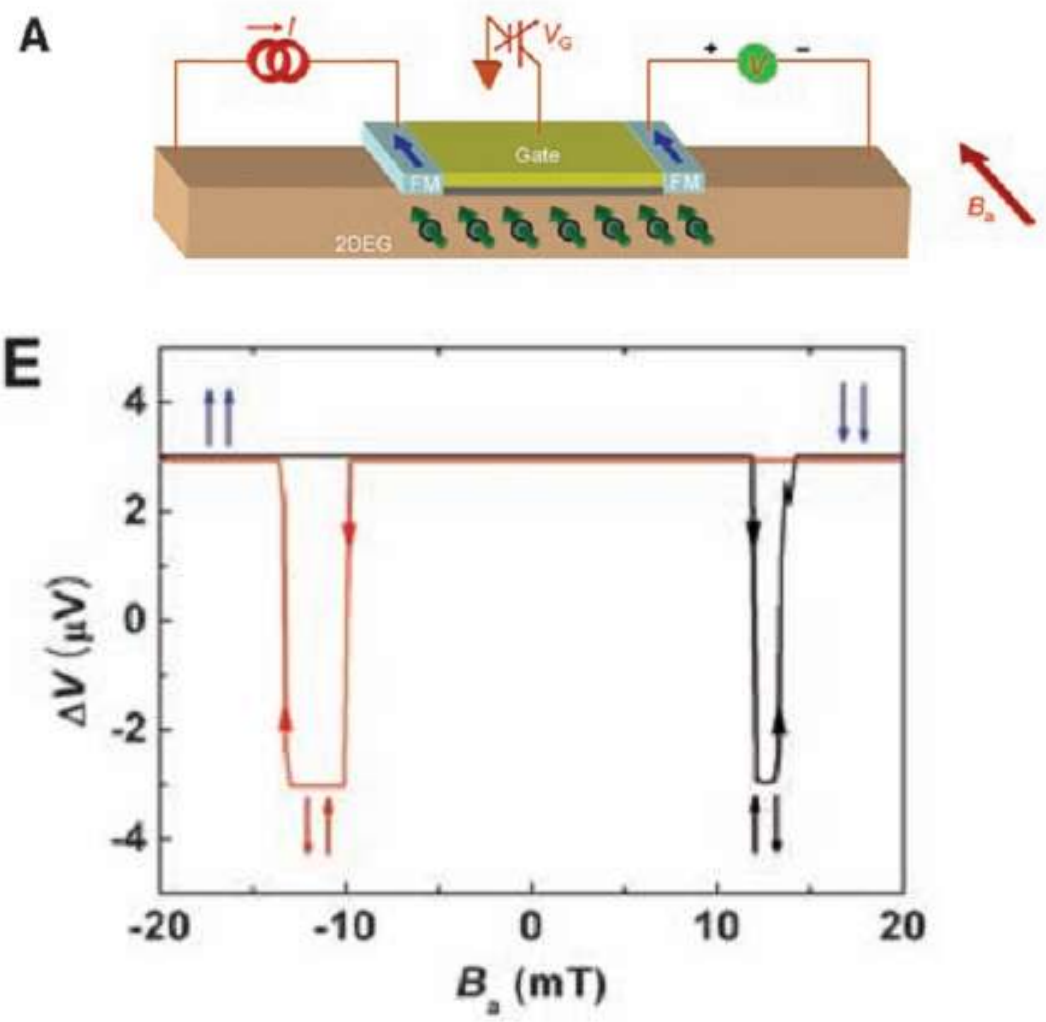


Marchenko, et al. Nature Commun. (2012)

Rashba effect for Spin-FET

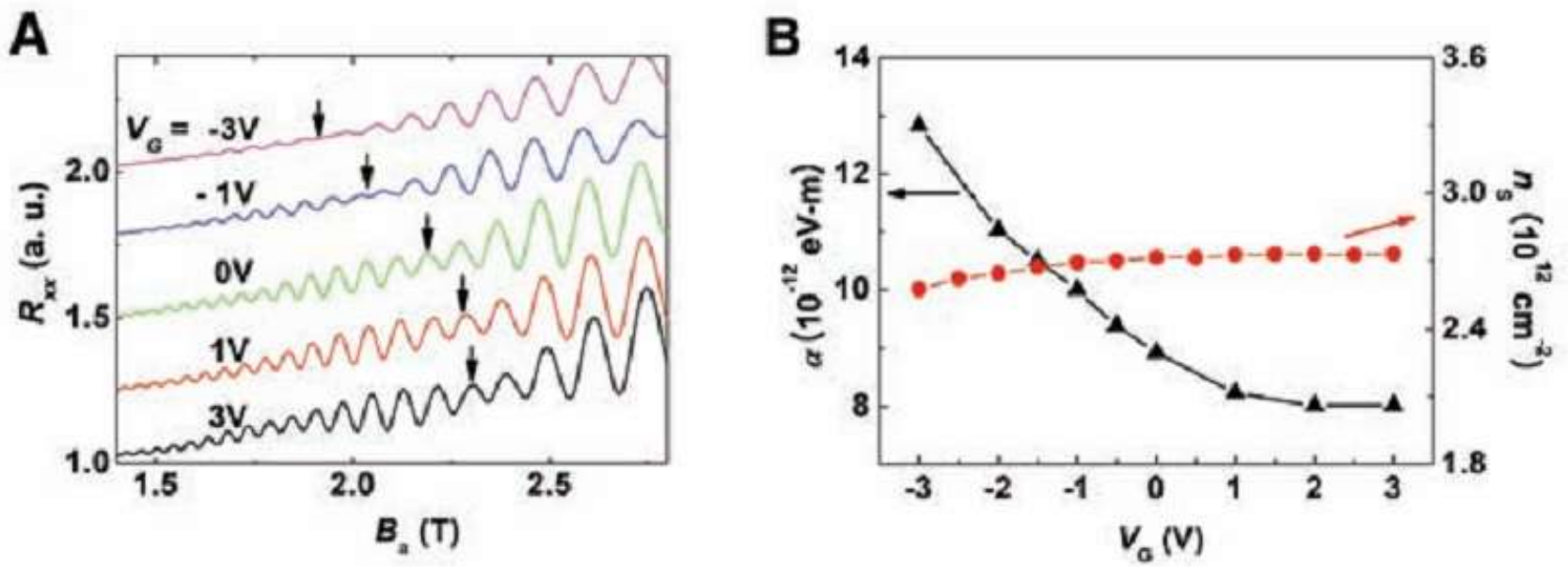
InAs channel



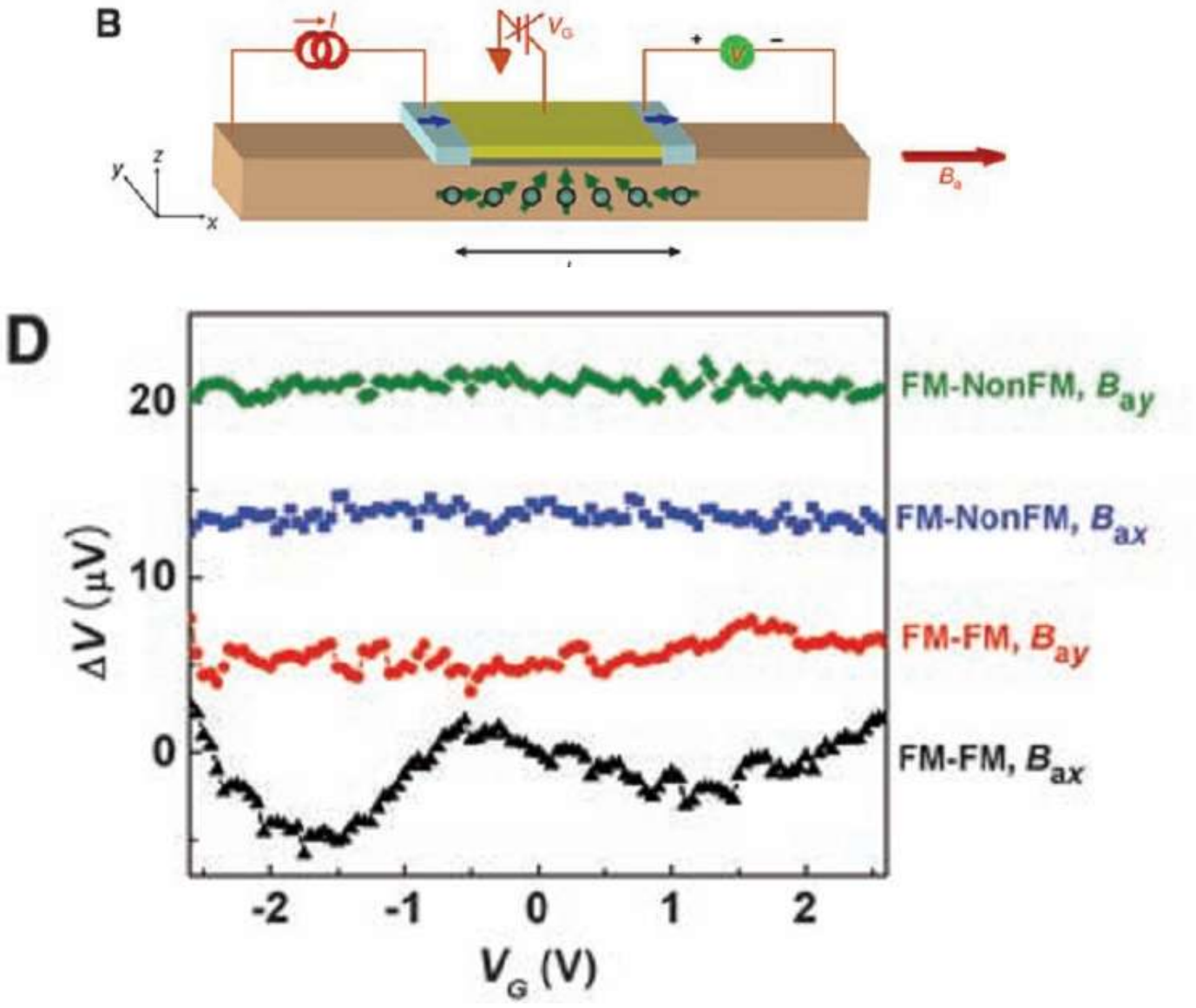


Koo, et al, Science (2009)

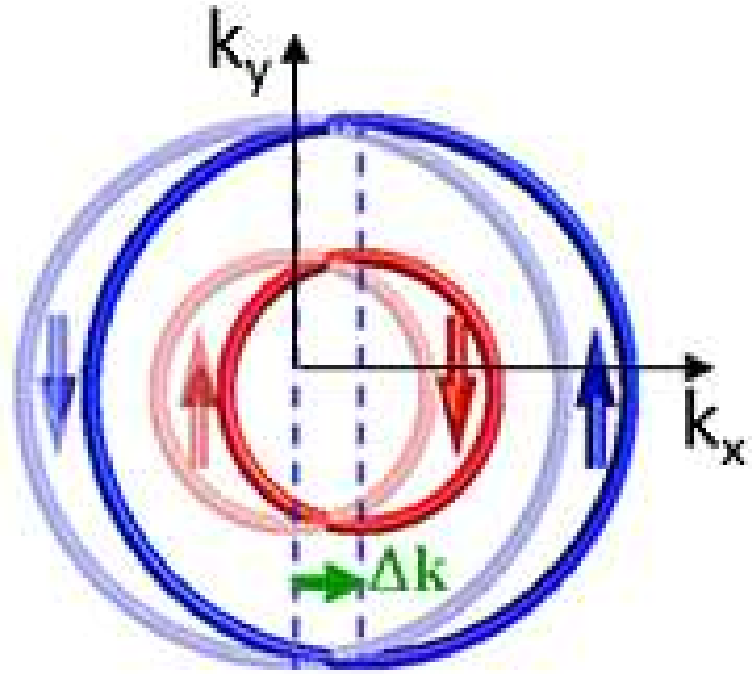
Rashba effect for Spin-FET



Rashba effect for Spin-FET



Edelstein effect

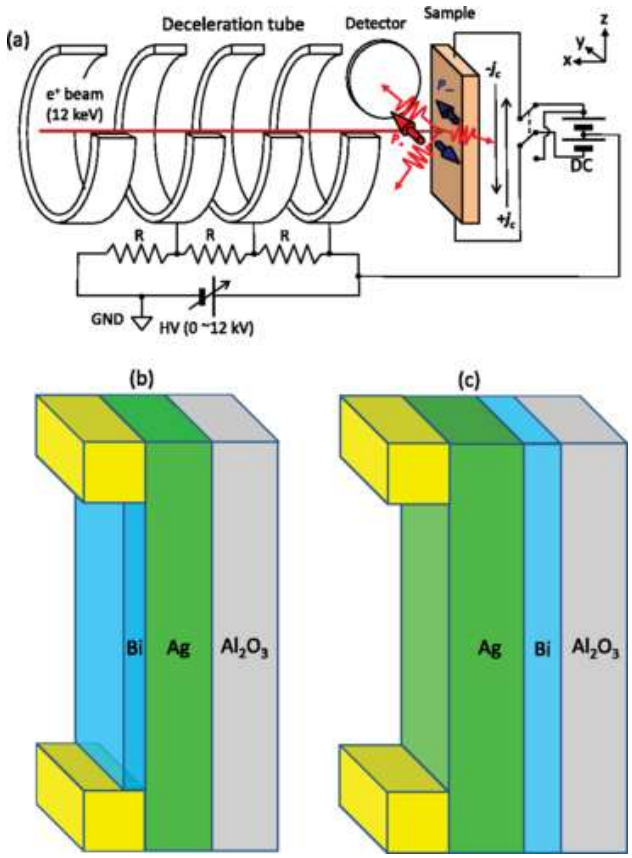


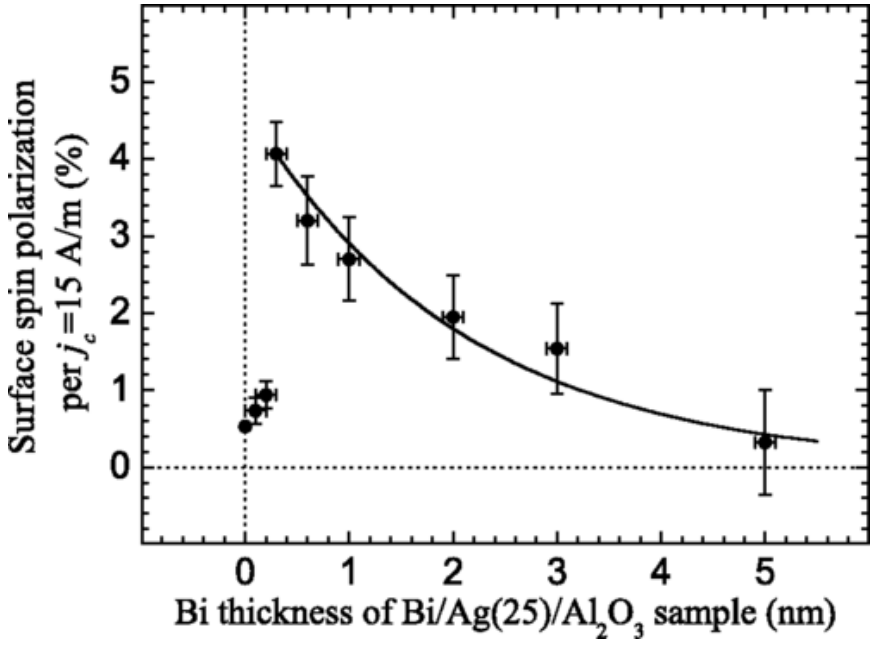
I

Edelstein effect

Bi/Ag

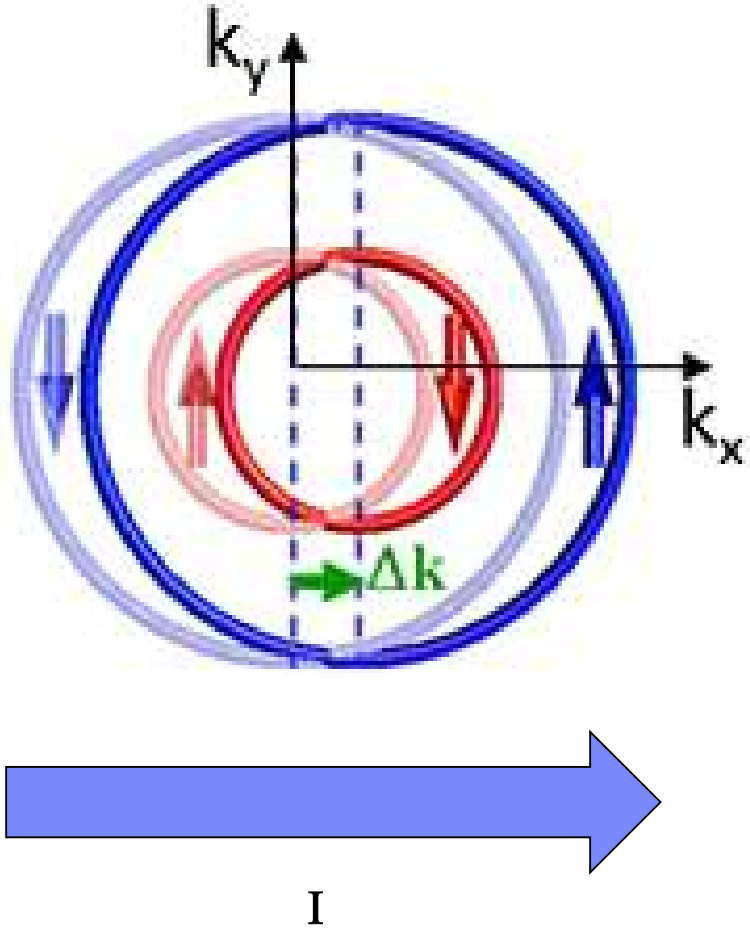
The spin polarized positron beam



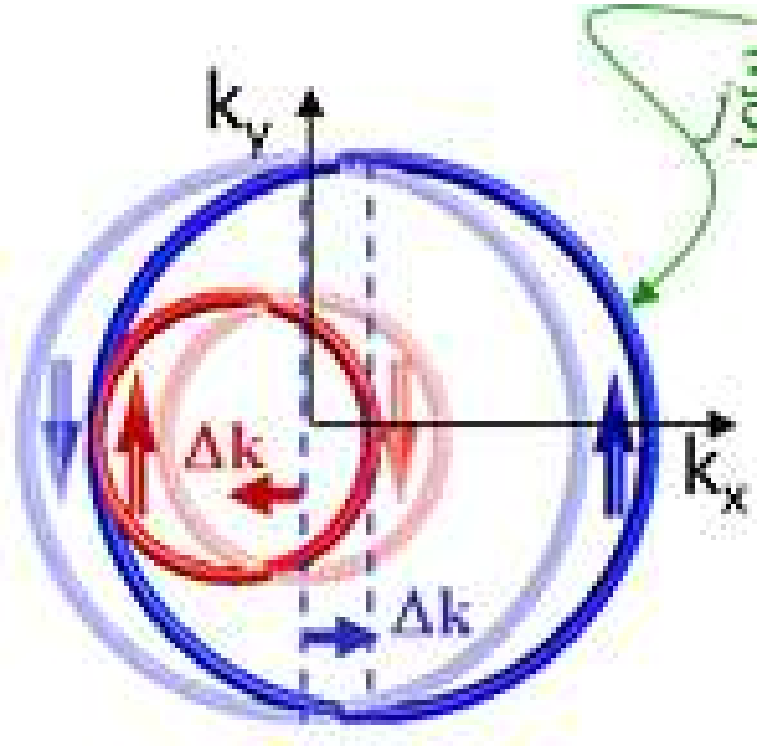


Zhang, et al. PRL (2015)

Edelstein effect



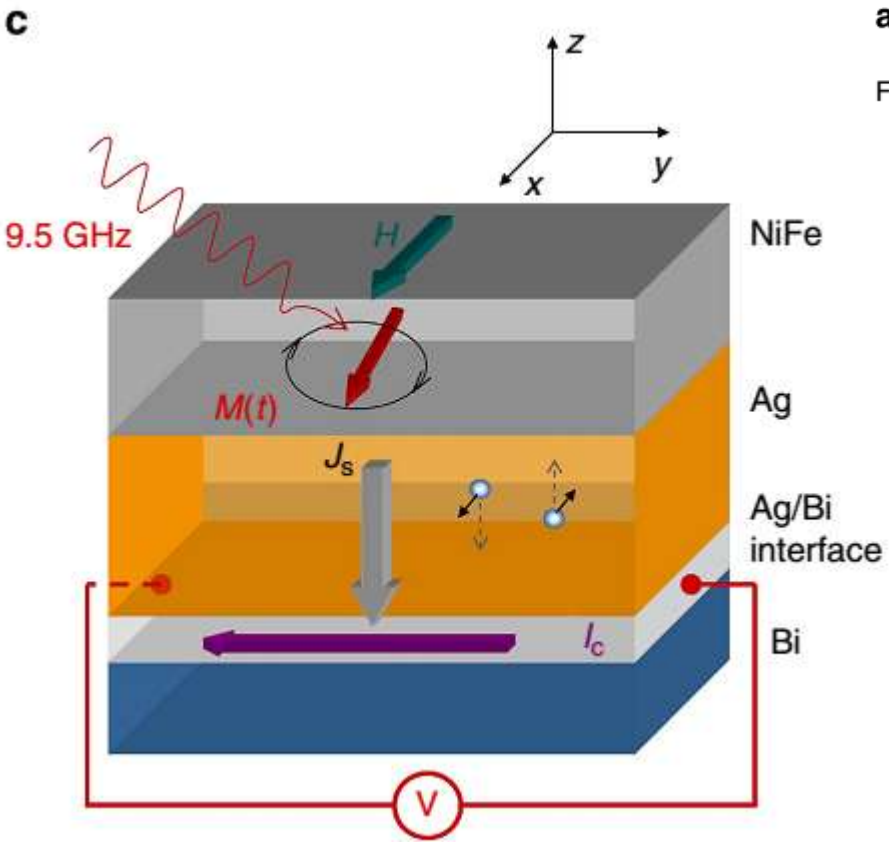
Spin injection

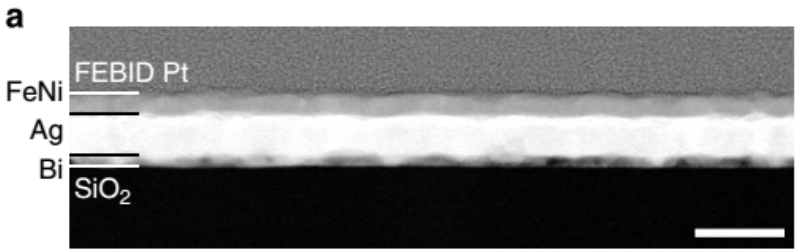


Charge current

Inverse Edelstein effect

Bi/Ag





Sanchez, et al. Nature Comm. (2013)

Inverse Edelstein effect

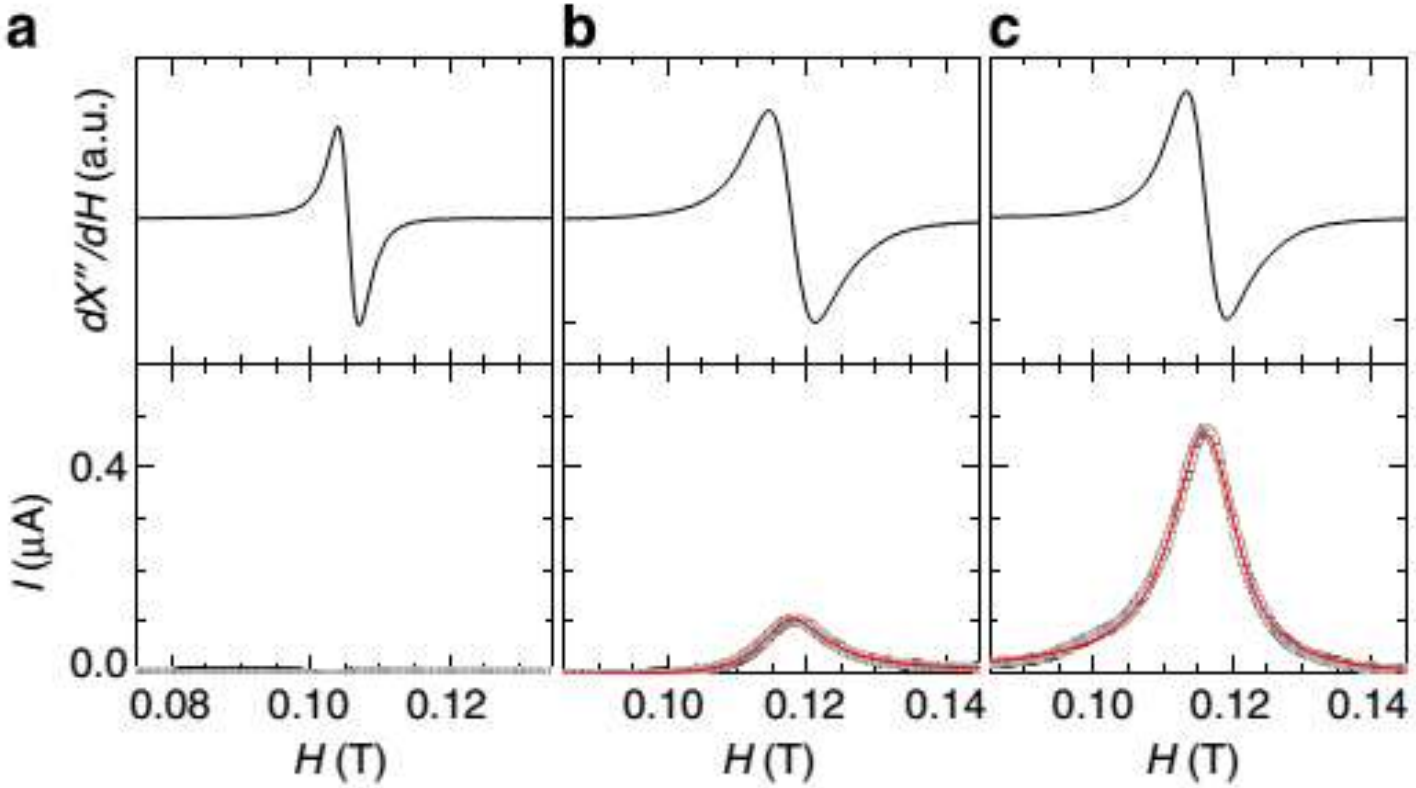


Figure 2 | Spin pumping results. FMR spectrum (top) and corresponding field dependence of the current I_C derived from the DC voltage V (bottom) for NiFe(15)/Ag(10) (**a**), NiFe(15)/ Bi(8) (**b**) and NiFe(15)/Ag(5)/Bi(8) (**c**) samples. Red lines are Lorentzian fits. The narrow FMR line and

Inverse Edelstein effect

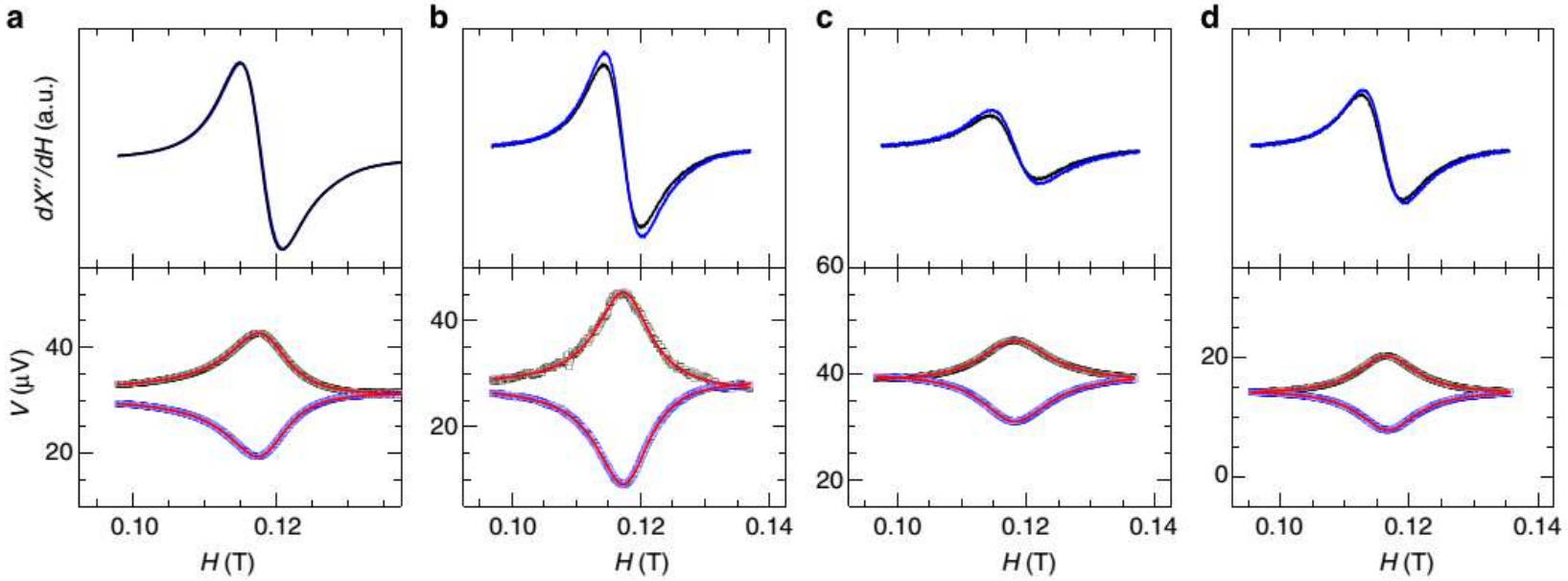
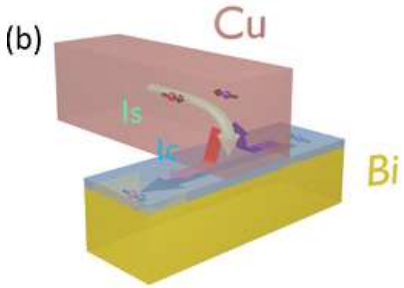
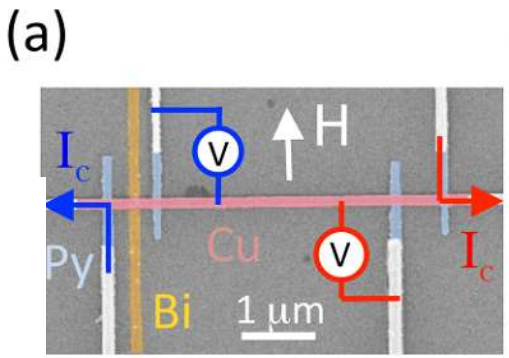


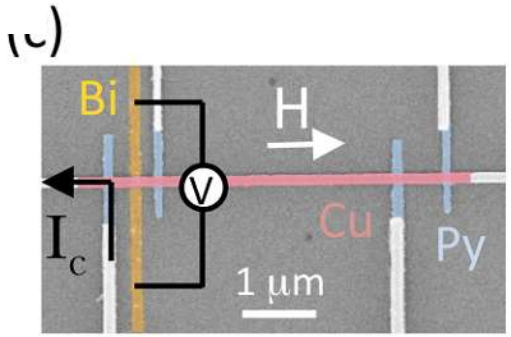
Figure 8 | FMR and measured voltage. Raw data of FMR-V curves on NiFe(15)/Ag(t)/Bi(8), in the series with length of 1.0 mm. (**a**) 0 nm of Ag. (**b**) 5 nm of Ag. (**c**) 10 nm of Ag. (**d**) 20 nm of Ag. The two voltage curves correspond to the parallel and antiparallel cases. Black and blue experimental data stand

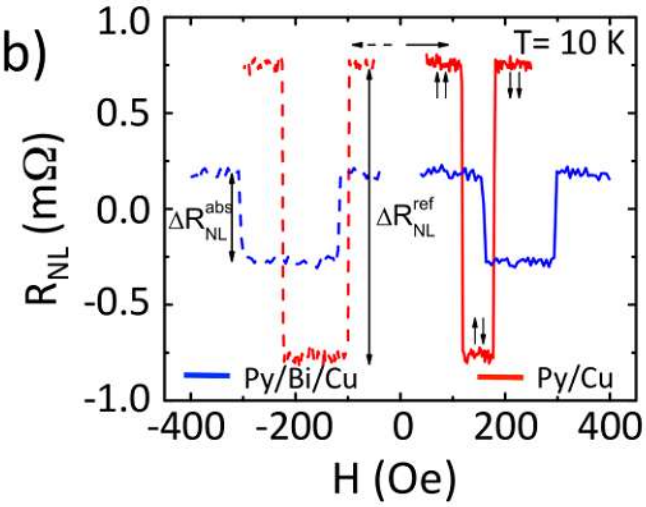
Inverse Edelstein effect

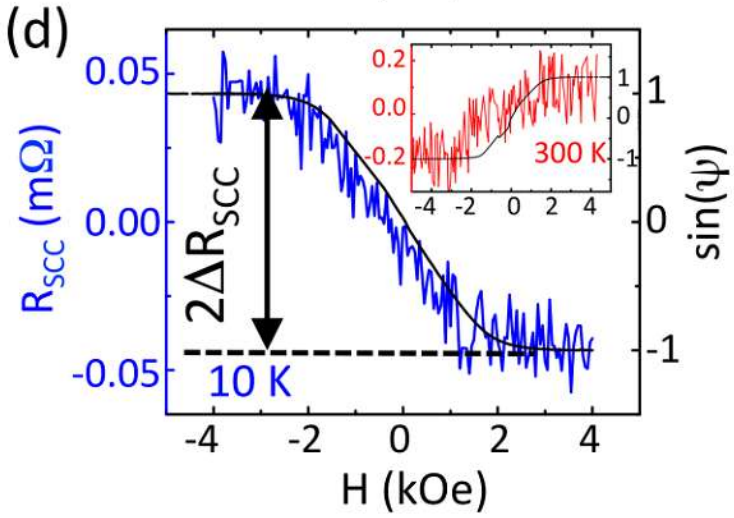
Bi/Cu





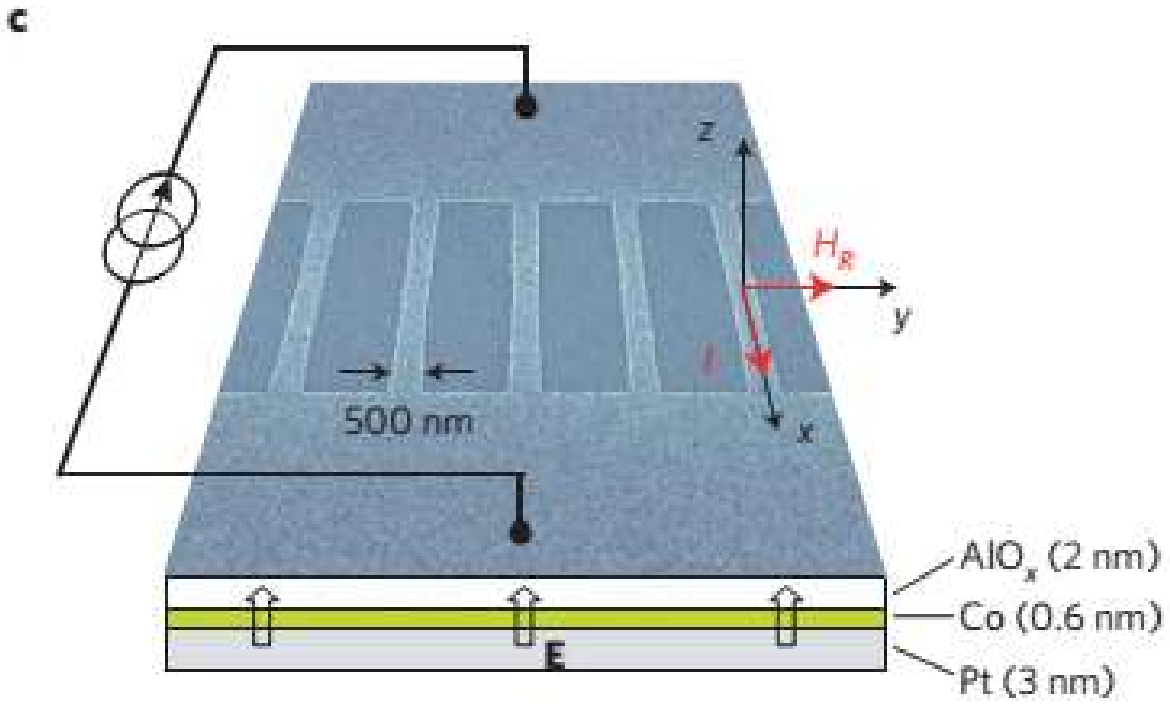






Isasa, et al. PRB (2016)

Edelstein spin torque



Miron, et al, Nature Materials (2010)
Miron, et al, Nature (2011)
Miron, et al, Nature Materials (2011)

Edelstein spin torque

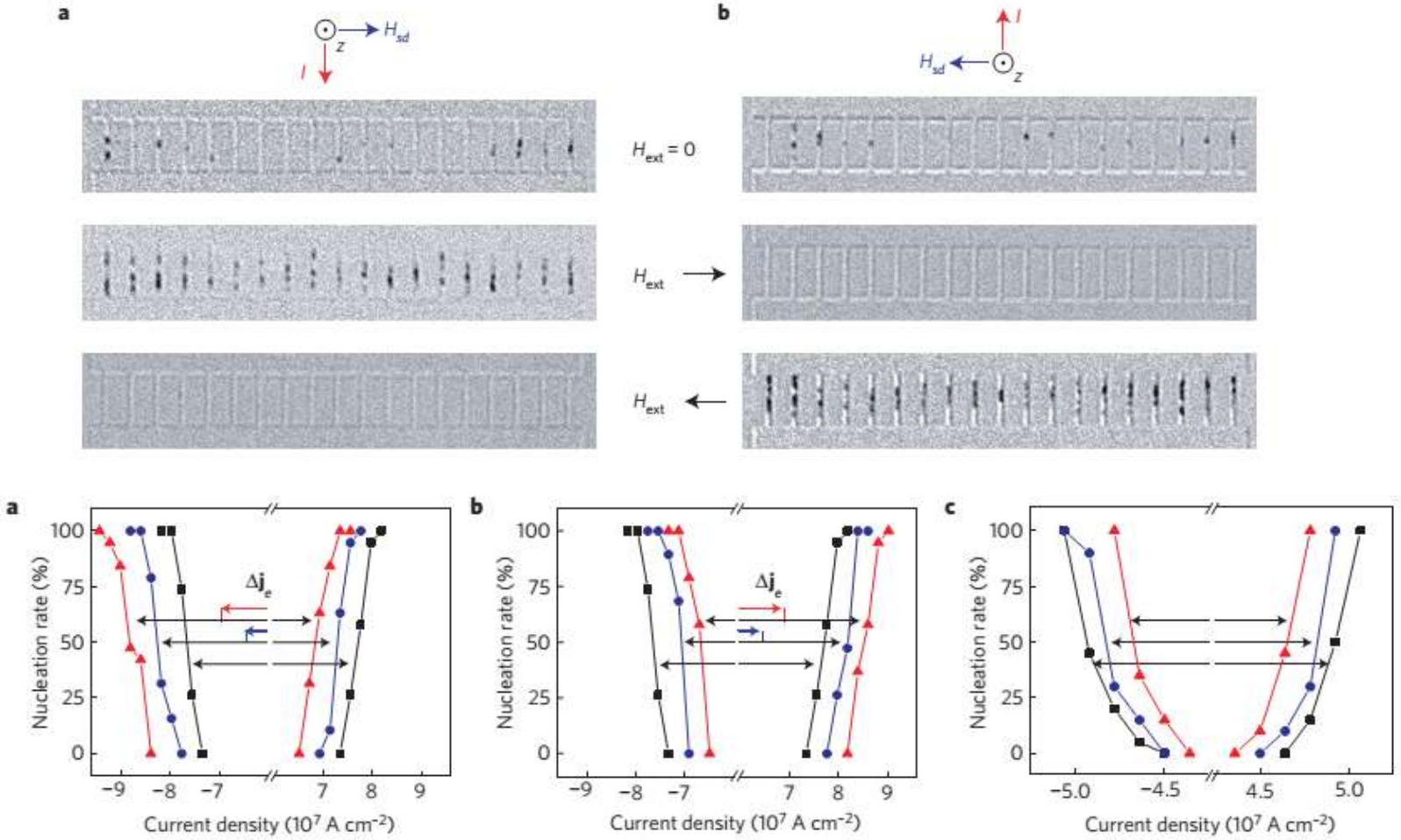
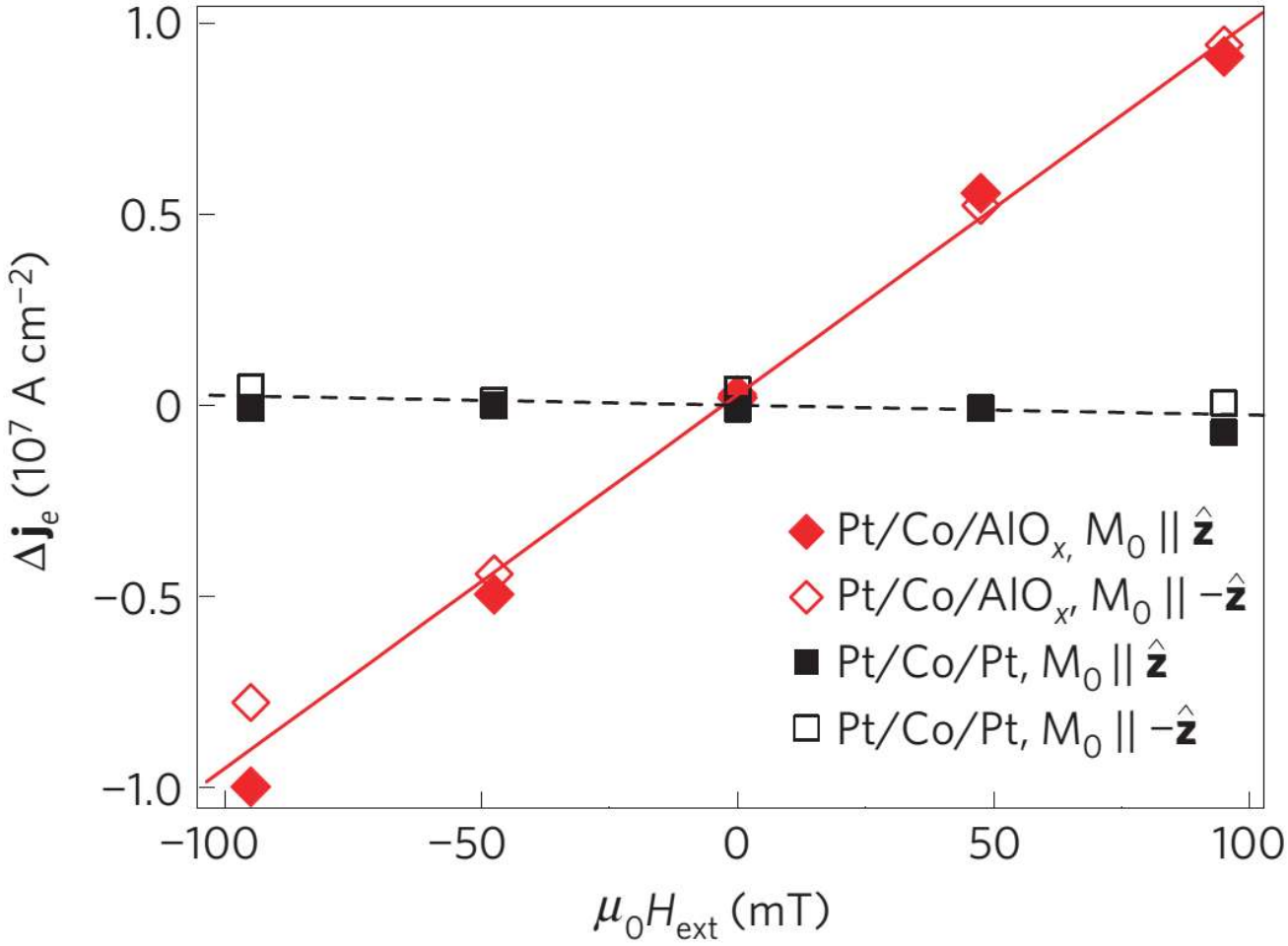
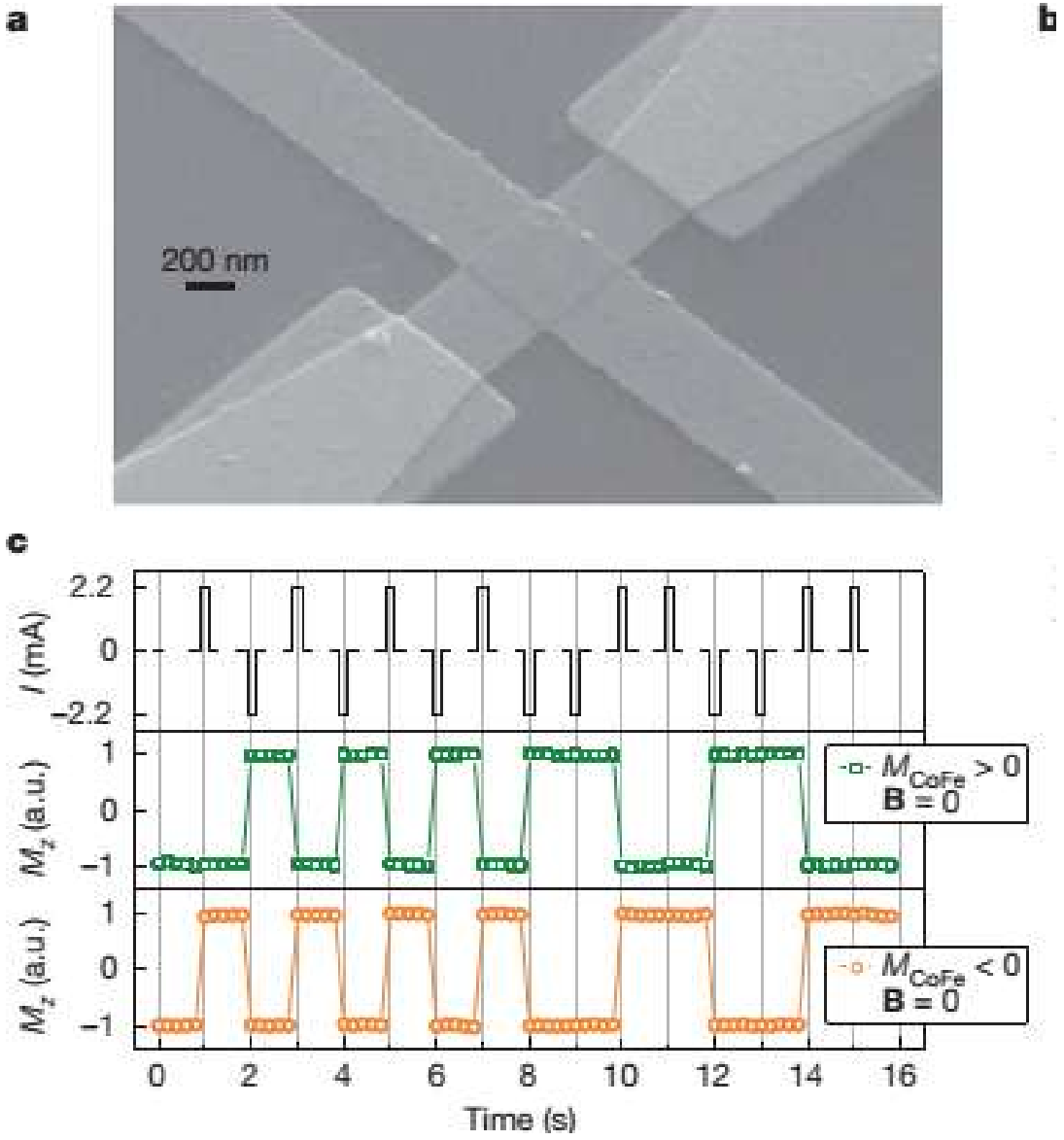


Figure 3 | Percentage of wires that present reversed magnetic domains after the injection of a current pulse as a function of current density and external field. a,**b**, Pt/Co/AlO_x wire array for $H_{ext} \parallel \hat{\mathbf{y}}$ (**a**) and $H_{ext} \parallel -\hat{\mathbf{y}}$ (**b**). **c**, Pt/Co/Pt wire array, $\mathbf{H}_{ext} \parallel -\hat{\mathbf{y}}$. The nucleation rate curves shift by an amount $\Delta \mathbf{j}_e$ proportional to H_{ext}, as indicated by red and blue arrows, reflecting the direction and magnitude of H_{sd}. Values of $\mu_0 H_{ext}$ are 0 mT (black squares), ±47.5 mT (blue dots), ±95 mT (red triangles).

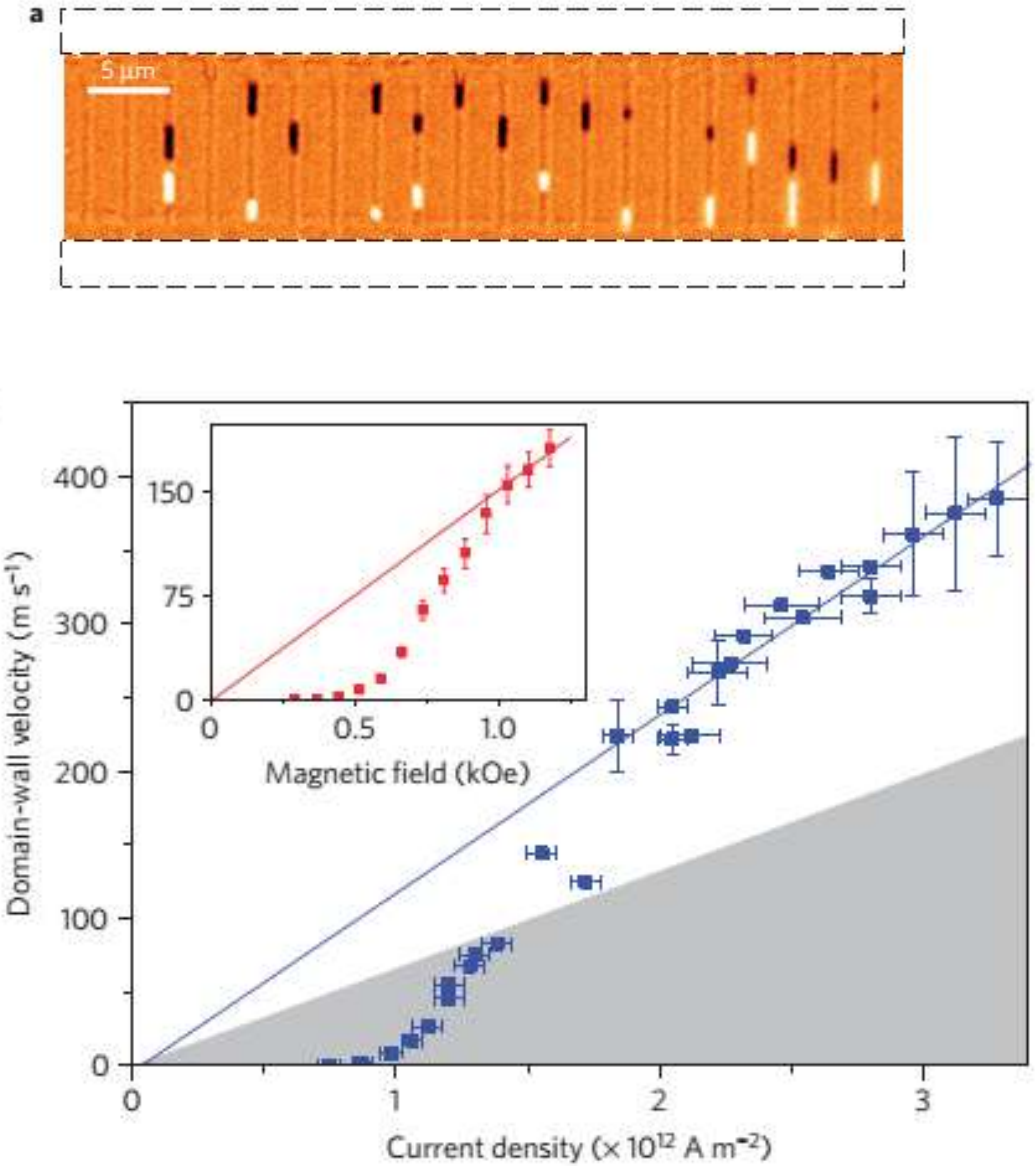
Edelstein spin torque



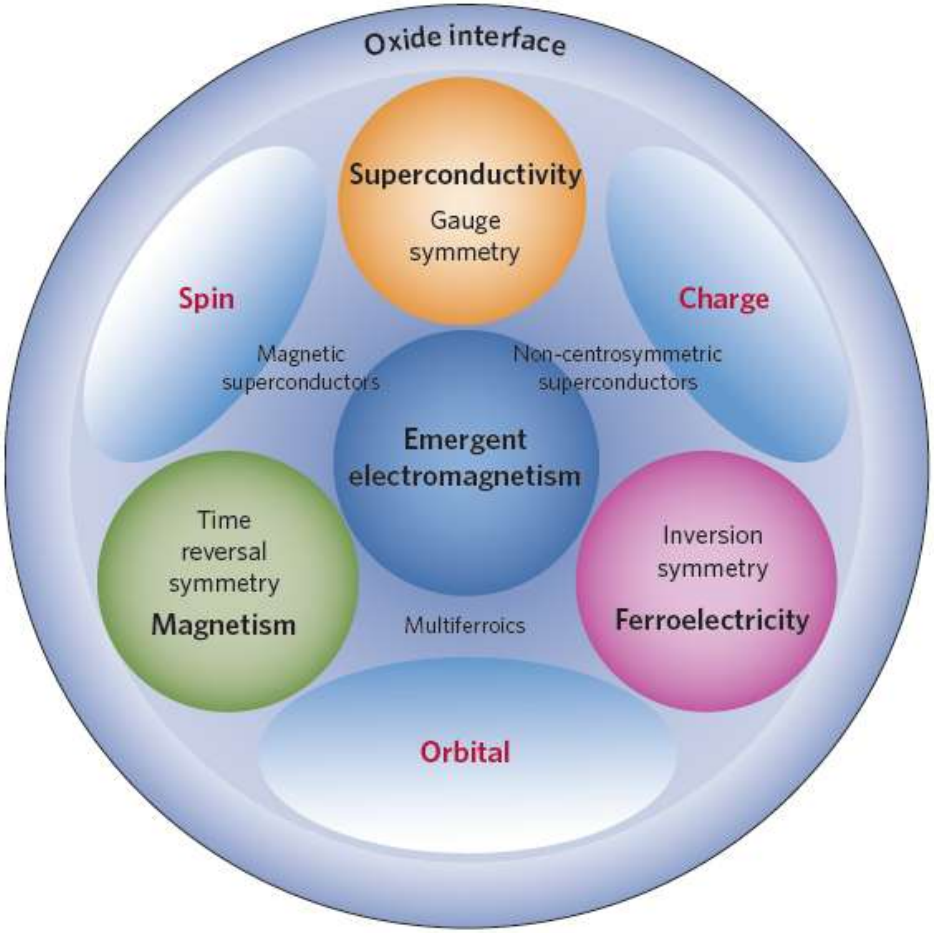
Edelstein spin torque



Edelstein spin torque

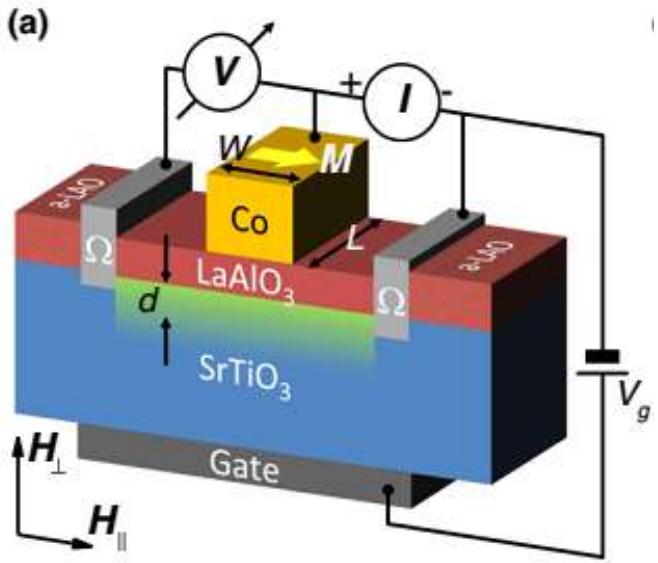


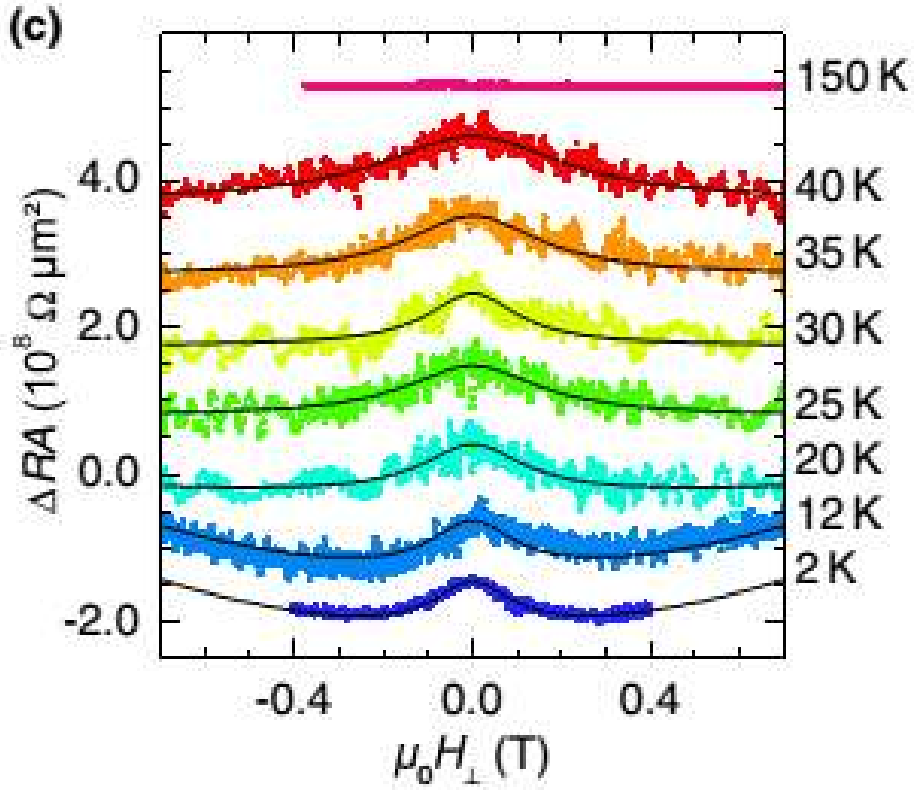
Inverse Edelstein in Oxide interface



Hwang, et al. Nat. Mater. (2012)

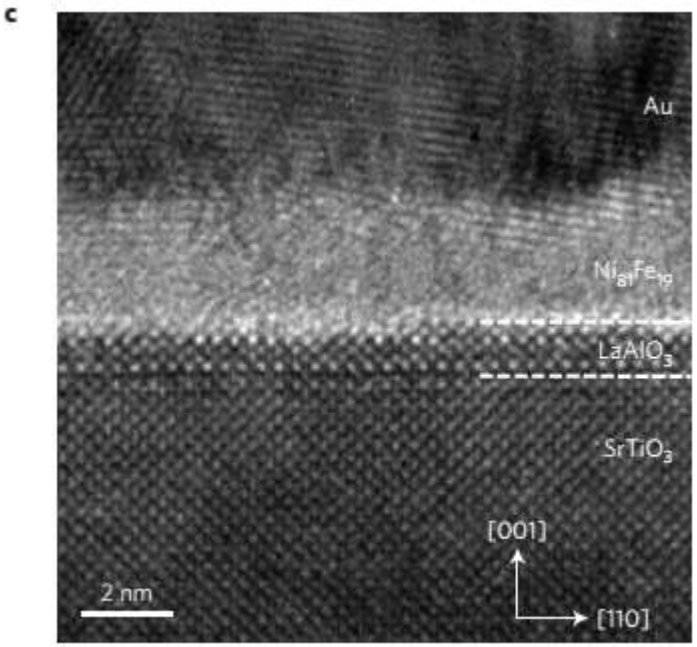
Inverse Edelstein in Oxide interface

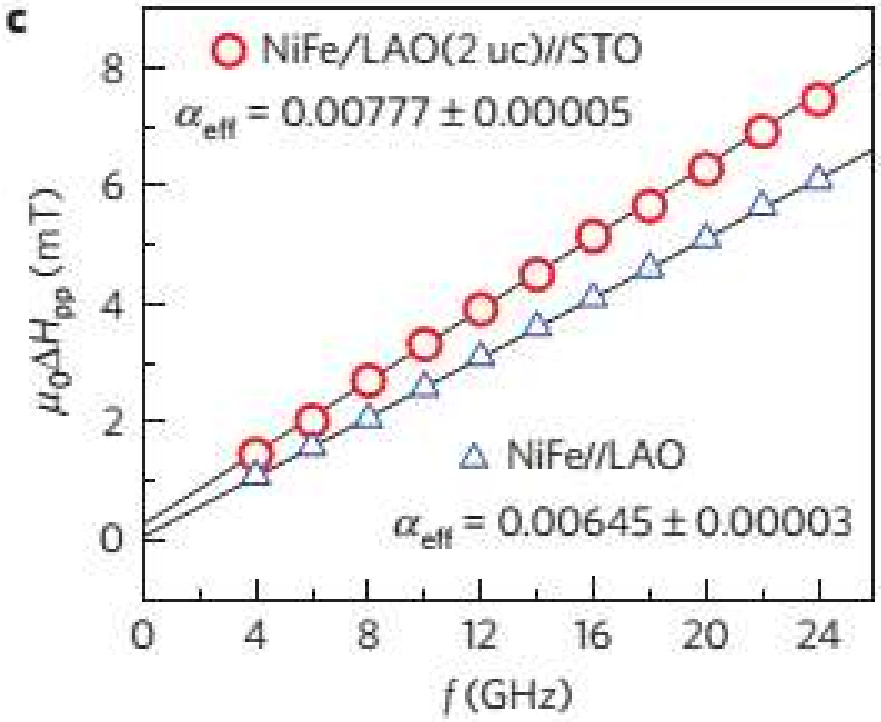




Reyren, et al, PRL (2012)

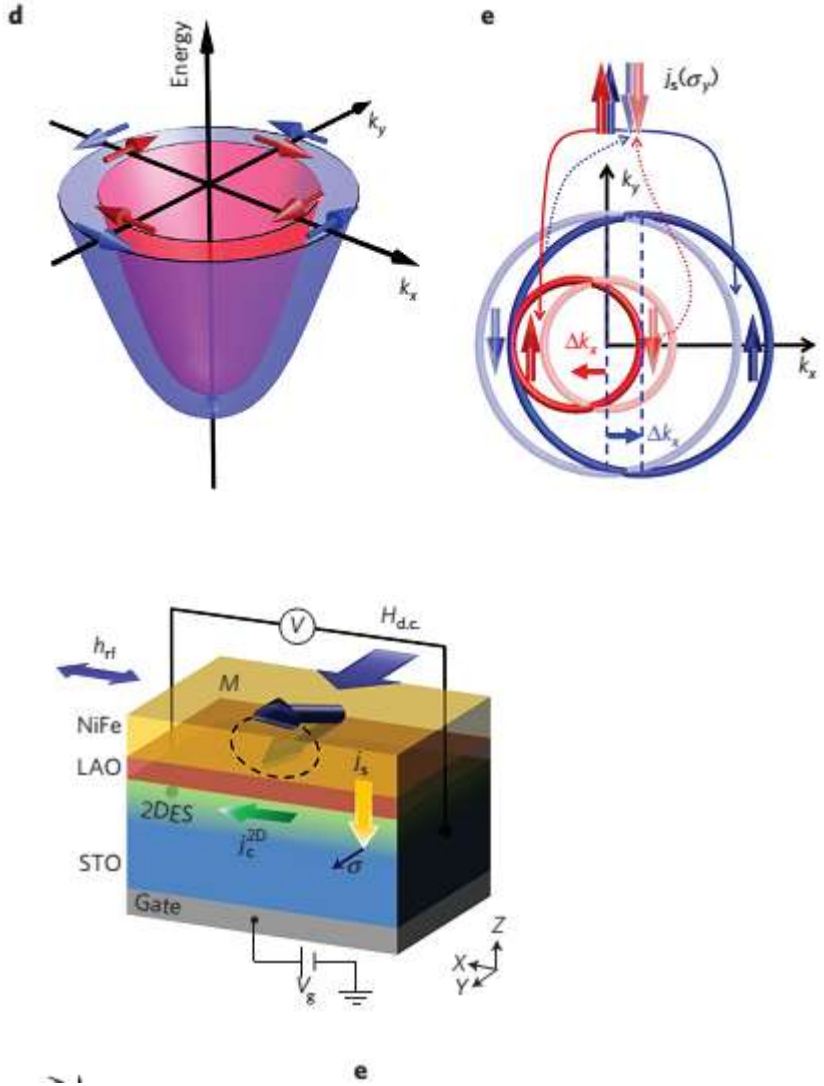
Inverse Edelstein in Oxide interface

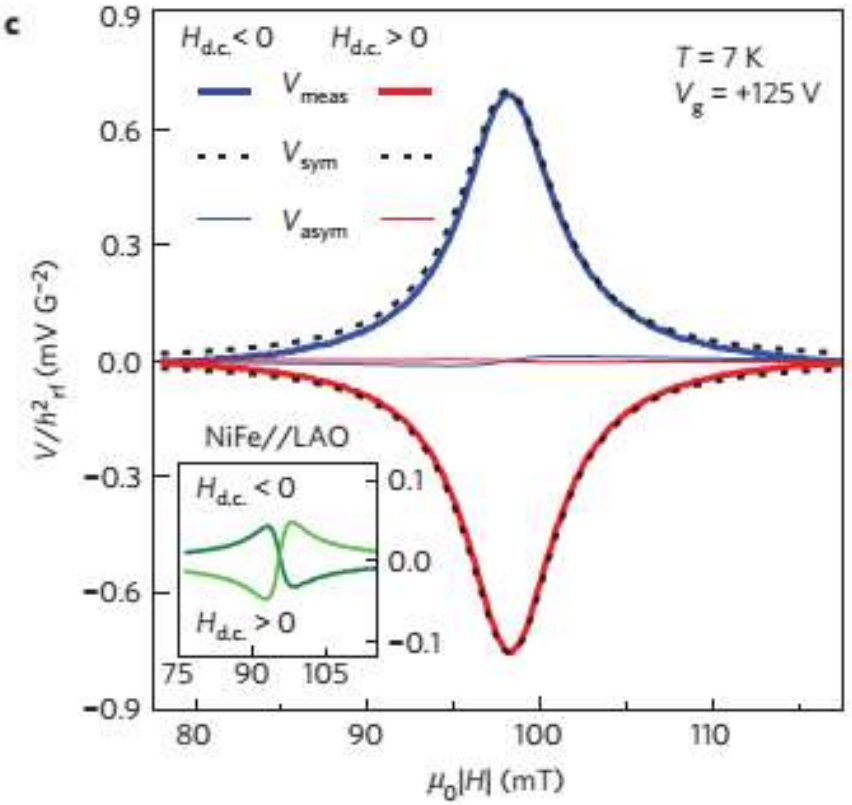




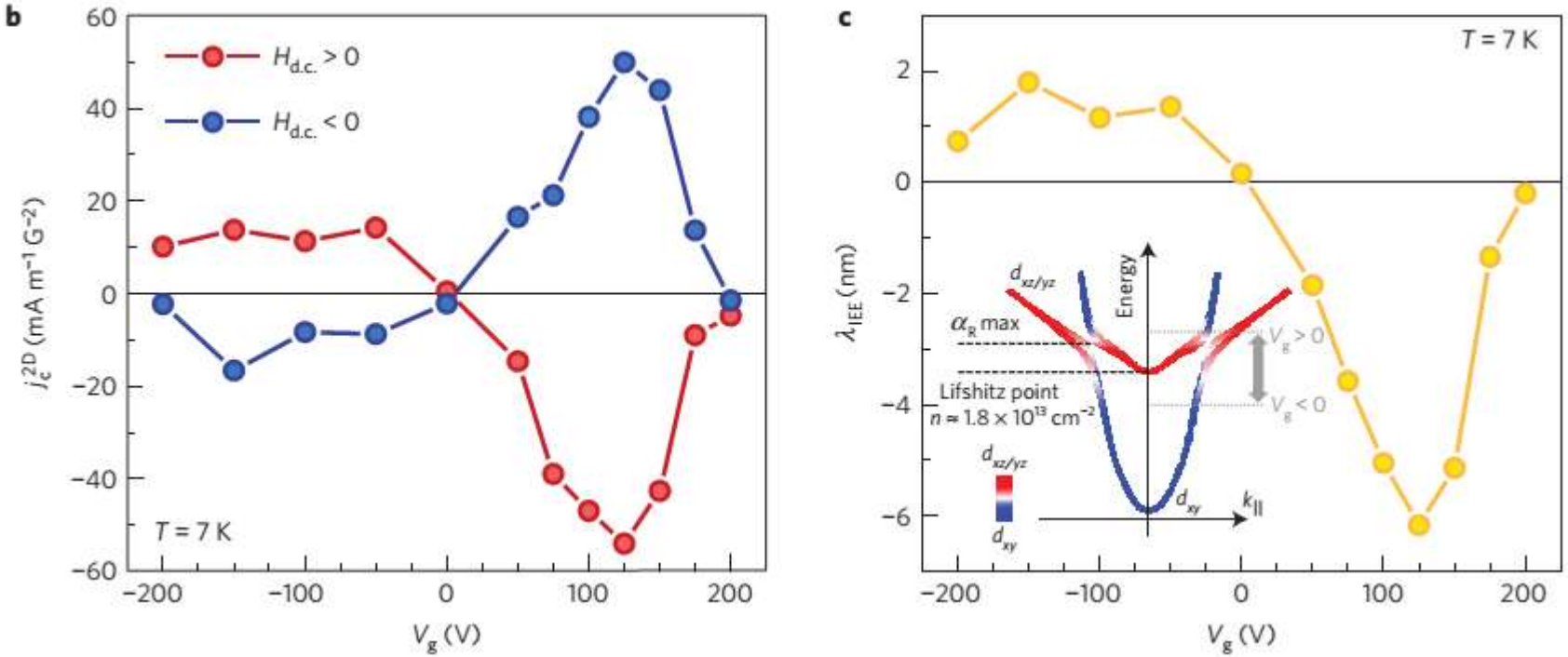
Lesne, et al, Nature Materials (2016)

Inverse Edelstein in Oxide interface



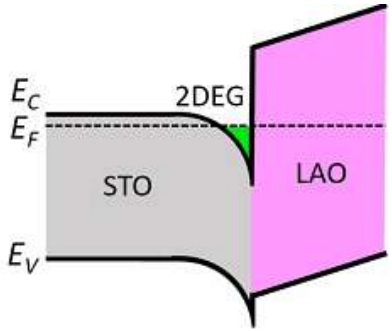


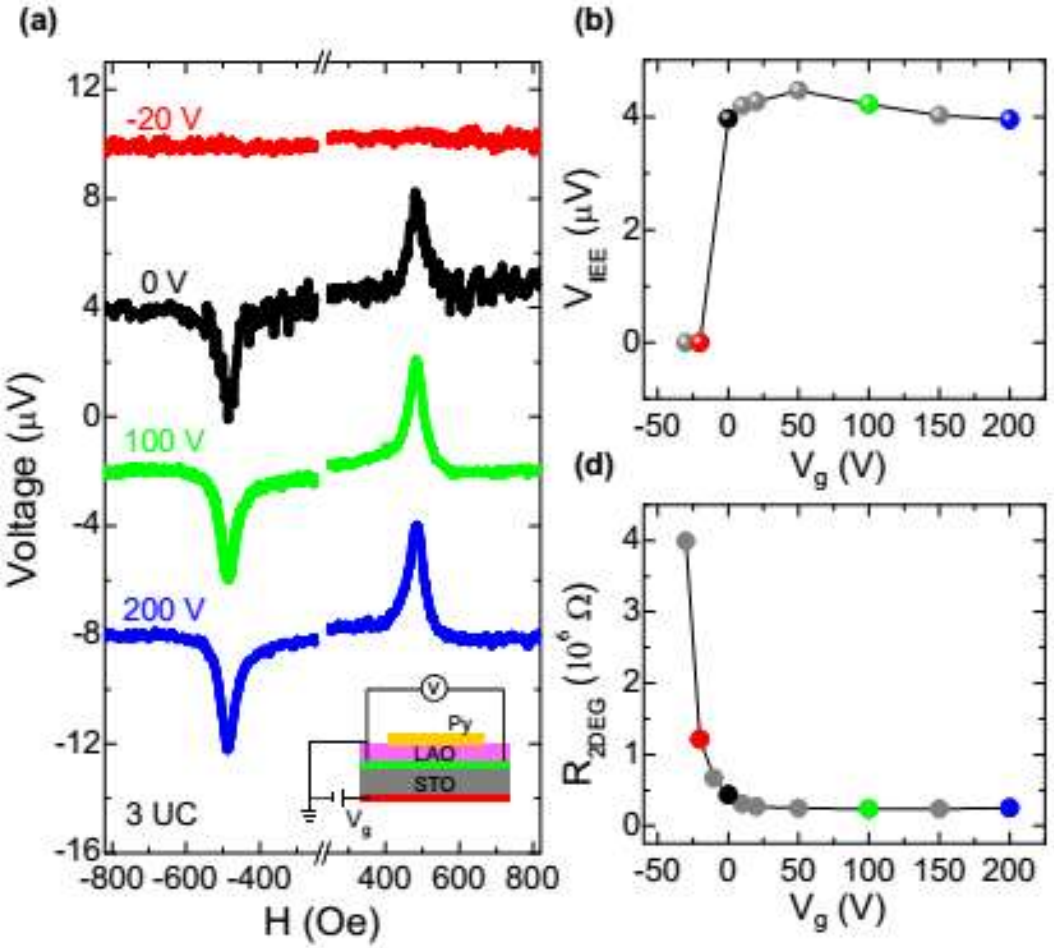
Inverse Edelstein in Oxide interface



Inverse Edelstein in Oxide interface

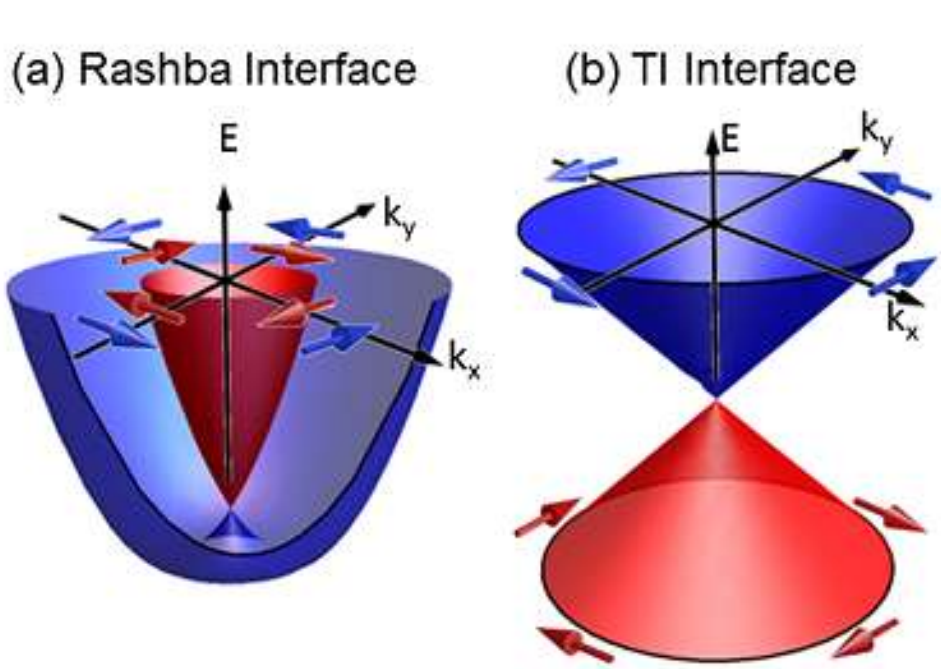
Room temperature

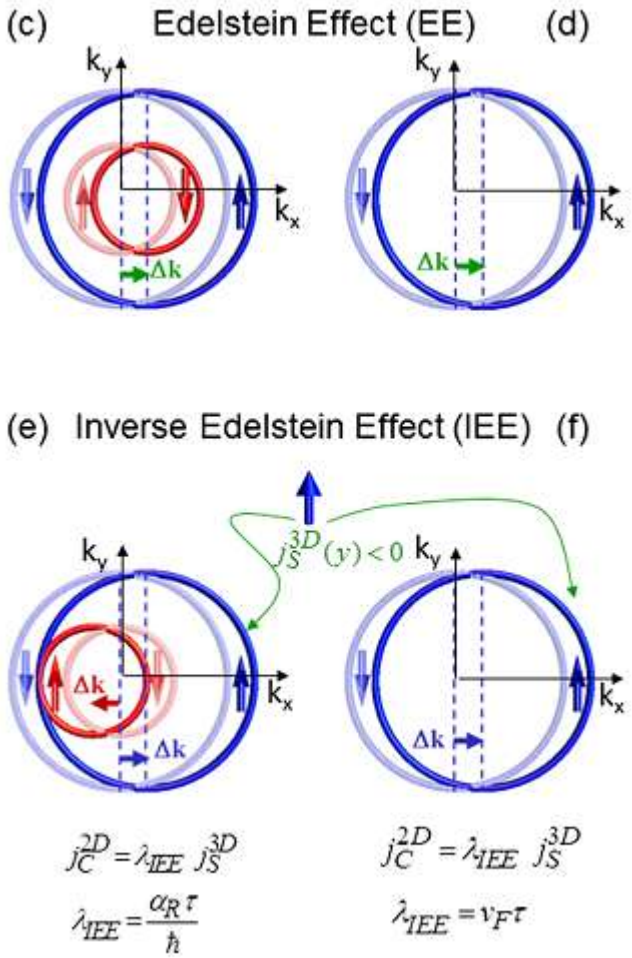




Song, et al, Science Advance (2017)

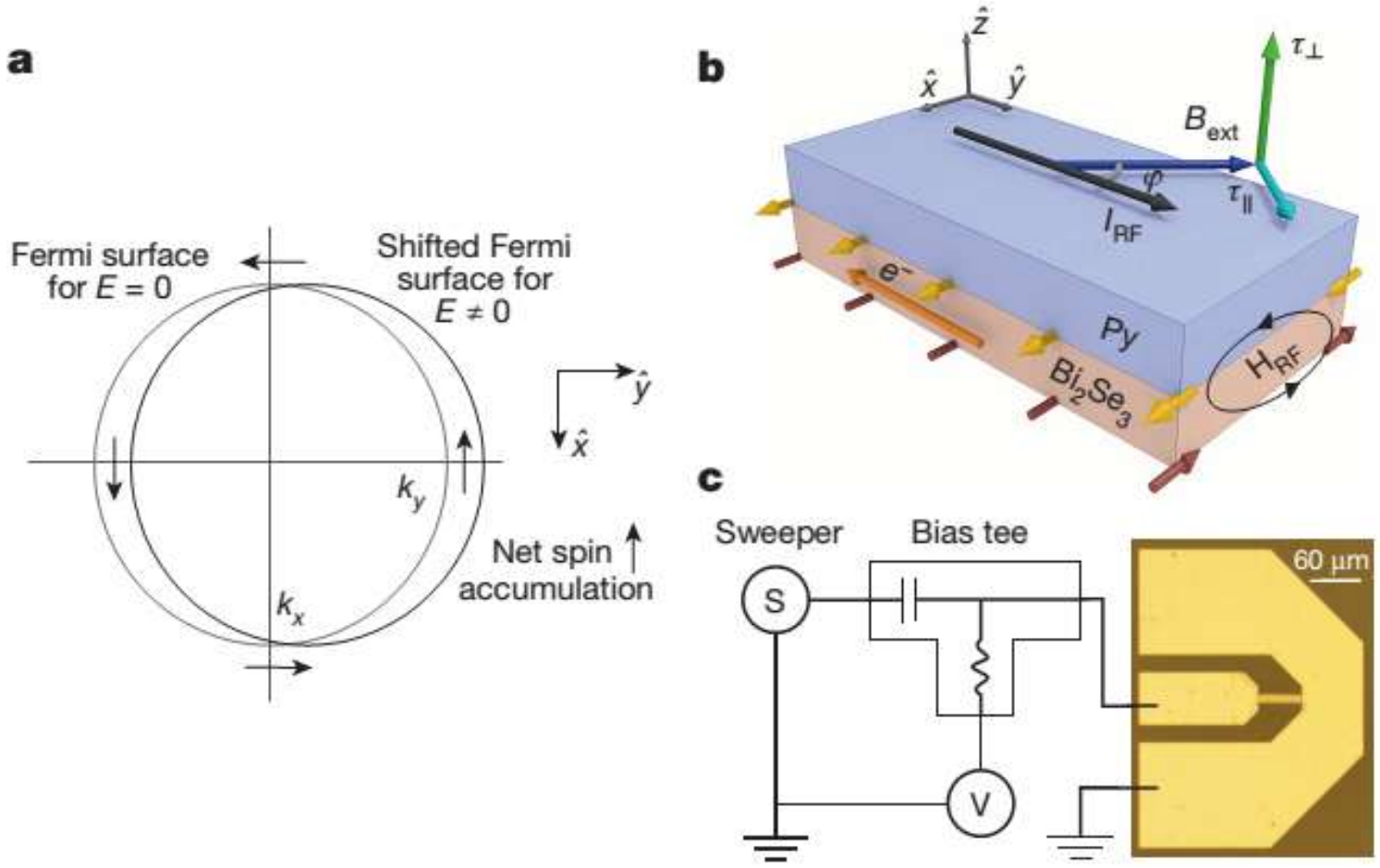
Inverse Edelstein in TI





Sanchez, et al. PRL (2016)

Inverse Edelstein in TI



Mellink, et al, Nature (2014)

Inverse Edelstein in TI

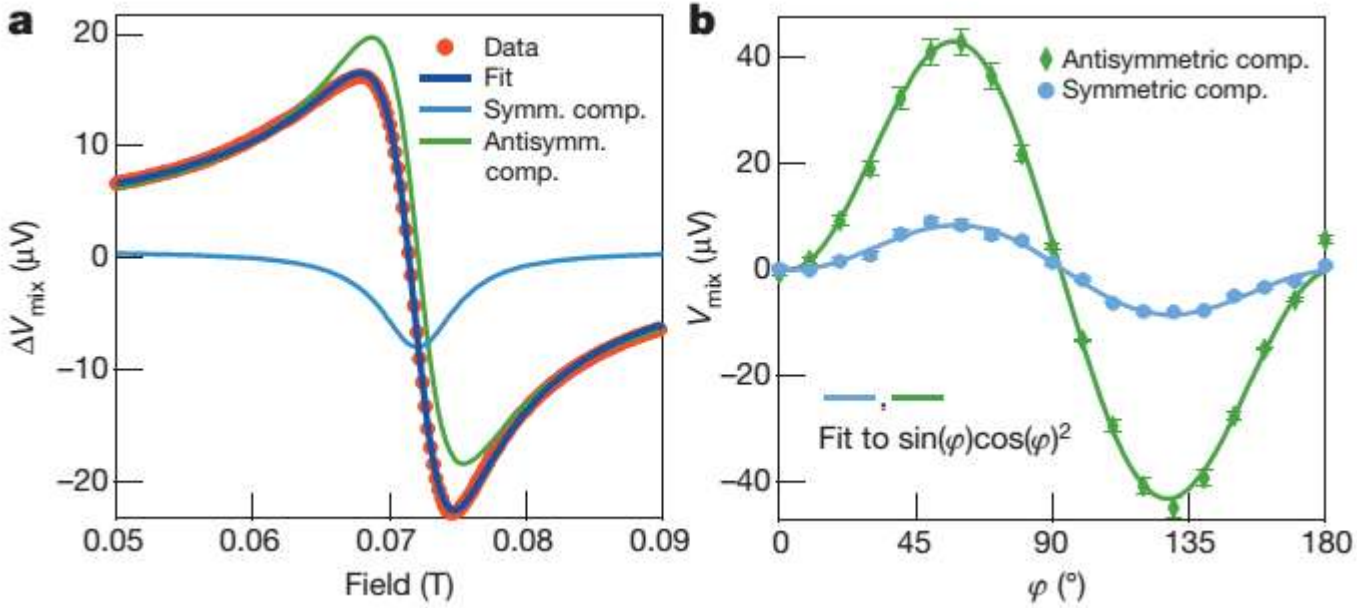
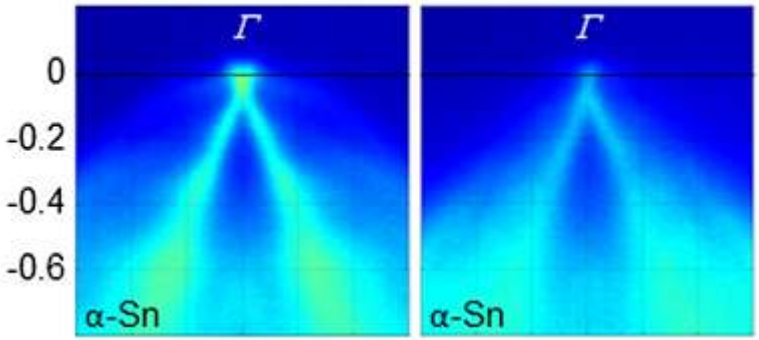


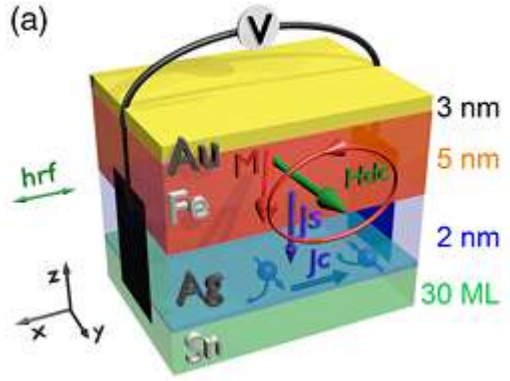
Table 1 | Comparison of room-temperature $\sigma_{s,\parallel}$ and $\theta_{s,\parallel}$ for Bi_2Se_3 with other materials

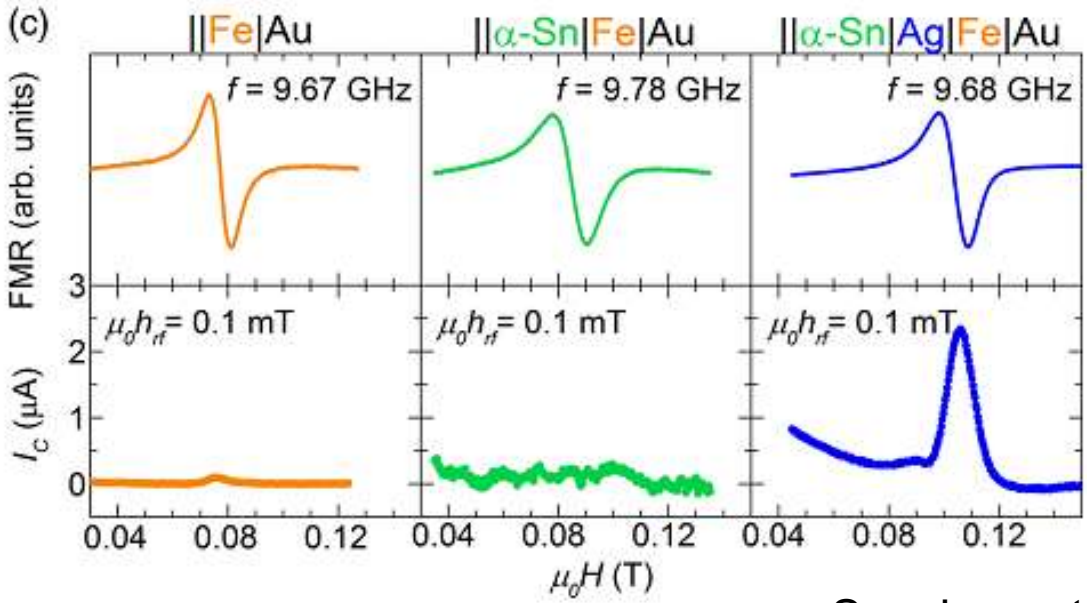
Parameter	Bi_2Se_3 (this work)	Pt (ref. 4)	β-Ta (ref. 6)	Cu(Bi) (ref. 23)	β-W (ref. 24)
$\theta_\parallel$	2.0–3.5	0.08	0.15	0.24	0.3
$\sigma_{S,\parallel}$	1.1–2.0	3.4	0.8	—	1.8

$\theta_\parallel$ is dimensionless and the units for $\sigma_{S,\parallel}$ are $10^5 \hbar/2e\ \Omega^{-1}\,m^{-1}$.

Inverse Edelstein in TI

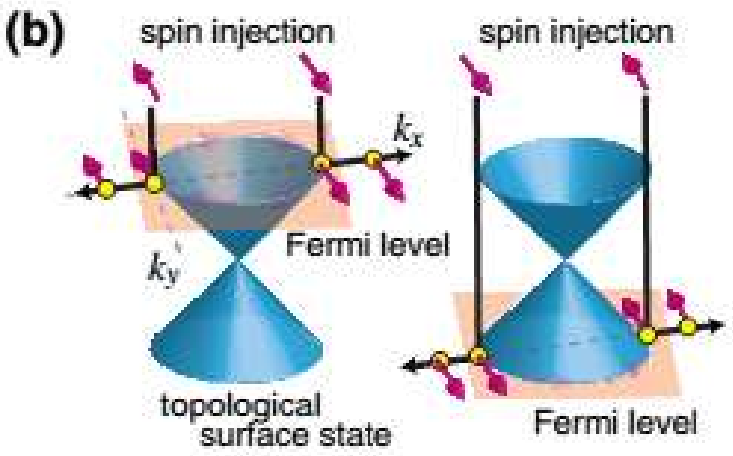


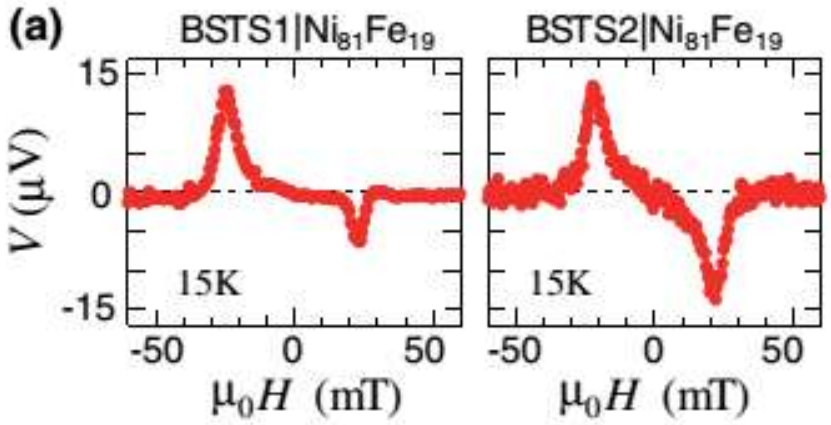


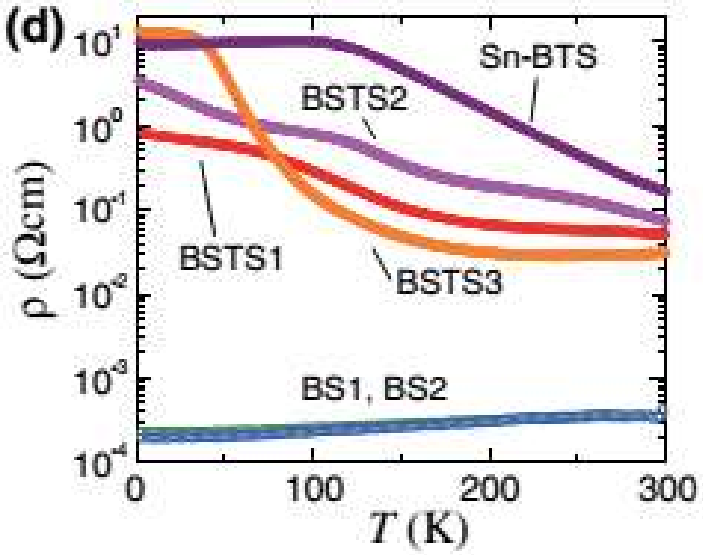


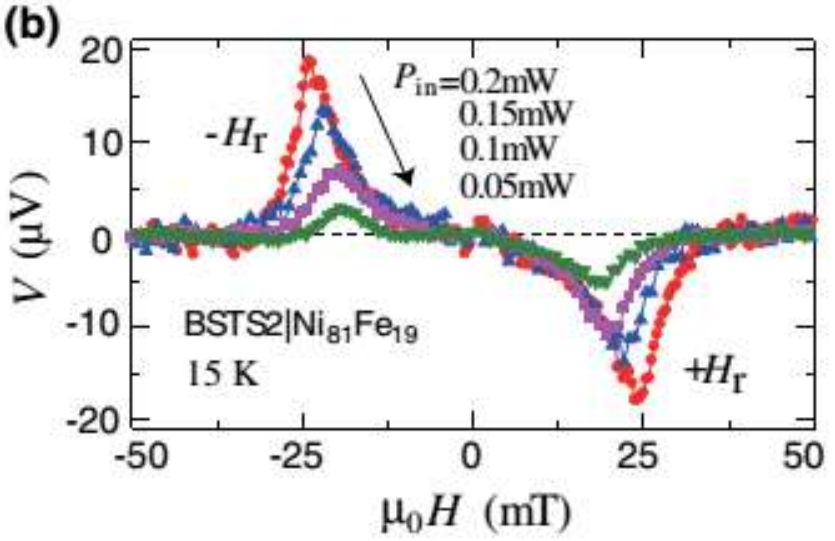
Sanchez, et al. PRL (2016)

Inverse Edelstein in TI



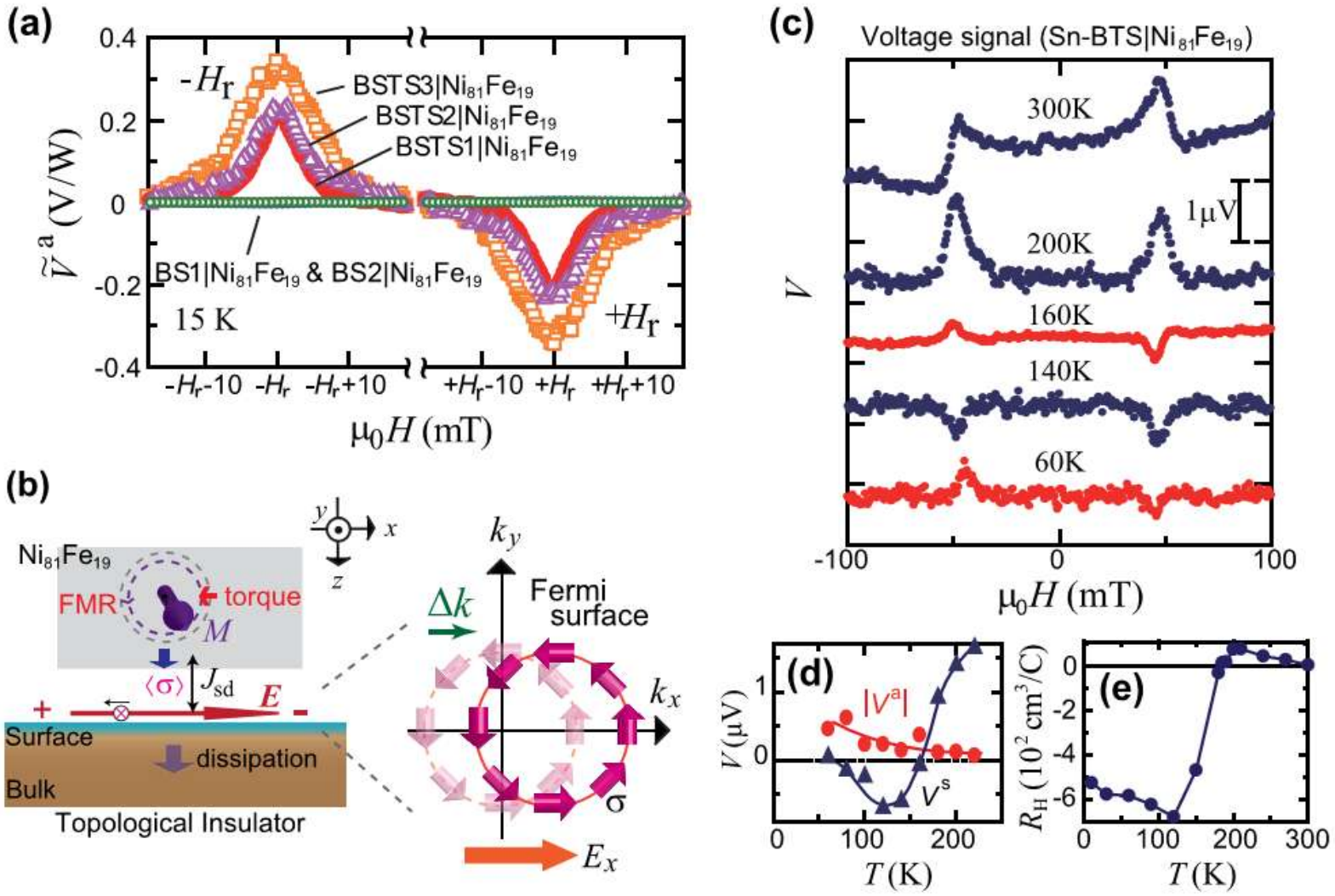






Shiomi, et al. PRL (2016)

Inverse Edelstein in TI



Inverse Edelstein in TI

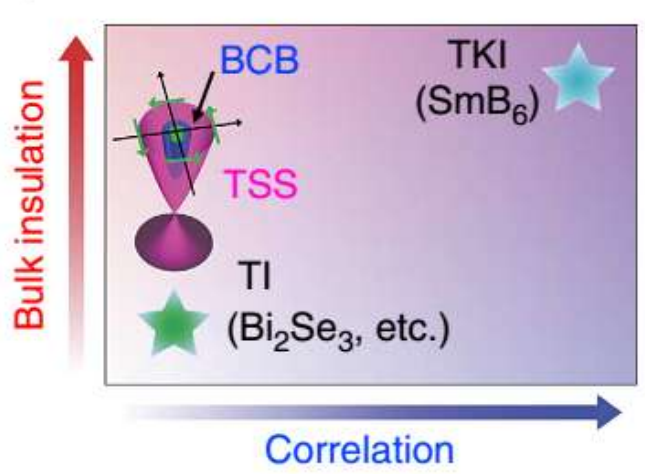
experimental data, the value of η is estimated to be $\sim 10^{-4}$ for BSTS1 and BSTS2. Here, because of imperfect insulation of bulk states, about 15% of the injected spins contribute to the spin-electricity conversion effect [11].

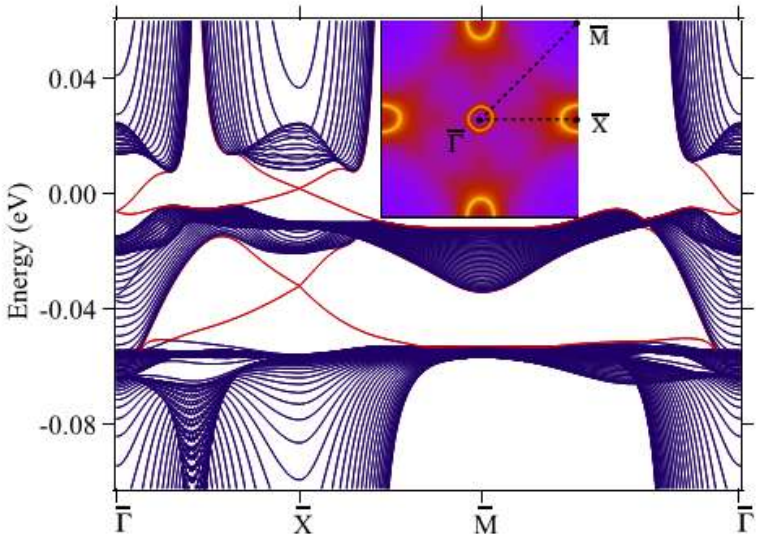
Note that, since the spin pumping induces spin polarization directly on the Fermi level of the surface state, the voltage generation is obviously dominated by the surface spin polarization, in contrast to experiments with circularly polarized light [29,30] where interband excitations generates electron-hole pairs and photocurrents. Also, as already noted, the spin-electricity conversion effect in the present surface-electron system is different from the

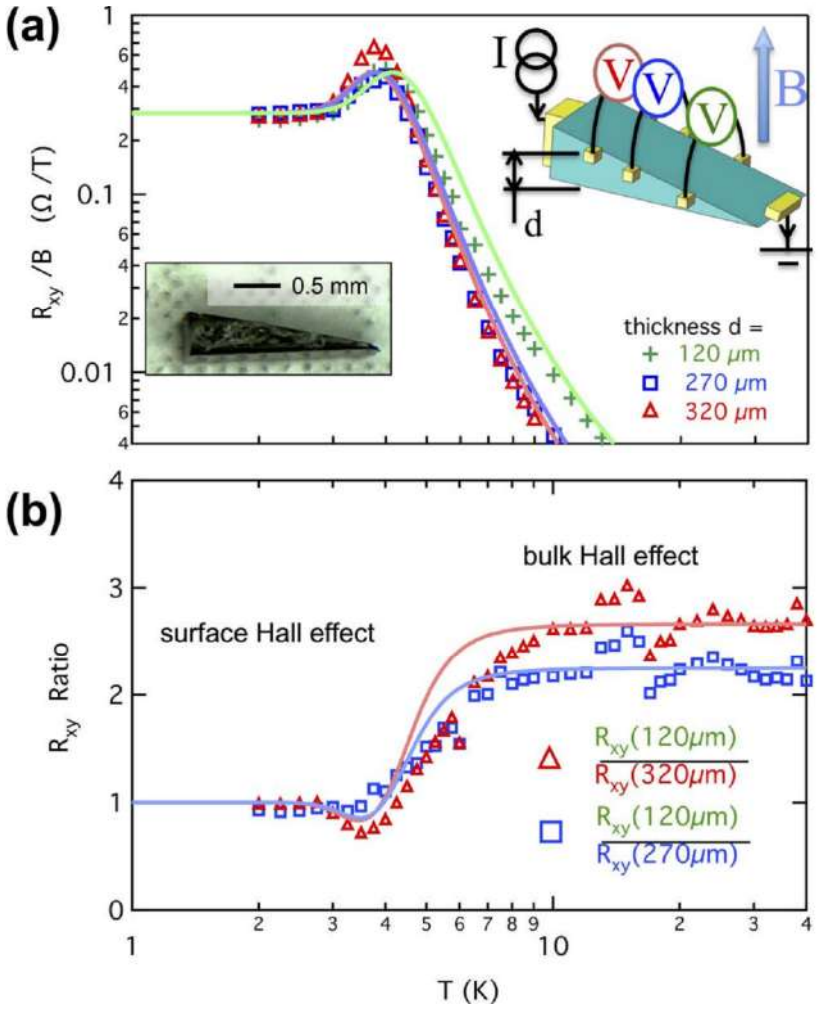
Challenge: Conduction from the Unavoidable bulk states

Inverse Edelstein in TI

SmB_6: A topological Kondo insulator



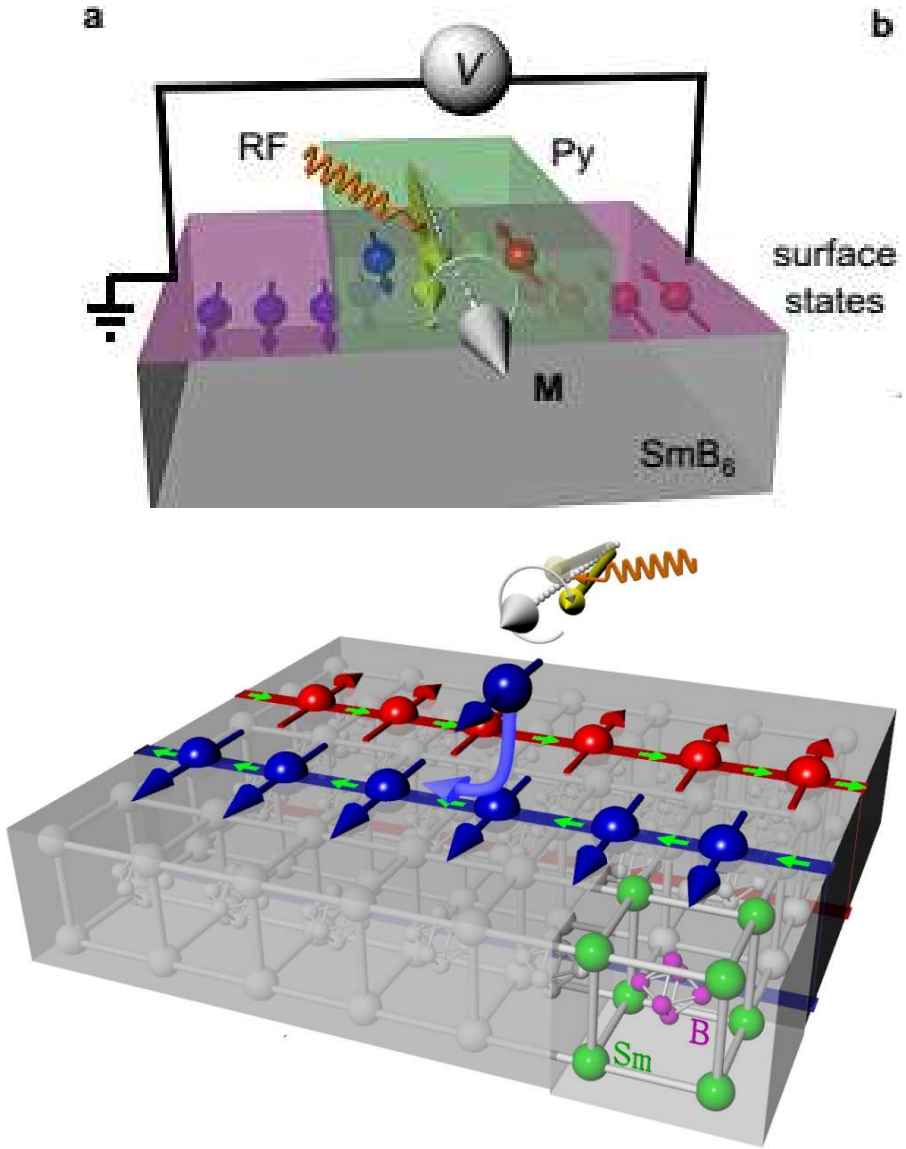




Fu et al., PRL (2013)

Kim et al, Scientific Reports (2013)

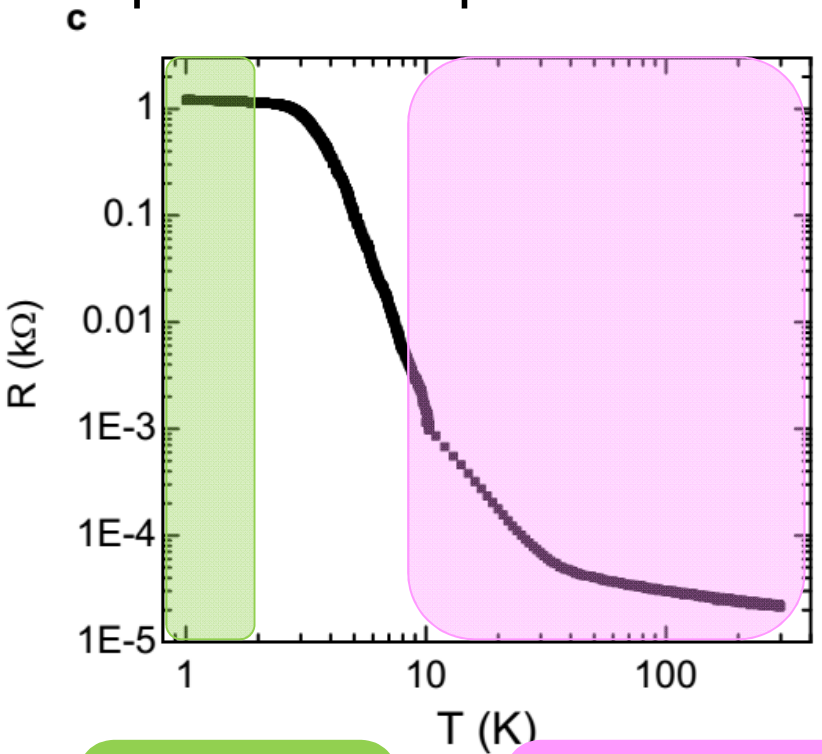
Inverse Edelstein in TI



Song, et al. Nature Commun. (2016)

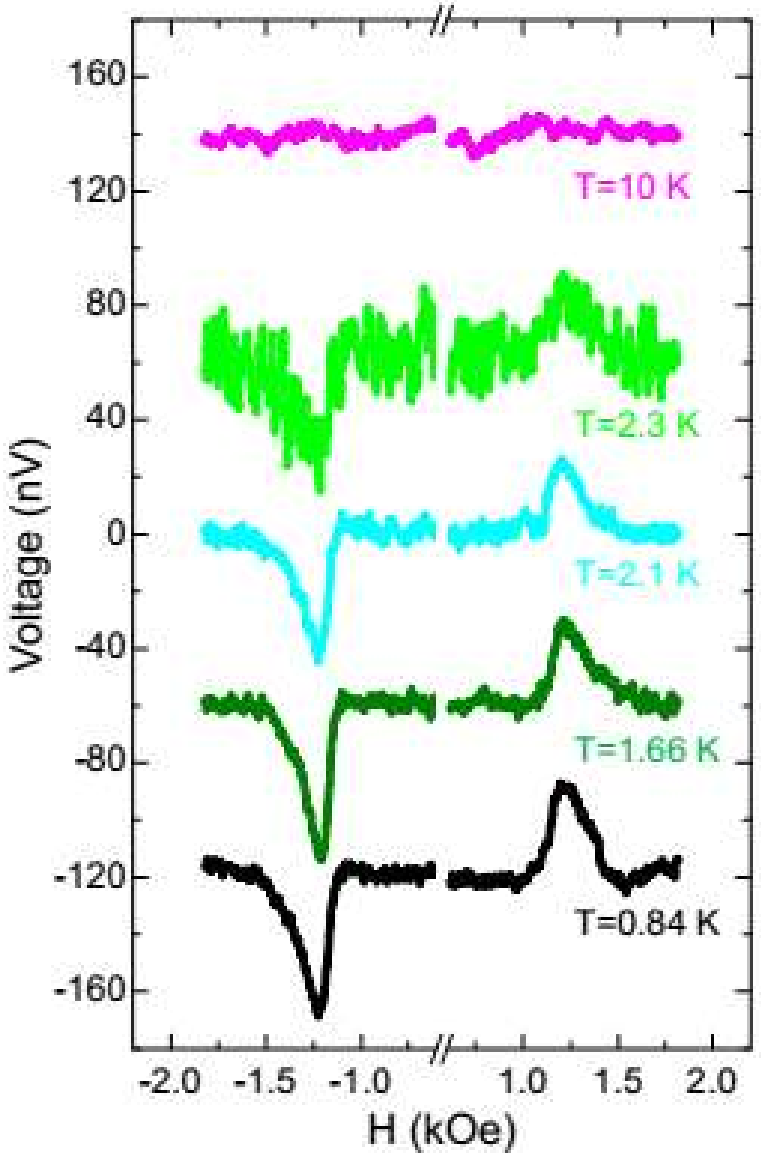
Inverse Edelstein in TI

Temperature dependence



Surface states

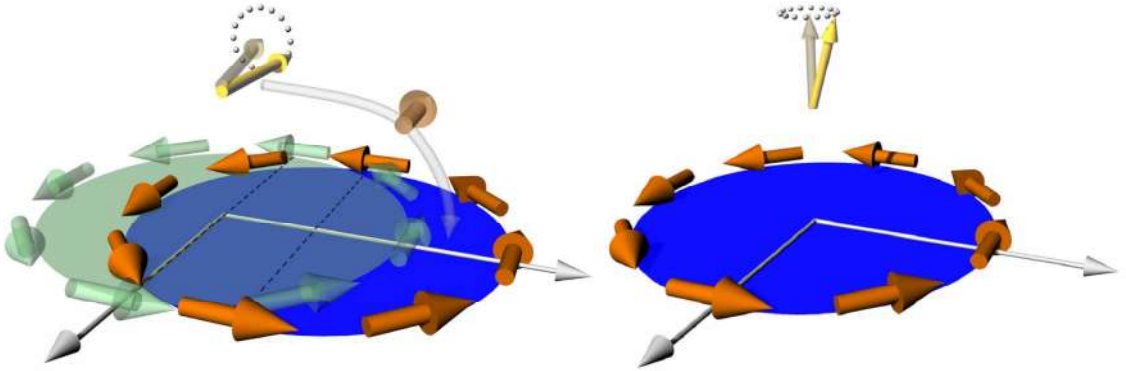
Bulk states

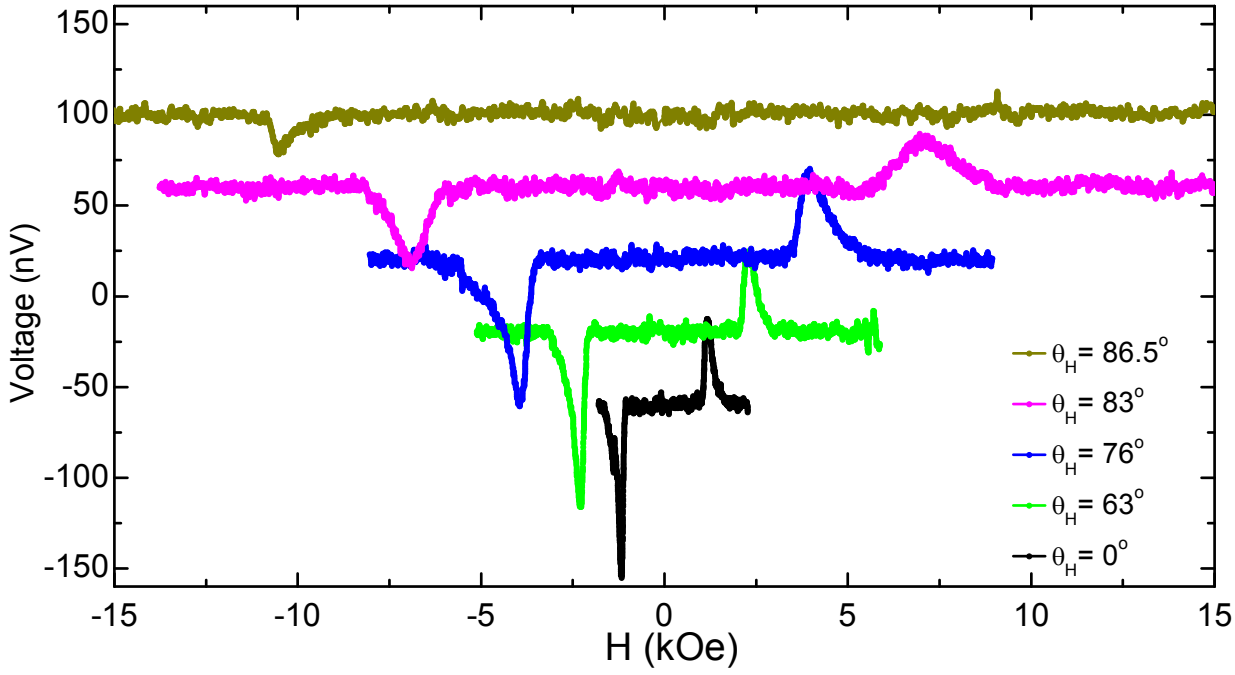


94

Inverse Edelstein in TI

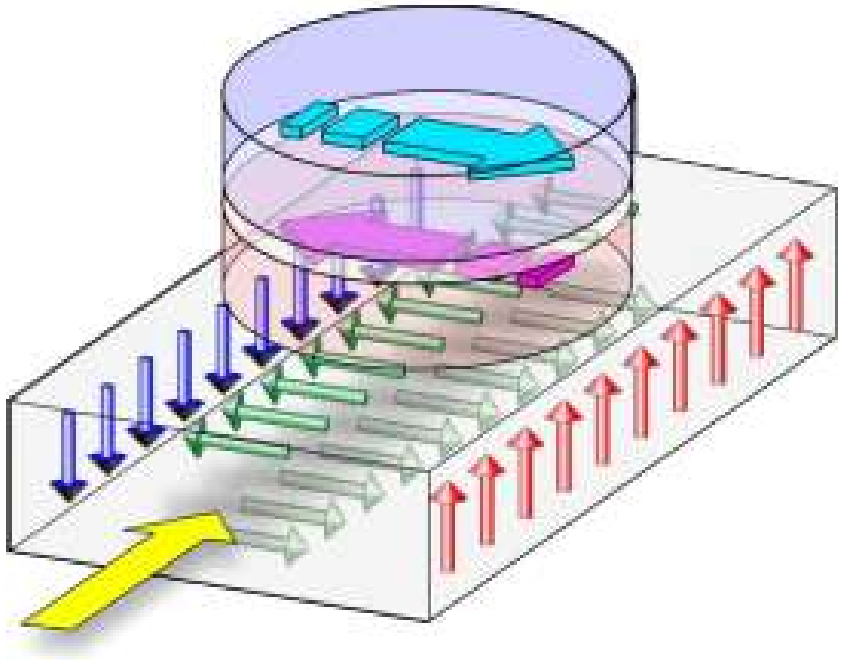
Angle dependence





Summary of this class

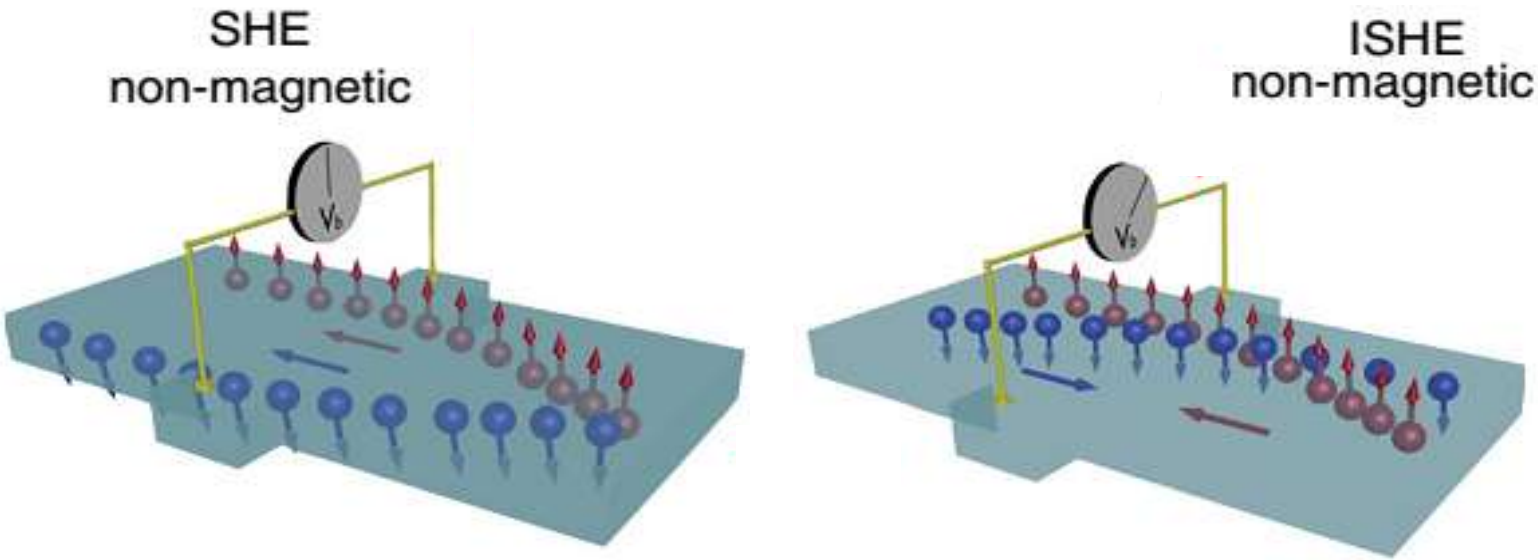
1. Spin orbit torque



$$\tau_{ST} = \frac{\hbar}{2}\hat{m} \times (\hat{\sigma} \times \hat{m})$$

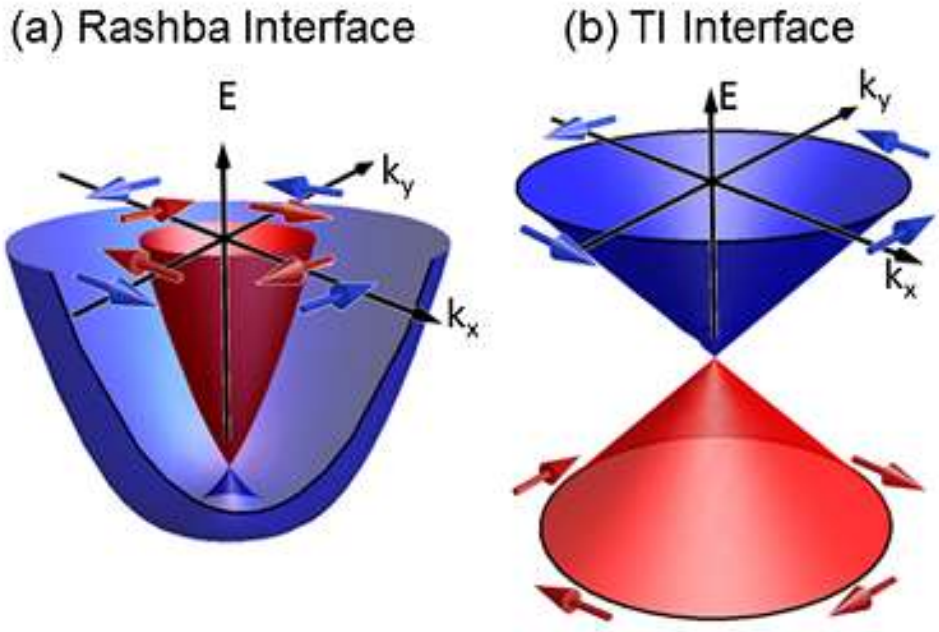
Summary of this class

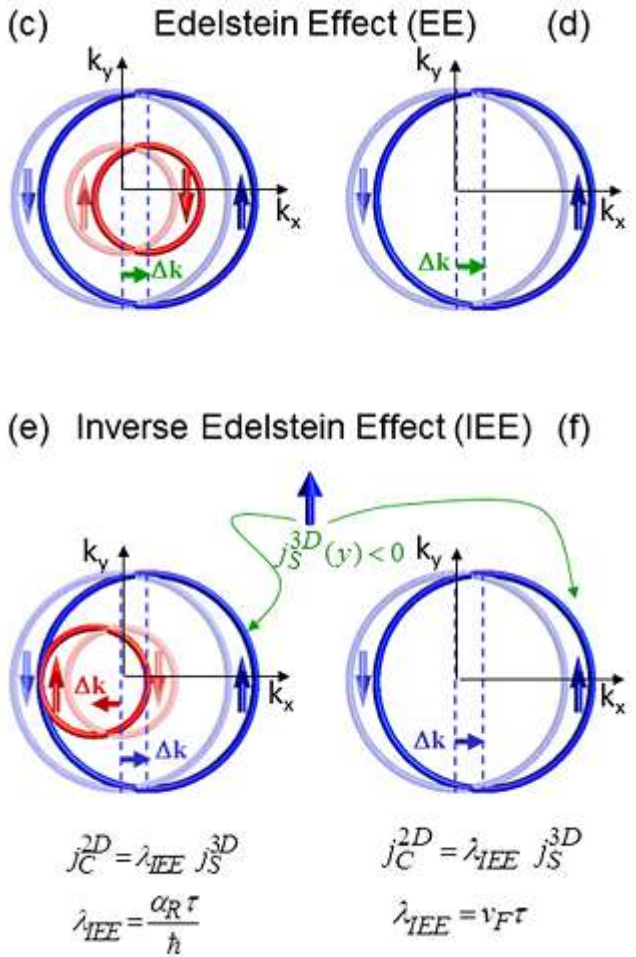
2. Spin Hall effect



Summary of this class

3. Rashba-Edelstein effect





下一节课: Nov. 30th

Chapter 6: Spin Caloritronics

课件下载：
http://www.phy.pku.edu.cn/~LabSpin/teaching.html